

A Computer Model for Circular and Linear Bubble Plumes

by

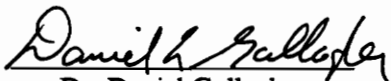
Wendy Cox Royston

Thesis submitted to the Faculty of the
Virginia Polytechnic Institute and State University
in partial fulfillment of the requirements for the degree of
MASTER OF SCIENCE
IN
ENVIRONMENTAL ENGINEERING

APPROVED:



Dr. John C. Little, Chair



Dr. Daniel Gallagher



Dr. Robert C. Hoehn

August 19, 1996

Blacksburg, Virginia

Keywords: bubble plume, hypolimnetic aeration, artificial circulation

c.2

LD
5655
V255
1976
R697
c.2

A COMPUTER MODEL FOR CIRCULAR AND LINEAR BUBBLE PLUMES

by

Wendy Cox Royston

Dr. John Little, Chairman

Department of Environmental Engineering

(ABSTRACT)

The purposes of this research were to implement the circular plume model developed by Wuest *et al.* (1992) and to develop and verify a linear plume model based on the circular model. The linear model developed is the first that models a bubble plume generated by a linear source in thermally stratified water and considers the effects of gas transfer between the bubbles and surrounding water.

The basis for both models is eight differential flux equations which are solved numerically using Euler's method. Knowledge of ambient temperature, dissolved solids, dissolved oxygen, and dissolved nitrogen profiles as well as gas input rate, diffuser dimensions, and initial bubble size are required to implement the models.

The implementation of the circular model was successful as the results obtained corresponded with those reported by Wuest *et al.* (1992). The linear model made predictions very similar to those made by the circular model and, therefore, was also considered to perform well. Comparisons of the linear model with available data met with limited success. Initially, the linear model's

predictions of laboratory scale plume velocity data resulted in overpredictions of 40 to 50 percent when compared to actual data. Error in predictions of laboratory scale oxygen transfer data were greater than 100 percent. The model fared better when its predictions were compared to full scale data; the predicted temperature was within 7 percent of that measured at three depths and the predicted oxygen concentration was within 4, 20, and 38 percent for the three depths. Some of the discrepancies in the data likely result from the fact that the Froude number used in the model to calculate initial velocity was derived for a circular, rather than a linear, source. Determination of the appropriate linear Froude number would likely improve the model's predictions.

ACKNOWLEDGMENTS

First, I would like to thank my advisor, Dr. John Little, for providing guidance and support throughout this project. I would also like to thank Dr. Daniel Gallagher and Dr. Robert Hoehn for serving on my committee. Thanks to the entire Environmental Engineering Division faculty and staff who have assisted me throughout my time at Virginia Tech. I would also like to express my gratitude to Dr. Robert Stern, my undergraduate advisor, whose guidance on my honor's thesis helped to make this thesis possible.

Thanks are also expressed to the Virginia Water Resources Research Center for providing financial support.

I would also like to say "Thank you" to my family and friends who have supported me through these last few years. Thanks to Dan McGinnis for helping me learn FORTRAN. A special thanks goes to my parents for their help and encouragement. Finally, a very special thank you to my husband Keith, for his support, encouragement, and immeasurable assistance through the past 3 1/2 years.

TABLE OF CONTENTS

ABSTRACT	ii
ACKNOWLEDGMENTS	iv
LIST OF FIGURES	vii
LIST OF TABLES	x
NOTATION USED IN CIRCULAR AND LINEAR PLUME MODELS	xi
INTRODUCTION	1
ARTIFICIAL CIRCULATION.....	1
HYPOLIMNETIC AERATION.....	2
BUBBLE PLUMES.....	3
OBJECTIVES.....	5
LITERATURE REVIEW	6
JETS AND PLUMES.....	7
CHARACTERISTICS OF BUBBLE PLUMES.....	8
SIMPLE PLUMES IN UNSTRATIFIED ENVIRONMENTS.....	10
SIMPLE PLUMES IN STRATIFIED ENVIRONMENTS.....	13
BUBBLE PLUMES IN UNSTRATIFIED ENVIRONMENTS.....	13
<i>Early Studies</i>	14
<i>Later Studies</i>	20
BUBBLE PLUMES IN STRATIFIED ENVIRONMENTS.....	23
GAS TRANSFER IN BUBBLE PLUMES.....	26
<i>Speece and Rayyan, 1973</i>	27
<i>Speece and Murfee, 1973</i>	28
<i>Rayyan and Speece, 1977</i>	28
<i>Tsang, 1990</i>	29
<i>Wuest et al., 1992</i>	29
SUMMARY OF PLUME THEORIES.....	31
MODEL DEVELOPMENT	33
WUEST ET AL. 'S CIRCULAR BUBBLE PLUME MODEL (1992).....	33
<i>Wuest et al. Model Equations</i>	33
<i>Wuest et al. Model Assumptions</i>	36
<i>Wuest et al. Solution Procedure</i>	38
CIRCULAR MODEL PROGRAM.....	40
<i>Circular Model Program Development</i>	40
<i>Circular Model Validation</i>	42
<i>Circular Model Sensitivity Analysis</i>	42
LINEAR PLUME MODEL.....	43
<i>Linear Model Equations</i>	43
<i>Linear Model Assumptions</i>	45

<i>Linear Model Solution Procedure</i>	48
LINEAR MODEL PROGRAM DEVELOPMENT.....	49
<i>Linear Model Validation</i>	49
<i>Linear Model Sensitivity Analysis</i>	54
RESULTS AND DISCUSSION	58
CIRCULAR PLUME MODEL VS. WUEST ET AL. MODEL.....	58
REVISED CIRCULAR PLUME MODEL VS. WUEST <i>ET AL.</i> MODEL.....	67
LINEAR PLUME MODEL VS. REVISED CIRCULAR PLUME MODEL.....	72
<i>Testing End Entrainment Assumption under Simulated Full Scale Conditions</i>	81
LINEAR PLUME MODEL VS. PROVOST'S (1973) VELOCITY DATA.....	82
LINEAR PLUME MODEL VS. WEN'S (1974) OXYGEN CONCENTRATION DATA.....	92
LINEAR PLUME MODEL VS. TVA DATA.....	96
SENSITIVITY ANALYSES.....	98
SUMMARY AND CONCLUSIONS	107
LITERATURE CITED	109
APPENDIX A: AMBIENT PROFILES	113
TEMPERATURE PROFILES.....	113
DISSOLVED SOLIDS PROFILES.....	114
DISSOLVED OXYGEN PROFILES.....	115
DISSOLVED NITROGEN PROFILES.....	116
APPENDIX B: CIRCULAR PLUME PROGRAM	117
APPENDIX C: LINEAR PLUME PROGRAM	129
VITA	141

LIST OF FIGURES

FIGURE 1. TYPICAL BUBBLE PLUME. (FROM LEMCKERT AND IMBERGER, 1993).	9
FIGURE 2. COMPARISON OF PLUME VELOCITIES FOR CIRCULAR MODEL WITH ADJUSTED AMBIENT DENSITY PROFILE WITH WUEST <i>ET AL.</i> 'S RESULTS FOR JULY AND NOVEMBER.	61
FIGURE 3. COMPARISON OF WATER VOLUME FLUXES FOR CIRCULAR MODEL WITH ADJUSTED AMBIENT DENSITY PROFILE WITH WUEST <i>ET AL.</i> 'S RESULTS FOR JULY AND NOVEMBER.	61
FIGURE 4. COMPARISON OF BUBBLE RADII FOR CIRCULAR MODEL WITH ADJUSTED AMBIENT DENSITY PROFILE WITH WUEST <i>ET AL.</i> 'S RESULTS FOR JULY AND NOVEMBER.	62
FIGURE 5. COMPARISON OF TEMPERATURES FOR CIRCULAR MODEL WITH ADJUSTED AMBIENT DENSITY PROFILE WITH WUEST <i>ET AL.</i> 'S RESULTS FOR JULY.....	63
FIGURE 6. COMPARISON OF TEMPERATURES FOR CIRCULAR MODEL WITH ADJUSTED AMBIENT DENSITY PROFILE WITH WUEST <i>ET AL.</i> 'S RESULTS FOR NOVEMBER.....	63
FIGURE 7. COMPARISON OF DENSITIES FOR CIRCULAR MODEL WITH ADJUSTED AMBIENT DENSITY PROFILE WITH WUEST <i>ET AL.</i> 'S RESULTS FOR JULY.....	64
FIGURE 8. COMPARISON OF DENSITIES FOR CIRCULAR MODEL WITH ADJUSTED AMBIENT DENSITY PROFILE WITH WUEST <i>ET AL.</i> 'S RESULTS FOR NOVEMBER.....	64
FIGURE 9. COMPARISON OF PLUME VELOCITIES FOR REVISED CIRCULAR MODEL WITH WUEST <i>ET AL.</i> 'S RESULTS FOR JULY AND NOVEMBER.....	69
FIGURE 10. COMPARISON OF WATER VOLUME FLUXES FOR REVISED CIRCULAR MODEL WITH WUEST <i>ET AL.</i> 'S RESULTS FOR JULY AND NOVEMBER.....	69
FIGURE 11. COMPARISON OF BUBBLE RADII FOR REVISED CIRCULAR MODEL WITH WUEST <i>ET AL.</i> 'S RESULTS FOR JULY AND NOVEMBER.....	70
FIGURE 12. COMPARISON OF PLUME TEMPERATURES FOR REVISED CIRCULAR MODEL WITH WUEST <i>ET AL.</i> 'S RESULTS FOR JULY AND NOVEMBER.....	70
FIGURE 13. COMPARISON OF DENSITIES FOR REVISED CIRCULAR MODEL WITH WUEST <i>ET AL.</i> 'S RESULTS FOR JULY.....	71
FIGURE 14. COMPARISON OF DENSITIES FOR REVISED CIRCULAR MODEL WITH WUEST <i>ET AL.</i> 'S RESULTS FOR NOVEMBER.....	71
FIGURE 15. COMPARISON OF PLUME VELOCITIES FOR LINEAR MODEL WITH END ENTRAINMENT WITH REVISED CIRCULAR MODEL FOR JULY.....	74
FIGURE 16. COMPARISON OF PLUME VELOCITIES FOR LINEAR MODEL WITH END ENTRAINMENT WITH REVISED CIRCULAR MODEL FOR NOVEMBER.....	74

FIGURE 17. COMPARISON OF WATER VOLUME FLUXES FOR LINEAR MODEL WITH END ENTRAINMENT WITH REVISED CIRCULAR MODEL FOR JULY	75
FIGURE 18. COMPARISON OF WATER VOLUME FLUXES FOR LINEAR MODEL WITH END ENTRAINMENT WITH REVISED CIRCULAR MODEL FOR NOVEMBER.	75
FIGURE 19. COMPARISON OF BUBBLE RADII FOR LINEAR MODEL WITH END ENTRAINMENT WITH REVISED CIRCULAR MODEL FOR JULY.....	76
FIGURE 20. COMPARISON OF BUBBLE RADII FOR LINEAR MODEL WITH END ENTRAINMENT WITH REVISED CIRCULAR MODEL FOR NOVEMBER.	76
FIGURE 21. COMPARISON OF PLUME TEMPERATURES FOR LINEAR MODEL WITH END ENTRAINMENT WITH REVISED CIRCULAR MODEL FOR JULY	77
FIGURE 22. COMPARISON OF PLUME TEMPERATURES FOR LINEAR MODEL WITH END ENTRAINMENT WITH REVISED CIRCULAR MODEL FOR NOVEMBER.	77
FIGURE 23. COMPARISON OF PLUME DENSITIES FOR LINEAR MODEL WITH END ENTRAINMENT WITH REVISED CIRCULAR MODEL FOR JULY.....	78
FIGURE 24. COMPARISON OF PLUME DENSITIES FOR LINEAR MODEL WITH END ENTRAINMENT WITH REVISED CIRCULAR MODEL FOR NOVEMBER.	78
FIGURE 25. COMPARISON OF LINEAR MODELS WITHOUT END ENTRAINMENT TO PROVOST'S PLUME VELOCITY DATA FOR 0.20 METER DEPTH.	86
FIGURE 26. COMPARISON OF LINEAR MODELS WITHOUT END ENTRAINMENT TO PROVOST'S PLUME VELOCITY DATA FOR 0.30 METER DEPTH.	86
FIGURE 27. COMPARISON OF LINEAR MODELS WITHOUT END ENTRAINMENT TO PROVOST'S PLUME VELOCITY DATA FOR 0.40 METER DEPTH.	87
FIGURE 28. COMPARISON OF LINEAR MODELS WITHOUT END ENTRAINMENT TO PROVOST'S PLUME VELOCITY DATA FOR 0.60 METER DEPTH.	87
FIGURE 29. COMPARISON OF LINEAR MODEL WITHOUT END ENTRAINMENT WITH FROUDE NUMBER OF 0.5 TO PROVOST'S PLUME VELOCITY DATA FOR 0.20 METER DEPTH.	90
FIGURE 30. COMPARISON OF LINEAR MODEL WITHOUT END ENTRAINMENT WITH FROUDE NUMBER OF 0.5 TO PROVOST'S PLUME VELOCITY DATA FOR 0.30 METER DEPTH.	90
FIGURE 31. COMPARISON OF LINEAR MODEL WITHOUT END ENTRAINMENT WITH FROUDE NUMBER OF 0.5 TO PROVOST'S PLUME VELOCITY DATA FOR 0.40 METER DEPTH.	91
FIGURE 32. COMPARISON OF LINEAR MODEL WITHOUT END ENTRAINMENT WITH FROUDE NUMBER OF 0.5 TO PROVOST'S PLUME VELOCITY DATA FOR 0.60 METER DEPTH.	91

FIGURE 33. SENSITIVITY OF MAXIMUM PLUME RISE HEIGHT TO INITIAL BUBBLE RADIUS FOR CIRCULAR AND LINEAR MODELS.	100
FIGURE 34. SENSITIVITY OF MAXIMUM PLUME RISE HEIGHT TO GAS INPUT RATE FOR CIRCULAR AND LINEAR MODELS.	100
FIGURE 35. SENSITIVITY OF MAXIMUM PLUME RISE HEIGHT TO INITIAL PLUME AREA FOR CIRCULAR AND LINEAR MODELS.	101
FIGURE 36. SENSITIVITY OF MAXIMUM PLUME RISE HEIGHT TO FROUDE NUMBER FOR CIRCULAR AND LINEAR MODELS.	101
FIGURE 37. SENSITIVITY OF MAXIMUM PLUME RISE HEIGHT TO ENTRAINMENT COEFFICIENT FOR CIRCULAR AND LINEAR MODELS.	102
FIGURE 38. SENSITIVITY OF MAXIMUM PLUME RISE HEIGHT TO AMBIENT TEMPERATURE PROFILE FOR CIRCULAR PLUME MODEL.	103
FIGURE 39. SENSITIVITY OF MAXIMUM PLUME RISE HEIGHT TO AMBIENT TEMPERATURE PROFILE FOR LINEAR PLUME MODEL.	103
FIGURE 40. SENSITIVITY OF MAXIMUM PLUME RISE HEIGHT TO AMBIENT DISSOLVED SOLIDS PROFILE FOR CIRCULAR PLUME MODEL.	104
FIGURE 41. SENSITIVITY OF MAXIMUM PLUME RISE HEIGHT TO AMBIENT DISSOLVED SOLIDS PROFILE FOR LINEAR PLUME MODEL.	104
FIGURE 42. SENSITIVITY OF MAXIMUM PLUME RISE HEIGHT TO AMBIENT DISSOLVED OXYGEN PROFILE FOR CIRCULAR PLUME MODEL.	105
FIGURE 43. SENSITIVITY OF MAXIMUM PLUME RISE HEIGHT TO AMBIENT DISSOLVED OXYGEN PROFILE FOR LINEAR PLUME MODEL.	105
FIGURE 44. SENSITIVITY OF MAXIMUM PLUME RISE HEIGHT TO AMBIENT DISSOLVED NITROGEN PROFILE FOR CIRCULAR PLUME MODEL.	106
FIGURE 45. SENSITIVITY OF MAXIMUM PLUME RISE HEIGHT TO AMBIENT DISSOLVED NITROGEN PROFILE FOR LINEAR PLUME MODEL.	106

LIST OF TABLES

TABLE 1. SUMMARY OF α VALUES IN PLUME THEORIES.....	32
TABLE 2. EIGHT FLUX EQUATIONS USED BY WUEST <i>ET AL.</i> (1992) FOR THE CIRCULAR PLUME MODEL.....	34
TABLE 3. DEFINITIONS OF THE EIGHT FLUX VARIABLES (FROM WUEST <i>ET AL.</i> , 1992).....	35
TABLE 4. EQUATIONS OF STATE AND PARAMETER APPROXIMATIONS USED BY WUEST <i>ET AL.</i> (1992) FOR THE CIRCULAR PLUME MODEL.	37
TABLE 5. INPUT VALUES FOR JULY AND NOVEMBER (WUEST <i>ET AL.</i> , 1992).	39
TABLE 6. EIGHT FLUX EQUATIONS FOR THE CIRCULAR PLUME MODEL (MODIFIED FROM WUEST <i>ET AL.</i> , 1992).	46
TABLE 7. DEFINITIONS OF THE EIGHT FLUX VARIABLES FOR LINEAR MODEL (MODIFIED FROM WUEST <i>ET AL.</i> , 1992).	47
TABLE 8. VALUES FROM PROVOST (1973) USED TO TEST LINEAR MODEL VELOCITY PREDICTIONS.	53
TABLE 9. VALUES FROM WEN (1974) USED TO TEST LINEAR MODEL OXYGEN TRANSFER PREDICTIONS. ...	56
TABLE 10. PROFILES USED TO TEST LINEAR MODEL PREDICTIONS OF TVA DATA.....	57
TABLE 11. PREDICTED AND MEASURED PLUME VELOCITIES AT DIFFERENT AIR FLOWRATES.	85
TABLE 12. COMPARISON OF LINEAR MODEL PLUME VELOCITY PREDICTIONS WITH FROUDE NUMBER EQUAL TO 0.5 TO PROVOST'S (1973) MEASURED DATA.	89
TABLE 13. COMPARISON OF LINEAR MODEL OXYGEN INPUT RATE PREDICTIONS TO WEN'S (1974) MEASURED DATA.	94
TABLE 14. EFFECT OF VARYING INITIAL BUBBLE SIZE ON LINEAR MODEL'S OXYGEN TRANSFER PREDICTIONS FOR GAS FLOWRATE EQUAL TO 0.0017 NM ³ /s.	95
TABLE 15. COMPARISON OF LINEAR MODEL OXYGEN AND PLUME TEMPERATURE PREDICTIONS TO TVA (1994) MEASURED DATA.	97
TABLE A-1. JULY TEMPERATURE PROFILES.	113
TABLE A-2. NOVEMBER TEMPERATURE PROFILES.....	113
TABLE A-3. JULY DISSOLVED SOLIDS PROFILES.....	114
TABLE A-4. NOVEMBER DISSOLVED SOLIDS PROFILES.....	114
TABLE A-5. JULY DISSOLVED OXYGEN PROFILES.....	115
TABLE A-6. NOVEMBER DISSOLVED OXYGEN PROFILES.....	115

NOTATION USED IN CIRCULAR AND LINEAR PLUME MODELS

- b Plume radius (circular model) (m)
b Plume width (linear model) (m)
 c_O Concentration of dissolved oxygen (mol/m^3)
 c_N Concentration of dissolved nitrogen (mol/m^3)
D Depth of diffuser below lake surface (m)
 D_O Dissolved oxygen flux (mol/m^3)
 D_N Dissolved nitrogen flux (mol/m^3)
Fr Froude number (dimensionless)
 F_S Dissolved solids flux (salinity flux) (kg/s)
 F_T Temperature flux ($^\circ\text{C m}^3/\text{s}$)
g Acceleration due to gravity (9.81 m/s^2)
 G_O Gaseous oxygen flux (mol/m^3)
 G_N Gaseous nitrogen flux (mol/m^3)
K Solubility constant ($\text{mol/m}^3\text{-bar}$)
L Plume length (Length of diffuser, linear model) (m)
M Momentum flux (m^4/s^2)
 m_O Concentration of gaseous oxygen (mol/m^3)
 m_N Concentration of gaseous nitrogen (mol/m^3)
N Number of bubbles
p Total pressure (bar)
 p_O Partial pressure of oxygen (bar)
 p_N Partial pressure of nitrogen (bar)
r Bubble radius (m)
R Gas constant ($8.314 \times 10^{-5} \text{ bar}\cdot\text{m}^3/\text{mol}\cdot\text{K}$) (where K denotes temperature in Kelvin)
S Dissolved solids concentration (salinity)
T Temperature ($^\circ\text{C}$)
 T_K Absolute temperature (K)
 V_g Volume of gas per volume of bubble-water mix (dimensionless)
w Plume velocity (m/s)
 w_b Bubble slip velocity (m/s)
z Vertical coordinate (measured from diffuser toward lake surface) (m)
- α Entrainment coefficient (dimensionless)
 β Gas transfer coefficient (m/s)
 λ Spreading coefficient (Defined as the ratio of the bubble-containing radius to the plume radius for bubble plumes.) (dimensionless)
 μ Water volume flux (m^3/s)
 ρ Density

Subscripts:

a ambient
O oxygen
N nitrogen
p plume
w plume water
0 initial

I. INTRODUCTION

In the summer, lakes and reservoirs thermally stratify and oxygen can be depleted in the hypolimnion. This oxygen depletion can result in a number of problems in the water body. One potential hazard is a fish kill that occurs when the oxygen concentration falls below critical levels. Another problem is that the sediment may release ammonia, iron, phosphorus, sulfide, and manganese into the water when dissolved oxygen concentrations approach zero (Cole, 1983). If the water body is a drinking water source, poor drinking water quality may result. Fortunately, methods exist that can replenish the oxygen supply in the hypolimnion. Two of these methods are artificial circulation and hypolimnetic aeration.

Artificial Circulation.

The purpose of artificial circulation is to mix the water throughout the depth of the lake so that the oxygenated water at the lake's surface is continually distributed through the lake. Artificial circulation, which is also called destratification since it destroys the thermal stratification in the water body, produces an increase in both dissolved oxygen concentration and temperature in the bottom portions of the basin. The increase in dissolved oxygen concentration is a benefit; however, the increased temperature can create problems. Some fish require a cold water habitat which an increase in temperature may degrade. Humans prefer to drink cold water and may complain if their drinking water becomes warm. Artificial circulation can result in another problem if it is implemented in nutrient deficient lakes, namely that the circulation can return nutrients from the hypolimnion back to upper portions of the lake where algal growth may occur (Lorenzen and Fast, 1977; Cooke *et al.*, 1993). Obviously, the potential advantages and

disadvantages of destratification must be weighed before such a system is installed in a lake or reservoir.

Artificial circulation can be accomplished by three main methods: air release near the bottom of the water body to produce a rising bubble plume, vertical water jets flowing upwards from the bottom portions of the water, and mechanical mixing using pumps or propellers (Lorenzen and Fast, 1977; Cooke *et al.*, 1993).

Hypolimnetic Aeration.

The goal of hypolimnetic aeration is to increase the oxygen concentration in the hypolimnion without destroying the thermal stratification in the water body. By retaining thermal stratification, the problems associated with artificial circulation are eliminated. However, a potential problem exists with hypolimnetic aeration as well. It has been hypothesized that using air for hypolimnetic aeration could result in hypolimnetic supersaturation with nitrogen which could harm fish. Nitrogen supersaturation has been observed, but harm to fish from this process has yet to be seen (Cooke *et al.*, 1993). Both destratification and hypolimnetic aeration have other advantages and disadvantages depending on the particular circumstances of the water body in question.

Numerous methods have been devised for hypolimnetic aeration. Lorenzen and Fast (1977) divided these methods into three categories: mechanical agitation, air injection, and oxygen injection systems. Mechanical agitation involves first bringing hypolimnetic water to the surface where it is mechanically aerated in a splash basin and then returning it to the hypolimnion. Air injection systems include both upflow and downflow systems. In upflow systems, air is injected near the bottom of the lake. The air-water mixture then ascends in a riser tube to either the upper

portions of the hypolimnion (partial lift systems) or near the water surface (full lift systems). At the top of the riser, waste air is released to the atmosphere. The oxygenated water is injected back into the hypolimnion. One of the first successful hypolimnetic aeration systems (Bernhardt, 1967) was a full lift air injection type. Downflow systems involve pumping hypolimnion water downward with enough velocity that injected air is forced downward as well. Air must then be separated from the water in the hypolimnion. Oxygen injection can be accomplished through several methods as well. One method involves withdrawing hypolimnetic water, exposing it to pure oxygen under high pressure, and then inserting it back into the hypolimnion. Another method involves injecting pure oxygen into the bottom of the lake to form a rising oxygen bubble plume. A third method involves utilizing a downflow system with pure oxygen that would dissolve in the hypolimnetic water. (See also Cooke and Carlson, 1989 and Cooke *et al.*, 1993.)

Kortmann *et al.* (1994) have developed the layer aeration method for increasing oxygen concentrations in a water body. This method is a combination of artificial circulation and hypolimnetic aeration. The aerator is a full lift type that withdraws water from various depths, provides contact with the atmosphere, and releases the water at the appropriate depths. Although the temperature profiles in the lake are altered, the water body remains thermally stratified.

Bubble Plumes.

A method that has provided both reservoir destratification and hypolimnetic aeration is the use of diffusers to release air or oxygen at or near the bottom of a water body. For destratification systems, air is released that rises toward the surface, entraining surrounding water to form a plume. Near the bottom of the plume, surrounding water from the lake is drawn into the plume; at the surface, currents flow away from the plume. The net result is a mixing of the lake. Bubble

plumes can also be used for hypolimnetic aeration by controlling the height to which the plume rises so that the plume water is detained near the top of the hypolimnion. It is also possible to form small oxygen bubbles that dissolve completely before reaching the metalimnion.

Wuest *et al.* (1992) have developed a model that predicts the performance of a circular diffused aeration system in a lake or reservoir. Eight flux equations, including water volume, momentum, temperature, dissolved solids, dissolved oxygen, dissolved nitrogen, gaseous oxygen, and gaseous nitrogen fluxes provide the basis for the model. Profiles for ambient temperature, dissolved solids, dissolved oxygen, and dissolved nitrogen are required to run the model.

The Tennessee Valley Authority (TVA) has developed a diffused aeration system that is linear in configuration. Oxygen is injected into the water through a porous hose which is installed in a line near the bottom of the reservoir (Mobley and Brock, 1996). The TVA system provides hypolimnetic aeration.

Currently, no model exists that assesses the performance, including effects of the system on temperature and dissolved oxygen profiles in the water body and the height to which the plume rises, for this and other linear diffused aeration systems. Such a model is needed so that the systems' performance in lakes and reservoirs can be predicted.

Objectives.

The objectives of this research were to:

- ♦ implement the model developed by Wuest *et al.* (1992) for circular plumes;
- ♦ verify the implementation of the circular model by comparing it to data presented in the Wuest *et al.* paper;
- ♦ convert the circular model to a linear model;
- ♦ verify the linear model through comparisons with both the circular model and data from previous studies; and
- ♦ use the linear model to predict the performance of the TVA system.

II. LITERATURE REVIEW

Bubble plumes were being used for engineering purposes as early as 1907, when a patent was obtained for a perforated pipe that served as a breakwater by releasing compressed air into the ocean. The mechanism by which the breakwater worked was unknown, and, in fact, the system did not work extremely well. It was not until 1936 that it was determined that the mechanism that caused the waves to break was a horizontal surface current generated by the rising plume (Bulson, 1968).

Turbulent bubble plumes have been studied as potential solutions to a number of diverse engineering problems. Bulson (1968) examined the feasibility of using bubble plumes as breakwaters in the ocean and determined that the amounts of air required were enormous and the costs therefore excessive. Some investigators, including Jones (1972), have investigated the possibility of using bubble plumes to contain oil spills. Others have considered bubble plumes to control saltwater intrusion into fresh water, to reduce the temperature of cooling water outfalls, and to prevent the freezing of harbors in the winter (Wilkinson, 1979). Since many early uses for bubble plumes relied on the plumes' vertical and surface velocities, early studies focused on these aspects and ignored other features such as bubble expansion and gas transfer.

A more recent application for bubble plumes is for lake and reservoir restoration, through both hypolimnetic aeration and artificial circulation. For this purpose, vertical plume velocity and gas transfer are the main parameters of concern. A significant amount of work has been done in this area, although most studies have focused on velocity and few have investigated the effects of gas transfer.

Jets and Plumes.

“A jet is the discharge of fluid from an orifice or slot into a large body of the same or similar fluid” (Fischer *et al.*, 1979). Jets flow due to an inertial force. Plumes are similar to jets in appearance but flow due to a buoyant force such as a temperature difference in the plume relative to its surroundings. Simple plumes are those in which the plume fluid is either the same as or miscible in the surrounding fluid, such as warm water rising in colder water. If the plume fluid is not miscible with the ambient fluid, a two-phase plume results. An example is air bubbles rising in water. Buoyant jets are jets that contain a buoyant force which acts in the same direction as the inertial force. Negative buoyant jets are those in which the buoyant force acts in the opposite direction, resulting in a reduction of flow velocity (Chen and Rodi, 1976).

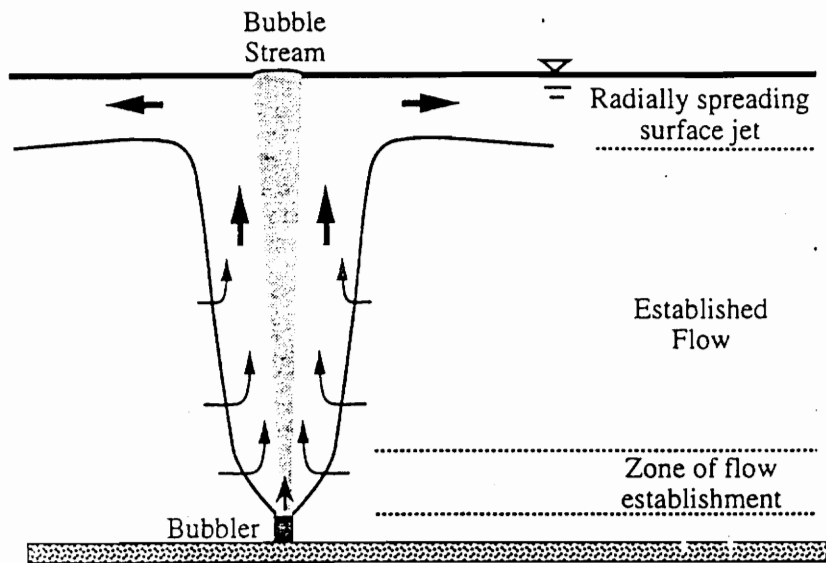
Flow in buoyant jets can be either laminar or turbulent depending on the Reynolds number. While the exact Reynolds number at which the transition from laminar to turbulent flow occurs cannot be accurately predicted, numbers above 2000 can generally be considered to be turbulent (Fischer *et al.*, 1979). In general, most jets of concern in engineering practice are turbulent as laminar flow becomes unstable close to the source (Morton, 1959).

Several studies of laminar flow in plumes have been performed. Although laminar flow studies are beyond the scope of this project, they do contain information that could increase understanding of the overall subject. For example, see Durst *et al.* (1986) for a discussion of bubble flow in laminar plumes and Priven *et al.* (1995) for a study of laminar buoyant jets in stratified environments. The considerable effort required by these investigators to ensure that the flow in their experiments remained laminar reinforced the contention that flow in most jets and plumes is turbulent.

Turbulent buoyant jets have been used for lake and reservoir destratification and for hypolimnetic aeration. In the literature, these buoyant jets are often referred to as bubble plumes since the buoyant force soon overshadows the inertial force (Kobus, 1968). This convention will be adopted here as well.

Characteristics of Bubble Plumes.

A schematic of a bubble plume is shown in Figure 1. An air source, typically with either a point, circular, or linear geometry, is located at a depth D from the surface of the water body. When the air exits the diffuser, small bubbles form and rise toward the surface. As the bubbles rise, they entrain water into their flow and to form a rising air-water plume. The plume has three zones: the zone of flow establishment; the zone of established flow; and the surface zone. In the zone of establishment, which is directly above the air supply, the plume width increases rapidly and flow is highly turbulent. In the zone of established flow, the plume width and velocity vary less dramatically. In the surface zone, the plume flows horizontally away from the plane or axis of the diffuser (Wilkinson, 1979). The depth of the surface zone has been found to be $0.25D$ for linear sources and slightly less for circular sources (Cederwall and Ditmars, 1970). The lateral extent of the surface current is typically four (Jones, 1972 and Wen, 1974) to six (Asaeda and Imberger, 1993) times the depth from the water surface to the diffuser.



Idealized Bubble Plume in Homogeneous Fluid Showing Flow Regions (Wilkinson 1979). (Thick Arrows Mark Major Flow Paths; Thin Arrows Indicate Entrainment Paths)

Figure 1. Typical Bubble Plume. (From Lemckert and Imberger, 1993).

Simple Plumes in Unstratified Environments.

Early plume studies focused on simple plumes. They modeled only the zone of established flow and did not attempt to describe the surface zone or the zone of flow establishment. These models typically concentrated on volume flux, momentum flux, and buoyancy flux equations with other aspects included depending on the particular theory. Investigators considered both linear (two dimensional) and circular (axisymmetric) plumes in air and water. All the models included what is known as the Boussinesq assumption: that while the density difference in the plume relative to its surroundings is significant in regards to buoyancy, the difference in density between the plume and the ambient fluid is negligible in regards to equations of motion (Orlob, 1983). The models also assumed that the vertical profiles followed a Gaussian distribution. The fluids in the models were assumed to be incompressible and, other than the vertical velocity of the plume, the ambient fluid was assumed to be stagnant. Morton (1959) introduced the important concepts of the entrainment coefficient and the spreading coefficient which were used in nearly all subsequent plume models.

The first significant study of simple plumes was performed by Rouse *et al.* (1952). They investigated plumes formed in air from both linear and point heat sources. Their assumptions included that the extent of the initial laminar flow zone was negligible compared to the turbulent zone, that pressure was hydrostatically distributed, that horizontal forces were negligible compared to vertical forces, and that vertical turbulent mixing was insignificant compared to horizontal turbulent mixing. In addition, they invoked the Boussinesq assumption.

Initial calculations led Rouse *et al.* (1952) to conclude that "... the convection zone will expand linearly with elevation; the maximum velocity will be independent of elevation; and the maximum incremental weight density will vary inversely with elevation." Based on these

conclusions, integral equations were derived for volume flux, momentum flux, kinetic energy flux, unit buoyant flux, and incremental weight flux. The five equations were integrated and the necessary constants were determined via temperature and velocity measurements above linear and point heat sources in the laboratory. A Gaussian profile was found to provide a good fit for the lateral distributions of both temperature and velocity.

The experimental results obtained by Rouse *et al.* (1952) were called into question by Kotsovinos and List (1977) as the 1952 results showed that the width of the plume velocity profile was larger than that of the temperature profile. Kotsovinos and List stated that the opposite was known to be true, and therefore the Rouse *et al.* results were questionable. However, the work by Rouse *et al.* was an important starting point for plume modeling.

Morton (1959) studied turbulent buoyant circular jets, which he called “forced plumes,” in both unstratified and stratified environments. The work concerning plumes in unstratified surroundings is discussed here; simple plumes in stratified environments are discussed in a following section.

The most significant contribution made by Morton was the concept of an entrainment coefficient. The entrainment coefficient, α , was “the ratio of the mean spread of inflow at the edge of a forced plume to the mean vertical speed on the plume axis” and was assumed constant. Another constant, λ , was defined as the ratio of the horizontal extent of the buoyancy profile to the horizontal extent of the velocity profile. The constants α and λ were determined experimentally to be 0.082 and 1.16, respectively. Gaussian distributions of velocity and buoyancy were assumed, and the Boussinesq assumption was made. Morton’s model was based on equations for momentum flux, mass flux, and buoyancy flux and the idea of a virtual point source with zero diameter which was normally below the actual source. Solutions to the model for plumes from an actual source

were found by first solving for the location of the virtual source and then using the equations derived for the plume formed at the virtual source.

Abraham (1960) investigated circular water jets in a salt solution. He found that, while the buoyancy was negligible compared to the inertia near the nozzle, it became very significant as distance from the nozzle increased. In this study, equations derived in previous studies (such as Morton, 1959), were altered so that the model could be solved for an actual source without calculating the location of the virtual source. Abraham's laboratory studies found that his model predicted the concentration along the centerline of the plume fairly well; the model's predictions of other variables, such as velocity, were not examined.

Kotsovinos and List (1977) completed what was only the third experimental study of two dimensional turbulent buoyant jets. The only other studies of plane buoyant jets had been performed by Rouse *et. al.* (1952), described previously, and by Lee and Emmons (1961, quoted in Kotsovinos and List, 1977) who measured temperature profiles above a linear fire. The focus of the Kotsovinos and List study was on the entrainment and mixing that occur in two-dimensional buoyant jets. Kotsovinos and List concluded that the entrainment coefficient was not the same in plumes as in jets and, in fact, was not constant as had been proposed by Morton (1959). They derived a set of equations to solve for the entrainment coefficient as a function of specific mass flux, specific momentum flux, specific buoyancy flux, and distance above the virtual origin.

This model contained several empirical constants; once their values were determined through laboratory experiments, the predictions made by the model were accurate. The study found that the spreading coefficient (defined as the velocity profile width versus temperature profile width) was greater for the two dimensional plume than for the circular plume (1.33 vs. 1.16) and that the half-width of the temperature profile varied linearly with distance above the source.

Simple Plumes in Stratified Environments.

Little work has been done concerning simple plumes in stratified environments. Only Morton (1959) has examined this topic in detail.

Morton (1959) noted that Gaussian distributions did not accurately describe plume profiles in stratified environments and therefore used a “top hat” distribution to describe the vertical flow of a plume in the presence of stratification. He also noted that, in a stratified environment, the plume reached its maximum height when its buoyancy was the same as the ambient buoyancy. However, the plume would first rise past this height due to its inertia; it would then slow, stop, and fall back to the level of neutral buoyancy where it would spread out.

A top hat profile assumes a constant average value across the width of the plume and does not affect the calculated height of maximum plume rise. However, the entrainment and spreading coefficients have different values: α is 0.116 and λ is 1.108 for round plumes. (As mentioned previously, α and λ were reported to be 0.082 and 1.16, respectively for round plumes in unstratified surroundings.) Morton also reported that stratification resulted in slightly greater widths in both plumes and jets.

Bubble Plumes in Unstratified Environments.

Bubble plume models borrowed heavily from the simple plume models that came before them. Early bubble plume theories did not examine gas transfer from the air bubbles to the surrounding water, ignoring the effects of gas absorption on the bubble size. The velocity, momentum, and buoyancy fluxes were evaluated in order to obtain the plume characteristics in the

zone of established flow. The main differences between these and simple plume theories were the inclusion of bubble slip velocity and the effects of the bubbles on buoyancy and momentum.

Early Studies.

One of the earliest attempts to predict the performance of a bubble plume was made by Kobus (1968). Since his model was for an unstratified environment, Gaussian profiles were used. He included the ideas of the virtual source and the entrainment coefficient that had been introduced in simple plume models. However, Kobus noted that the distance between the virtual source and the actual source was negligible when compared to the overall depth of the source and therefore was not likely to affect the model's results. Using equations for the volume, momentum, and buoyancy fluxes in the plume, he derived equations to predict the volume flux for both linear and circular source air bubble plumes. After noting that the momentum flux at any point in the plume was the sum of the initial momentum flux and the buoyancy flux at that point, he found that the buoyancy term grew rapidly and that the momentum flux was soon negligible. He also found that the rate of spread of the velocity profile and the bubble rise velocity in the plume depended only on air supply rate and were independent of orifice size, shape, and spacing. The centerline plume velocity depended only on depth of the source and rate of air supply. The rate of velocity profile spread was found to vary with air supply rate to the 0.15 power and the centerline velocity was found to be proportional to the air supply rate to the 1/4 power for a single orifice and to the 1/3 power for a linear source (row of orifices).

While Kobus did not directly mention bubble slip velocity, he did comment that the bubbles would reach a constant velocity soon after leaving the source. This velocity was found to be proportional to the air flowrate to the 0.15 power. Although Kobus noted that bubbles should

expand as pressure decreases when they rise, he considered this effect to be negligible and did not account for it in his model. His velocity predictions were found to be fairly accurate based on laboratory studies.

Bulson (1968) examined the feasibility of using linear bubble plumes as breakwaters and was therefore primarily concerned with the surface current produced. In his examination, he found that horizontal velocity varied with air supply rate to the 1/3 power. He obtained the equation

$$v_m^3 = kgQ$$

where:

v_m = horizontal surface current velocity (feet per second (ft/s))

k = constant

g = acceleration due to gravity

Q = quantity of air per second per foot of pipe.

The value for $k^{1/3}$ was found to be 1.46, and the centerline vertical plume velocity was $0.75v_m$ for the conditions Bulson examined. Since the vertical velocity was proportional to the horizontal velocity, vertical velocity also varied with air supply rate to the 1/3 power, as had been reported by Kobus (1968).

Cederwall and Ditmars (1970) developed a model that was very similar to that of Kobus (1968) with one important feature added. They introduced the concept of bubble slip velocity: a constant that described the difference between the total bubble velocity and the plume water velocity. In addition to conservation of mass, momentum, and buoyancy, they included the entrainment coefficient and the turbulent Schmidt number in their calculations. They studied both point and line sources in both stratified and non-stratified water. The entrainment coefficient, α ,

was found to be a function of the gas input rate. However, they quoted a previous source as stating that $\alpha = 0.16$ was a good approximation for a buoyant line source and provided the equation used by many other investigators when α is assumed to be constant:

$$\frac{dQ}{dx} = 2\pi b \alpha u_m$$

where: Q = volume flux,

x = vertical coordinate,

$\frac{dQ}{dx}$ = rate of entrainment (as the only change in volume flux comes from the

entrainment of surrounding water),

b = plume radius,

α = entrainment coefficient, and

u_m = centerline plume velocity.

Hussain and Narang (1977) modeled a two dimensional air bubble plume as a two phase jet. Entrainment was calculated as a function of the square root of the momentum flux, the jet velocity relative to its surroundings, and “the interfacial area between the jet and the surrounding region” (Hussain and Narang, 1977). However, comparisons of the predicted volume flux and jet half width with measured data revealed some disagreement, and these discrepancies were attributed to “uncertainty in specifying accurately the value of [the entrainment coefficient]” (Hussain and Narang, 1977). They concluded that more work should be done to better determine the value of the entrainment coefficient.

Wilkinson (1979) also studied two-dimensional bubble plumes. He noted that theories developed by Kobus (1968), Cederwall and Ditmars (1970) (described previously), and Speece and Rayyan (1973) (described in a following section) predicted data from laboratory scale experiments well but were inaccurate when used to predict full scale data with high air flowrates, such as that collected by Bulson (1968). Wilkinson proposed that plumes could be characterized by a Weber number which was the ratio of surface tension forces to buoyant forces in the zone of flow establishment. The equation for the Weber number is

$$W = \frac{\rho\beta_0^{4/3}}{\sigma g}$$

where: W = Weber number,

ρ = ambient fluid density,

β_0 = initial vertical buoyancy flux,

σ = surface tension at the air water interface, and

g = acceleration due to gravity.

Wilkinson hypothesized that plumes with low Weber numbers were similar to simple plumes and therefore could be described by the previously mentioned bubble plume theories while those with high Weber numbers could not.

Wilkinson defined a characteristic width and compared it to elevation above the virtual source for previous studies. The relationship was found to be linear for plumes with low Weber numbers; for the Bulson data which had a high Weber number, the characteristic width was constant and therefore independent of elevation. Nondimensional velocity and buoyancy parameters were defined as well. The velocity parameter was found to be constant in plumes with low Weber numbers but dependent on elevation for Bulson's data. In addition, a Gaussian profile

was found to fit the laboratory scale data well but did not fit Bulson's data. Evaluation of the buoyancy flux parameters indicated that full scale bubble plumes produce a weaker vertical current than the plumes with low Weber numbers. Another difference was found in the entrainment coefficient, which was found to be about twice as large for plumes with small Weber numbers. For plumes with high Weber numbers, the entrainment coefficient was found to decrease as the plume rose.

It therefore appears that a significant difference exists between laboratory scale plumes and full scale plumes with high gas flowrates, although the reason for the difference is not clear. Wilkinson proposed some explanations, but these were later shown by Tsang (1984) to be incorrect. Tsang also called into question the validity of using the Weber number to distinguish between strong and weak plumes. Regardless of the reason, however, it is important that the difference between small scale and large scale plumes is noted.

Milgram (1983) completed a thorough study of circular bubble plumes in unstratified environments. The basis for the model was four integral equations: gas volume flux, liquid volume flux, momentum flux, and buoyancy per unit height. All four equations depended on the local mean gas fraction and the three flux equations were functions of the local mean vertical velocity. The starting point for integrations was the bottom of the zone of established flow, as only this zone was modeled. The depth of the bottom of this zone was determined either by a method described by Chen and Rodi (1980, cited in Milgram, 1983) for simple plumes or by five outlet diameters, whichever was greater.

Milgram redefined λ , the spreading coefficient, for bubble plumes as the "ratio of 'gas-containing radius' to 'plume radius'" (Milgram, 1983) which has become the accepted definition of λ for bubble plumes. Milgram surveyed existing data and concluded that a constant λ value of 0.8

was sufficient for his model. He also noted that changing λ by 0.1 had only a very small effect on the results of his study, leading him to decide that the use of this approximate value was acceptable. The bubble slip velocity was also estimated using previous studies. Although his study found a range of bubble sizes which resulted in a range of bubble velocities, Milgram determined that a constant value of 0.35 meters per second (m/s) was sufficiently accurate for his theory. Again, changing the bubble slip velocity did not significantly alter the model's results. Milgram introduced a term that he called the momentum amplification factor, γ , which he defined as the ratio of total momentum flux to momentum flux of the mean flow and was therefore a measure of turbulent momentum flux. He used existing data to determine that the entrainment coefficient was not constant.

A main objective of Milgram's study was the development of semi-empirical equations for values of γ and α . The entrainment coefficient was determined to be a function of the bubble Froude number and two constants that he determined experimentally. The bubble Froude number, F_B , was defined as follows:

$$F_B = \Delta^{2/5} \times \left(\frac{L_M}{L_D} \right)$$

where: Δ = centerline gas fraction,

L_M = distance of turbulent bubble mixing motion, and

L_D = characteristic distance between bubbles.

Additional equations were provided for Δ , L_M , and L_D , but are not pertinent here. The momentum amplification factor was a function of the plume velocity squared, Δ , and several constants.

Milgram made a number of interesting discoveries during his full scale bubble plume study. The first was that the plume "wandered," meaning that previous studies that calculated

velocities based on time averages (Kobus, for example) reported greater plume width and smaller centerline velocities than actually occurred. Second, his model predicted a rapid increase in velocity immediately above the gas outlet, followed by a fairly rapid decrease which eventually became a gradual decrease. However, the deepest point at which velocity was measured in the field was above the region of rapid increase so this was not verified by the data. He found that his estimated value for λ of 0.8 was accurate except for very small or very low velocity plumes. However, for plumes in which the velocity was very large relative to the bubble slip velocity (likely true for depths greater than 10 to 20 meters (m) (Fannelop *et al.*, 1991)), λ approached 1.0. In regards to α , laboratory scale studies were found to have smaller than predicted entrainment coefficients. Milgram hypothesized that α might be constant for bubble Froude numbers exceeding 50, meaning that the characteristic distance between bubbles is small relative to the other terms in the equation.

Later Studies.

Laureshen and Rowe (1987) developed a model for a two-dimensional bubble plume based on a model by Rowe and Poon (1985, cited in Laureshen and Rowe, 1987) for a circular plume. They noted that the vertical volume flux of water in a two phase plume is less than in a simple plume because of the bubble slip that occurs. In addition, the bubbles in bubble plumes expand as they rise due to decreasing pressure, which results in an increasing buoyancy flux as the plume rises. Equations for the conservation of the gas phase and the liquid phase as well as an equation for the conservation of momentum were the basis for the model. A fully turbulent flow was assumed, and “the effects of surface tension, density and pressure fluctuations and interfacial mass transfer” were ignored. The bubble slip velocity was assumed to be a constant 0.25 m/s. Bubbles

were assumed to be small and spherical; the model was not developed for plumes with large or cap-shaped bubbles. Three factors, the entrainment coefficient α , the spreading coefficient λ , and the momentum amplification factor γ , (after Milgram, 1983), were assumed to be functions of the plume Weber numbers and empirical constants.

The model was tested using data from Kobus (1968) (weak plumes) and Bulson (1968) (strong plumes) and it was confirmed that the three factors were functions of the Weber number. While the equation for the Weber number was not the same for linear plumes as for round plumes, the equations and constants developed previously by Rowe and Poon (1985, cited in Lareshen and Rowe, 1987) predicted α , λ , and γ for two dimensional plumes reasonably well. Lareshen and Rowe believed that these factors along with the equations developed would accurately predict the average plume flow properties. By incorporating the Weber number into their calculations, it is likely that they eliminated the problem described previously by Wilkinson (1979).

Leitch and Baines (1989) further investigated bubble plumes in unstratified surroundings by focusing on weak bubble plumes. Unlike the rest of the plume models presented in this paper, the work by Leitch and Baines was largely experimental. They presented a method for measuring plume volume flux and used their method to demonstrate some characteristics of bubble plumes.

The results of the study indicated that for weak plumes in an unstratified environment, the liquid volume flux and the total momentum increase linearly with height above a virtual origin. Liquid volume flux was also determined to vary with the square root of the air flowrate according to the equation

$$Q_L = 5.0Q_B^{1/2}(z - z_0)$$

where: Q_L = liquid flowrate,

Q_B = gas flowrate,

z = elevation above the source, and

z_0 = elevation of the virtual source

for the air flowrates and depths used in the study. The maximum vertical liquid velocity was a function of gas flowrate as well:

$$w_L = 11.3Q_B^{0.37}$$

where: w_L = maximum liquid velocity and

Q_B = gas flowrate.

Bubble slip velocity was also examined and found to be constant (above the initial zone of flow establishment) at approximately 0.23 m/s. The bubble spread was found to vary with gas flowrate; less spread occurred for lower flowrates, and for flowrates greater than 6 cm³/s,

$$b = 0.2z^{1/2}$$

where: b = lateral extent of bubbles (denoted λ by other investigators) and

z = height above source.

The entrainment coefficient was examined as well. While the entrainment coefficient was found to vary, Milgram's (1983) method of solving for α as a function of the bubble Froude number was found to be inaccurate for the weak plumes investigated. Instead, α was found to depend upon the inflow into the bubble wakes and the gas flowrate.

While this study provided insight into the mechanics of the bubble plume, the results and relationships obtained must be used with care. The experimental procedure investigated weak

plumes only, and, as Wilkinson (1979) demonstrated, weak plume results cannot necessarily be applied to stronger plumes.

Fannelop *et al.* (1991) originally intended to study linear bubble plumes in shallow (1 m) water to determine the magnitude of the vertical and horizontal (surface) currents produced (as opposed to Bulson (1968) who performed a similar study in deep water). They were interested in the size of the circulating cell produced by the plume. Gaussian profiles were assumed, α was estimated to be 0.08, and λ was estimated to be 0.85 from their studies of a two dimensional plume. The size of the cell was found to be dependent on gas flowrate.

Unfortunately, after performing their experiments, Fannelop *et al.* (1991) decided to focus on the cells produced by non-buoyant vertical jets in their discussion. However, they did contribute useful values for α and λ for linear bubble plumes. They also found that varying the bubble slip velocities over a range of 0.05 to 0.5 m/s had little effect on predicted plume width but had a fairly significant effect on the predicted plume velocity in deep water.

Bubble Plumes in Stratified Environments.

Several investigators expanded the work done concerning bubble plumes in unstratified environments to stratified environments. A major difference in these models is the use of a “top hat” distribution, which was found by Morton (1959) to describe plumes in stratified environments better than a Gaussian distribution. The vertical density differences in the water body have a significant effect on the height to which the plume will rise and therefore must be incorporated into these theories. In addition, even if the water in the plume reaches its neutral buoyancy depth and spreads out as described by Morton (1959), the air bubbles will continue rising to the surface unless they dissolve into the surrounding liquid. Since none of the models discussed in this section

consider gas transfer between the bubbles and the water, the bubbles in these theories all rise to the water surface. The rising bubbles entrain more fluid and additional plumes can be formed above the original plume.

While Cederwall and Ditmars (1970) focused on unstratified water bodies in their study, they did mention bubble plumes in stratified water. They considered a situation in which a liquid of one density at the bottom is covered by a second liquid of lower density and introduced the concept of “complete uncoupling” of the plume water and air bubbles. Complete uncoupling occurred when the plume water would not cross the density difference while the bubbles would continue to rise to the surface. The buoyancy and momentum flux equations from their model for unstratified water are altered slightly to account for the density difference. They noted that more work should be done to examine bubble plumes in stratified environments.

The first known work that focused on bubble plumes in stratified environments was done by McDougall (1978). He used the equations for conservation of mass, momentum, and buoyancy developed by Morton, Taylor, and Turner (1956, cited in McDougall, 1978) but also considered bubble expansion, bubble slip, and stratification. The entrainment coefficient and the bubble slip velocity were considered to be constant, and top hat buoyancy and velocity distributions were assumed. McDougall defined two new constants: M measured the “relative importance of the volume flux of gas at the source and the total water depth in the non-dimensional solutions” (McDougall, 1978), and C , which was called the stratification parameter, described the stability of the surrounding stratification relative to the source strength.

McDougall suggested that the liquid in bubble plumes would follow the same pattern as described by Morton (1959) for simple plumes; it would rise past its neutral buoyancy depth, then slow, stop, and fall back to that depth. The gas fraction of the bubble plume, however, would

continue rising to the top of the lake. This prompted McDougall to propose a double plume theory in which the inner plume contained the bubbles and the outer plume contained bubble-free liquid that could rise and spread out at various levels. The inner plume radius was seen experimentally to be about one-third the outer plume radius. The velocity of the outer plume was initially less than the velocity of the inner plume; the outer plume velocity slowed relative to the inner plume as the plume rose and eventually spread out at its level of neutral buoyancy. The double plume theory necessitated the use of two separate entrainment constants: one describing entrainment from the surrounding water to the outer plume and one for the entrainment of water from the outer plume to the inner plume. The actual values used for these two coefficients were not provided.

Schladow (1992) expanded upon the work done by McDougall (1978). He used a value for α of 0.083 and a bubble slip velocity of 0.3 m/s. He noted that both of these parameters probably varied with the flow conditions but that holding them constant should not have a significant effect on the model's prediction of the plume's features. He modified McDougall's equation for C and concluded that the new value for C along with McDougall's M value determined whether a given plume rose to the surface or spread out at one or more levels. Strongly stratified water bodies (which would have high C values) were more difficult to mix than less strongly stratified bodies.

Schladow (1993) presented the model from his 1992 paper and described the method by which he combined his plume model with the lake model DYRESM. He provided examples that demonstrated that this combined model could be used successfully to design lake mixing systems.

While Schladow's model seems to have been successful, his papers (1992, 1993) contain two potential flaws. First, he used Gaussian rather than top hat distributions in his model which have been shown to misrepresent the actual profiles in stratified water. Second, Schladow refers to

a previous study as stating that λ is 0.3, a value that compares to McDougall (1979) but seems low when compared to those obtained by other authors.

Asaeda and Imberger (1993) presented what is perhaps the most complex of the models for a bubble plume in a stratified environment. Their model included “an upward-moving bubble core, an inner plume consisting of a mixture of bubbles and relatively dense fluid, an annular downdraught, and beyond that a horizontal intrusion flow” (Asaeda and Imberger, 1993). They assumed a top hat distribution and constant values for the bubble slip velocity and for α , noting that previous studies showed that α could vary between 0.04 and 0.12. They used three different entrainment coefficients for the different regions of their plume but did not present the actual values used. Three new parameters were introduced to describe the plume’s behavior and these three parameters were used for design of lake destratification systems.

Their laboratory scale experiments showed that high gas flowrates resulted in one plume that reached the top of the tank while lower flowrates resulted in a vertical series of plumes. Very low gas flowrates resulted in an unsteady plume with irregular turbulent eddies, and the plumes wandered a great deal.

Gas Transfer in Bubble Plumes.

Only a few studies of bubble plumes have considered gas transfer between the bubbles and the surrounding liquid. If bubble plumes are to be used for lake aeration, gas transfer is one of the most significant components of the model. The five bubble plume models that account for gas transfer are discussed below.

Speece and Rayyan, 1973.

Speece and Rayyan (1973) were the first to incorporate gas transfer into a bubble plume model. Their purpose was to derive a model for hypolimnetic aeration and therefore they developed their model for an unstratified environment. Equations for the rate of water discharge, water momentum flux, air-water buoyancy flux and water kinetic energy flux were derived for both zero and non-zero bubble slip velocities. They assumed that the bubble spread was small compared to the plume expansion and used a value for λ of 0.2. They assumed, but did not attempt to verify in their full scale study, that both λ and α were constant. Increasing α from the 0.03 used in the model resulted in a decrease in predicted velocity, an increase in predicted plume width, and an increase in predicted water flowrate.

The data collected showed that the proposed model predicted the data well. Less than 13 percent error was found for the predictions of centerline velocities at various depths and flowrates. The plume diameter was as predicted for shallow water but was significantly smaller than predicted for deep water. Dye studies found that the hypolimnion did not mix with the upper layers of the lake as a result of the plume and it was assumed that complete uncoupling, as proposed by Cederwall and Ditmars (1970), occurred. Although Wilkinson (1979) found that the Speece and Rayyan theory was not accurate when used to predict the performance of full scale plumes with high flowrates, the theory seemed accurate for the flowrates examined in their study.

In addition to the theory presented, Speece and Rayyan provide an excellent, although now out dated, review of studies of bubble formation and bubble velocity.

Speece and Murfee, 1973.

Speece and Murfee (1973) presented a purely practical guide to designing hypolimnetic aeration systems. The first step involves choosing the height to which the plume should rise based on the depth of the hypolimnion. A graph is provided from which a bubble size is selected to correspond with the maximum height of plume rise desired. Air flow rate and diffuser type to provide the appropriate bubble size are then selected. Finally, the oxygen requirement is determined and the area of diffuser units required is calculated.

As mentioned, this approach is purely practical and does not consider the properties of bubble plumes. Some difficulties could result from the use of this method. For example, the bottom of the metalimnion is assumed to be 15 meters from the water surface. Difficulties may occur if this procedure is used to size aeration systems for lakes whose profiles do not conform to this depth. Another problem is that Speece and Murfee give no guidance concerning the selection of the air flowrate and diffuser type to obtain the desired bubble size, and bubble size is very difficult to predict.

Rayyan and Speece, 1977.

In 1977, Rayyan and Speece presented a model for hypolimnetic aeration in a stratified water body based on the Cederwall and Ditmars (1970) bubble plume model. They added terms to account for non-linear stratification and oxygen transfer. The basis for this model were equations for volume flux, oxygen flow, momentum flux, and buoyancy flux. An equation for the conservation of heat was also included. Predicted plume velocity and diameter agreed with data measured in the laboratory and in the field with an error of only 10 percent. Predicted maximum plume rise height and temperature distribution were also accurate. Oxygen transfer predictions

were not tested. Rayyan and Speece used Gaussian velocity and buoyancy profiles, but this probably did not make a difference as their predictions were concerned with the hypolimnion.

Rayyan and Speece found that their oxygen plume stopped when it reached the thermocline. Mixing occurred between the metalimnion and epilimnion, but the hypolimnion did not mix with the layers above it.

Tsang, 1990.

Tsang (1990) also developed a model for oxygenating bubble plumes. Tsang based his model on conservation of mass (water volume flux), conservation of energy, volumetric gas flux, bubble number (assumed constant), bubble radius, gas transfer across the bubble surface, and bubble expansion due to decreasing pressure. Because this model was for bubble plumes in unstratified surroundings, the expansion angle of the plume was assumed to be small and constant. While this is likely an accurate assumption for plumes in weakly stratified environments or for high gas flowrates, Asaeda and Imberger's (1983) work showed that this is probably not true when the environment is strongly stratified or when the plume is weak. Therefore, Tsang's model, which appeared very thorough, could be used only for hypolimnetic aeration or for predicting plume performance in unstratified water bodies.

Wuest *et al.*, 1992.

The most recent bubble plume model for stratified water bodies that includes gas transfer was developed by Wuest *et al.* (1992). The basis for this model was eight differential flux equations. Water volume flux, momentum flux, temperature flux, dissolved solids flux, dissolved oxygen flux, dissolved nitrogen flux, gaseous oxygen flux, and gaseous nitrogen flux were all

considered. The change in momentum as the plume rose was considered equal to the buoyant force at that height. The entrainment coefficient was assumed to be a constant 0.11; the spreading coefficient was assumed to be 0.8, and the bubble slip velocity was a function of bubble radius. Top hat profiles were assumed.

The eight differential equations were solved numerically along with a number of equations of state that varied with depth. The predicted height of maximum plume rise and the amount of oxygen transferred to the water were found to be most sensitive to initial bubble size (which had to be estimated) and gas flowrate. The value assumed for α had a significant effect on the predicted height of maximum plume rise. Initial plume area and initial plume velocity were not found to have a significant effect on either of the two predictions.

A comparison was made between the predicted height of maximum plume rise as a function of initial bubble radius for the model with and without gas exchange. For bubbles less than 0.01 m in radius, the model without gas exchange greatly overpredicted the height of maximum plume rise. For example, for 0.001 m (1 mm) radius bubbles, the model without gas exchange predicted that the plume would rise approximately 20 meters higher than was predicted when gas exchange was considered. This was the result of bubble dissolution which would be more pronounced in smaller bubbles. Therefore, the inclusion of gas transfer is important to bubble plume models not only for oxygen supply predictions but also for the accurate determination of the height of maximum plume rise.

As this model was used as the basis for the linear model proposed in this thesis, the methods used by Wuest *et al.* in developing the model are discussed in greater detail in the Model Development portion of this paper.

Summary of Plume Theories.

A significant number of plume theories exist. Not all studies examined the same topics and those that did sometimes found opposing results. However, there are some issues about which most theories tend to agree. For example, while the entrainment coefficient, α , is probably not constant, reasonable predictions can be made when it is assumed to be constant. (See Table 1 for a summary of reported values for α .) The spreading coefficient, λ , is considered by most to be constant but there are two differing views as to its value. Some authors (Cederwall and Ditmars, 1970; Speece and Rayyan, 1977; McDougall, 1978; Schladow, 1992 and 1993) have found the value to be in the 0.2 to 0.3 range while others (Milgram, 1983; Fannelop *et al.*, 1991; Wuest *et al.*, 1992) have found that it is 0.8 or larger. Bubble slip velocity is known to vary with bubble size but estimates of a constant 0.2 to 0.3 m/s give reasonable results. For linear sources, vertical plume velocity appears to be a function of gas flowrate to the 1/3 power. Finally, the velocity and buoyancy profiles resemble a Gaussian distribution in unstratified water but are better described by a top hat distribution in stratified water.

Some issues concerning bubble plumes remain unresolved. Weak plumes seem to have different characteristics from strong plumes, but the reason for this difference is not clear. Therefore, it is still uncertain whether a single bubble plume theory can describe all bubble plumes. Most of the work done has focused on circular plumes and unstratified environments. Better data concerning the entrainment and spreading coefficients for linear plumes in stratified surroundings are needed.

Table 1. Summary of α Values in Plume Theories.

Investigator	α (Axisymmetric Plumes)	α (Two Dimensional Plumes)
Morton (1959)	0.082 (unstratified) 0.116 (stratified)	
Cederwall and Ditmars (1970)		0.16
Fannelop <i>et al.</i> (1991)		0.08
Schladow (1992, 1993)	0.083	
Asaeda and Imberger (1993)	0.04-0.12	
Speece and Rayyan (1973)	0.03	
Wuest <i>et al.</i> (1992)	0.11	

III. MODEL DEVELOPMENT

Wuest *et al.*'s Circular Bubble Plume Model (1992).

As mentioned in the previous section, Wuest *et al.* (1992) developed a model for a bubble plume generated by a circular source in a stratified water body. Since the model developed in this paper is based on the model presented by Wuest *et al.*, their model will be explained in more detail here.

Wuest *et al.* Model Equations.

The core of the circular plume model is a set of eight differential equations for the volume, momentum, temperature, salinity, dissolved oxygen, dissolved nitrogen, gaseous oxygen, and gaseous nitrogen fluxes. (See Table 2.) (Definitions of the eight flux variables are provided in Table 3.) The volume flux is the change in the plume volume with height and is equal to the water entrained into the plume. The Boussinesq assumption allows the contribution of the gas volume to be neglected. The momentum flux equation, which again invokes the Boussinesq assumption, is based on the buoyant flux in the inner, bubble containing portion of the plume and the outer, bubble-free portion of the plume. The change in temperature with height (neglecting the gas heat content) is a result of the entrainment of ambient water, and therefore depends on the water volume flux and the ambient water temperature. Similarly, the total dissolved solids flux results from the volume flux and ambient salinity. The dissolved oxygen and dissolved nitrogen fluxes are functions of both the entrainment of ambient water and the diffusion of the gases through the bubble surfaces into the surrounding water. The gaseous oxygen and nitrogen fluxes result from diffusion of the gases either into or out of the bubbles based on the mass transfer coefficient, the

Table 2. Eight Flux Equations Used by Wuest *et al.* (1992) for the Circular Plume Model.

Flux	Equation
Water Volume Flux	$\frac{d\mu}{dz} = 2\alpha(\pi\mu M)^{1/2}$
Momentum Flux	$\frac{dM}{dz} = \frac{\rho_a - \rho_p}{\rho_p} g \lambda^2 \frac{\mu^2}{M} + \frac{\rho_a - \rho_w}{\rho_p} g \frac{\mu^2}{M} (1 - \lambda^2)$
Temperature Flux	$\frac{dF_T}{dz} = 2\alpha(\pi M)^{1/2} T_a$
Salinity Flux	$\frac{dF_S}{dz} = 2\alpha(\pi M)^{1/2} \rho_a S_a$
Dissolved Oxygen Flux	$\frac{dD_O}{dz} = 2\alpha(\pi M)^{1/2} c_{O_a} + \frac{4\pi r^2 N}{\frac{M}{\mu} + w_b} \beta_O (K_O p_O - \frac{D_O}{\mu})$
Dissolved Nitrogen Flux	$\frac{dD_N}{dz} = 2\alpha(\pi M)^{1/2} c_{N_a} + \frac{4\pi r^2 N}{\frac{M}{\mu} + w_b} \beta_N (K_N p_N - \frac{D_N}{\mu})$
Gaseous Oxygen Flux	$\frac{dG_O}{dz} = -\frac{4\pi r^2 N}{\frac{M}{\mu} + w_b} \beta_O (K_O p_O - \frac{D_O}{\mu})$
Gaseous Nitrogen Flux	$\frac{dG_N}{dz} = -\frac{4\pi r^2 N}{\frac{M}{\mu} + w_b} \beta_N (K_N p_N - \frac{D_N}{\mu})$

Table 3. Definitions of the Eight Flux Variables (from Wuest *et al.*, 1992).

Variable	Equation	Units
Plume Water Volume Flux	$\mu = \pi b^2 w$	m ³ /s
Momentum Flux	$M = \pi b^2 w^2$	m ⁴ /s ²
Temperature Flux	$F_T = \mu T$	°Cm ³ /s
Dissolved Solids Flux	$F_S = \mu S \rho_w$	kg/s
Dissolved O ₂ and N ₂ Fluxes	$D_i = \mu c_i$ (i = O, N)	mol/s
Gaseous O ₂ and N ₂ Fluxes	$G_i = \pi b^2 \lambda^2 (w + w_b) m_i$ (i = O, N)	mol/s

saturation concentration of the gas, the concentration of the gas in the surrounding water, and the total number of bubbles per unit height.

The eight flux equations required that a number of other factors be calculated. These factors include the ambient profiles for temperature, dissolved solids, dissolved oxygen, and dissolved nitrogen; the initial plume velocity at the source (which can be calculated from an additional equation if the Froude number is assumed to be a constant 1.6); the initial plume radius; the air flowrate in the diffuser; and the number of bubbles produced (or the initial bubble radius). From these factors, the pressure, partial pressures of oxygen and nitrogen, ambient density, plume density, plume water density, gas volume in the plume, bubble radius, bubble slip velocity, oxygen and nitrogen gas transfer coefficients, and oxygen and nitrogen solubility (based on Henry's law) constants at any depth could be obtained. The equations used in the calculation of these factors are shown in Table 4. The entrainment coefficient, α , is 0.11 and the spreading coefficient, λ , is 0.8.

Wuest *et al.* Model Assumptions.

In order to make the task of modeling the bubble plume manageable, it was necessary for Wuest *et al.* to make a number of assumptions. First, they made the Boussinesq assumption which had been used in all previously known plume models. This assumption states that the difference in density in the plume and ambient water is negligible in the mass terms. The gas mass density was neglected. Second, a "top hat" distribution, rather than a Gaussian distribution, was assumed for all components of the model. Horizontally, the extent of the temperature and the dissolved solids, oxygen, and nitrogen was assumed to equal the plume radius, while the radius of the inner core of the plume containing the bubbles was only a fraction of the total radius, represented by the plume

Table 4. Equations of State and Parameter Approximations Used by Wuest *et al.* (1992) for the Circular Plume Model.

Parameter	Equation	Notes
Total Pressure	$p = p_s + 10^{-5} \rho_{ave} g(z_s - z)$	units: bar
Partial Pressures	$p_i = \left[\frac{m_i}{m_O + m_N} \right] p = \left[\frac{G_i}{G_O + G_N} \right] p$	I = species (oxygen or nitrogen) units: bar
Ambient and Plume Water Densities	$p_j = 999.868 + 10^{-3} \times [65.185T_j - 8.4878T_j^2 + 0.05607T_j^3] + f_s S_j$	j = species (ambient or plume) $f_s = 0.802 \text{ kg} \cdot \text{m}^{-3} (\text{‰})^{-1}$ or $= 0.705 \times 10^{-3} \text{ kg} \cdot \text{m}^{-3} (\mu\text{S}/\text{cm})^{-1}$
Density of Bubble-Water Plume Mixture	$\rho_p = (1 - V_g) \rho_w$	units: kg/m^3
Gas Volume - Ideal Gas Law	$V_g = \frac{(m_O + m_N)}{p} RT_K$	T_K = Temperature in Kelvin dimensionless
Gas Volume - Van der Waals Gas Law (Implicit)	$\left[\frac{V_g}{m_O + m_N} - 32 \times 10^{-6} \right] \times [p + 1.4 \times 10^{-6} \times \frac{(m_O + m_N)^2}{V_g^2}] = RT_K$	dimensionless
Bubble Radius	$r = \sqrt[3]{\frac{3V_g \lambda^2 b^2 (w + w_b)}{4N}}$	N = number of bubbles units: m
Initial Plume Velocity	$w_0 = Fr \times \sqrt{2\lambda b g \frac{\rho_a - \rho_p}{\rho_p}}$	Fr = Froude Number (assumed to be 1.6) units: m/s
Bubble Slip Velocity	$w_b = 4474r^{1.375}$ $w_b = 0.23$ $w_b = 4.202r^{0.547}$	$r < 6.67 \times 10^{-4}$ $7.0 \times 10^{-4} < r$ and $r < 5.1 \times 10^{-3}$ $r > 5.1 \times 10^{-3}$ r units: meters w_b units: m/s
Oxygen and Nitrogen Gas Transfer Coefficient	$\beta = 0.6r$ $\beta = 4 \times 10^{-4}$	$r < 6.67 \times 10^{-4}$ $r > 6.67 \times 10^{-4}$ β units: m/s
Molecular Oxygen Solubility Constant	$K_O = 2.125 - 0.05021T + 5.77 \times 10^{-4} T^2$	units: $\text{mol m}^3/\text{bar}$
Molecular Nitrogen Solubility Constant	$K_N = 1.042 - 0.0245T + 3.171 \times 10^{-4} T^2$	units: $\text{mol m}^3/\text{bar}$

radius multiplied by λ . The plume was assumed to be fully turbulent and the surrounding water was assumed to have no currents. Although the plume is turbulent, the turbulent transport of temperature, momentum, dissolved solids, and dissolved gases was considered negligible as compared to the advective transport of these substances. Next, it was assumed that bubbles were produced at a constant rate and were distributed equally over the area of the circular source. The number of bubbles was assumed to remain constant, and all bubbles at a given height were assumed to be spherical and of uniform size. Gas exchange between the bubbles and surrounding plume water for all gases except for oxygen and nitrogen was neglected. Finally, the initial properties of the plume, including temperature, dissolved oxygen, dissolved nitrogen, and dissolved solids, were assumed to be the same as in the ambient water in the lake at the same depth.

Wuest *et al.* Solution Procedure.

The first step in solving the model was to determine the initial conditions. Because the plume water was assumed to have the characteristics of the lake water initially, the temperature, dissolved solids, dissolved oxygen, and dissolved nitrogen profiles were used to determine the respective initial values. The equations for the initial values for the eight flux variables are the definitions of the variables shown in Table 3. The equation for the initial plume velocity was shown in Table 4.

Wuest *et al.* implemented their model for two different seasons. Data was gathered and the model was run in both July and November. The initial conditions varied based on the month in question. A summary of the initial conditions used is provided in Table 5. The ambient profiles used are shown in Appendix A.

Table 5. Input Values for July and November (Wuest *et al.*, 1992).

Month	July	November
Diffuser Depth (m)	65	65
Initial Plume Size (m²)	20 (b ₀ ≈2.5m)	20 (b ₀ ≈2.5m)
Gas Input Rate (Nm³/s)¹	0.0062, oxygen	0.014, air
Initial Plume Velocity (m/s)	0.125	0.172
Initial Bubble Radius (m)	0.001	0.006

¹ m³/s, normalized to 1 bar and 0° C.

Wuest *et al.* solved their model using Euler's method. Euler's method was the first method devised to solve differential equations numerically. The method involves dividing a function into a discrete number of steps and approximating the value of the function at each step based on tangent lines. The slope of the line tangent to the function at the initial value, which must be known, is calculated. This slope is then used to estimate the function's value at the next step, and so on. The method becomes increasingly accurate as the step size becomes smaller (Boyce and DePrima, 1992). Wuest *et al.* chose their vertical increment so that the flux variables changed by less than 0.01 percent from one step to the next. Once the initial values were obtained, the first step up was taken, and the eight differential equations (Table 2) were solved. Then the supporting equations (Table 4) were solved based on the results of the eight differential equations. This procedure was repeated until either the plume velocity reached zero or the plume reached the lake surface.

Circular Model Program.

Circular Model Program Development.

The computer program used to solve the equations for the circular plume model was developed using Microsoft FORTRAN Powerstation. The steps taken to solve the equations were the same as those outlined in Wuest *et al.*'s solution procedure.

First, the program asks the user for the initial parameters, including the radius of the diffuser, the initial bubble radius, the air flowrate, and the temperature, dissolved solids, dissolved oxygen, and dissolved nitrogen profiles. The profiles are entered in the form of a fourth order polynomial equation (i.e., $ax^4+bx^3+cx^2+dx+e$). The program allows the user to determine the number of intervals into which to divide the depth of the lake for Euler's method. The initial conditions are then calculated as described previously using the equations in Table 3. Next the

program enters a large “do loop.” In this loop, a step up, the size of which is determined by the number of intervals chosen by the user, is taken and the incremental changes in the eight differential flux equations shown in Table 2 are calculated. The change in the flux variables is added to the value of the flux variable from the previous step to obtain the new value of the flux variables at each step. Next the Table 4 equations are calculated. The program then returns to the beginning of the do loop for another iteration. The results of the program are saved to a data file. The program stops when the plume’s momentum is less than zero, implying that the plume has reached its maximum height, when the plume velocity reaches zero, or when the plume reaches the lake surface. A copy of the program is provided in Appendix B.

All equations in the program were taken directly from Wuest *et al.*’s paper with two exceptions. In the paper, two equations were given for the volume of gas in the plume. Upon obtaining a copy of the authors’ program, which was written in Basic, it was discovered that Van der Waals gas law, the second equation in the paper, was used in the calculation of gas volume. However, it was determined that the volume of gas calculated using the ideal gas law resulted in only 0.04 percent error as compared to that predicted by Van der Waals law. This calculation was performed at the diffuser depth of 65 meters used by Wuest *et al.* and, because the pressure is highest at that point, should have resulted in the greatest amount of error, meaning that the error throughout the lake would be less than 0.04 percent as a result of using the ideal gas law. Even at 500 meters, the error was calculated to be only 5 percent. Finally, changing the calculation of the volume of gas in a version of Wuest *et al.*’s program that had been re-written in FORTRAN resulted in only very small differences in the predictions. Therefore, the ideal gas law was used in all gas volume calculations in the program. The second exception was in the calculation of the number of moles of nitrogen and oxygen entering the plume which was required for the calculations

of the dissolved and gaseous concentrations of both gases. There was no equation for this provided in the paper so the ideal gas law was used. It was later determined that the paper's authors also used the ideal gas law for this calculation in their own computer program.

Circular Model Validation.

After the program was completed, its accuracy was reviewed by comparing its results to those reported by Wuest *et al.* As a first step, each point on their temperature, salinity, dissolved oxygen, and dissolved nitrogen profiles from both July and November was recorded. The points were plotted using Microsoft Excel Version 5.0 and a curve was fitted to each profile. The equations for the curves were used as the profiles requested by the computer program and were listed in Appendix A. Values for air flowrate, initial velocity, diffuser radius, and initial bubble size were taken from the Wuest *et al.* paper. Rather than using the Froude number equation to determine the velocity in these comparisons, the initial velocity given by Wuest *et al.* was forced to be the initial velocity used by the program as using the Froude number equation resulted in slightly different velocities than those given in the paper. By patterning the data put into the FORTRAN program as closely as possible to that used in the Wuest *et al.* paper, it could be determined whether the program was working accurately. After comparisons between the model's predictions and the paper were completed, necessary alterations were made to create the final version of the circular model.

Circular Model Sensitivity Analysis.

Wuest *et al.* (1992) examined the sensitivity of the depth of maximum plume rise to initial bubble radius, air flowrate, initial plume area, initial Froude number (initial velocity), and the

entrainment factor. Therefore, a sensitivity analysis was performed on the circular plume model to determine its sensitivity to these same factors. Initial bubble radius was varied from 1.0×10^{-4} to 1.0×10^{-1} meters; oxygen input rate from 1.0×10^{-3} to 1.0×10^{-1} Nm³/s (m³/s normalized to standard conditions of 1 bar and 0°C); initial plume area from 3.14 to 50 m², initial Froude number from 1.0 to 2.0, and the entrainment factor from 0.05 to 0.20, which were the same intervals used by Wuest *et al.* except for the initial plume area, for which they reported a range of 0 to 50 m². In addition, the effects of the temperature, dissolved solids, oxygen, and nitrogen profiles on the velocity and height of maximum plume rise were examined. The temperature profile was increased by 5.0, 2.0, and 1.0 degrees and decreased by 1.0, 2.0, and 5.0 degrees. The effects of changing the slope of the temperature profile were explored as well. The salinity profile was altered by 0.01 and 0.02 percent in either direction, and the oxygen profile was varied by 0.2 and 0.1 mol/m³ in both directions. Since the nitrogen concentration was a constant 0.714 mol/m³ throughout the depth of the lake, the effect of changing the nitrogen concentration to 0.664 and 0.764 was determined.

Linear Plume Model.

Once the program for the circular plume was completed, the next step was to develop a model for an air bubble plume emitted from a linear source. This model was based directly on the circular plume model developed by Wuest *et al.* Because the plume is formed by a line source, the model will be called the linear model.

Linear Model Equations.

First, the eight differential flux equations and the initial conditions were modified from a circular to a rectangular geometry. This resulted in the differential flux equations shown in Table

6 and the initial conditions shown in Table 7. As before, the volume of gas was calculated using the ideal gas law. The supporting equations remained the same as in the circular model except for the bubble radius equation, which also had to be modified for a rectangular geometry. The revised bubble radius equation is as follows:

$$r = \sqrt[3]{\frac{3V_g \lambda b L (w + w_b)}{4\pi N}}$$

An approximation had to be made in the calculation of the initial plume velocity. While the circular model used the Table 4 initial plume velocity equation with the Froude number equal to 1.6 to find the initial velocity, a corresponding Froude number for a linear source could not be found in the literature. The equation used to calculate the initial velocity was altered from

$$Fr = \frac{w}{\sqrt{2\lambda b g \frac{\Delta p}{\rho}}}$$

for a circular source to

$$Fr = \frac{w}{\sqrt{gL \frac{\Delta p}{\rho}}}$$

for a linear source

where: Fr = Froude number,

w = vertical plume velocity,

ρ = density,

g = acceleration due to gravity,

λ = circular spreading coefficient,

b = circular plume radius, and

L = length of the linear plume.

The Froude number was assumed to be 1.6 near the linear source as well since no better approximation was available.

The entrainment coefficient, α , is 0.08 and the spreading coefficient, λ , is 0.85, as reported by Fannelop *et al.* (1991).

Linear Model Assumptions.

The linear model made the same assumptions as made by Wuest *et al.*'s circular model. Additional assumptions were necessary as well. The plume was assumed to be long, and, therefore, end effects were not considered. As such, the spreading coefficient was applied to the width only, and entrainment was considered to occur only along the sides of the plume. The plume was assumed to have an initial area of the length of the diffuser multiplied by the width of the diffuser. While some have found that the entrainment coefficient is not a constant, it was assumed to be constant for the purposes of this model since others have suggested that this is a good approximation and since Wuest *et al.* (1992) assumed it to be constant. Finally, since the circular entrainment coefficient was found to be proportional to the plume velocity and the circumference of the circle, the linear entrainment coefficient was assumed to be proportional to the plume velocity and the length of the two sides of the rectangle, as end effects were neglected.

Table 6. Eight Flux Equations for the Linear Plume Model (Modified from Wuest *et al.*, 1992).

Flux	Equation
Water Volume Flux	$\frac{d\mu}{dz} = 2\alpha Lw$
Momentum Flux	$\frac{dM}{dz} = \frac{\rho_a - \rho_p}{\rho_p} g\lambda Lb \frac{\mu^2}{M} + \frac{\rho_a - \rho_w}{\rho_p} gLb(1 - \lambda)$
Temperature Flux	$\frac{dF_T}{dz} = 2\alpha LwT_a$
Salinity Flux	$\frac{dF_S}{dz} = 2\alpha Lw\rho_a S_a$
Dissolved Oxygen Flux	$\frac{dD_O}{dz} = 2\alpha Lwc_{O_a} + \frac{4\pi r^2 N}{\frac{M}{\mu} + w_b} \beta_O (K_O p_O - \frac{D_O}{\mu})$
Dissolved Nitrogen Flux	$\frac{dD_N}{dz} = 2\alpha Lwc_{N_a} + \frac{4\pi r^2 N}{\frac{M}{\mu} + w_b} \beta_N (K_N p_N - \frac{D_N}{\mu})$
Gaseous Oxygen Flux	$\frac{dG_O}{dz} = -\frac{4\pi r^2 N}{\frac{M}{\mu} + w_b} \beta_O (K_O p_O - \frac{D_O}{\mu})$
Gaseous Nitrogen Flux	$\frac{dG_N}{dz} = -\frac{4\pi r^2 N}{\frac{M}{\mu} + w_b} \beta_N (K_N p_N - \frac{D_N}{\mu})$

Table 7. Definitions of the Eight Flux Variables for Linear Model (modified from Wuest *et al.*, 1992).

Variable	Equation	Units
Plume Water Volume Flux	$\mu = Lbw$	m ³ /s
Momentum Flux	$M = Lbw^2$	m ⁴ /s ²
Temperature Flux	$F_T = \mu T$	°Cm ³ /s
Dissolved Solids Flux	$F_S = \mu S \rho_w$	kg/s
Dissolved O ₂ and N ₂ Fluxes	$D_i = \mu c_i$ (i = O, N)	mol/s
Gaseous O ₂ and N ₂ Fluxes	$G_i = \lambda Lb(w + w_b)m_i$ (i = O, N)	mol/s

Linear Model Solution Procedure.

The steps taken in solving the linear model were the same as those taken in solving the circular model. Briefly, the initial conditions were calculated, a step up was taken, the new values for the flux variables were calculated, the supporting equations were calculated, and the process was repeated. The output was printed so that 100 steps (0.65 meters each) were saved to a data file each time the program was run.

Euler's method was used to numerically solve the eight differential equations, and the program was run under winter and summer conditions for a number of step sizes. For summer conditions, the results using 100,000 steps were compared to the results at the same depths using 200,000 steps. The largest difference incurred at any displayed depth as a result of increasing the number of steps to 200,000 was 0.05 percent. This error occurred in the momentum data; errors in the velocity, temperature, and density data were all below 0.05 percent. Therefore, 100,000 steps were considered sufficient to obtain reliable results for the summer data. For the winter data, 500,000 steps were required so that the maximum error created at any displayed depth by increasing the number of steps to 600,000 was 0.03 percent. Again, this maximum error occurred in the momentum data. To ensure that Euler's method accurately calculated the results, 500,000 steps were used in calculating all data based on Wuest *et al.*'s conditions for both the circular and linear plume models for both July and November conditions. As this corresponded to a step size of 0.00013 meters, the number of Euler's intervals for all other data sets was chosen so that the step size never exceeded this value. Each time the program was run under a different set of conditions, the results were tested to insure that adding additional steps resulted in an error of less than 0.05 percent at any given depth.

Linear Model Program Development.

Again, FORTRAN Powerstation was used as the programming language. The linear program was identical to the circular program with the exceptions noted above that the eight basic equations, the bubble radius equation, the number of bubbles equation, and the equation for the initial plume velocity were altered for the new geometry. (Appendix C presents the linear model FORTRAN program.)

Linear Model Validation.

The first step in determining whether the linear model was performing correctly was to compare its results to the circular model's results. The model was run as though the source was a 2.45m x 2.45m square, which had approximately the same area as the 2.5m radius circular source in the Wuest *et al.* paper which was used to test the circular model. After the number of steps necessary to prevent error from using Euler's method were determined, the linear model was run under both July and November conditions with initial conditions identical to those presented in the Wuest *et al.* paper.

The assumption that end entrainment could be neglected was tested as well. The linear model was run both with and without entrainment at the ends and both sets of results were compared to the circular model's results.

After the linear model was compared to the circular model, it was run for full scale conditions in a linear configuration to determine whether its predictions seemed reasonable. Temperature, salinity, dissolved oxygen, and dissolved nitrogen profiles as well as initial conditions from both seasons in Wuest *et al.*'s (1992) study were again used. The model was run for a

diffuser similar to that designed and used by Mobley and Brock (1996), and the results were recorded.

Since the model in this case was run for the configuration for which it was designed, the effects of end entrainment were again examined. The model was run twice for each season, once with and once without end entrainment. In this way, the effect of neglecting end entrainment on the linear model could be determined.

The linear model was then compared to data collected by Provost (1973), Wen (1974), and TVA (1994). The model's predictions of plume velocity were compared to Provost's study and the oxygen transfer predictions to Wen's work. Predicted oxygen concentrations and plume temperatures were compared to the data collected by TVA. Brief descriptions of these works follow.

Provost (1973). In 1973, Richard Provost completed a Master's thesis entitled *Circulation and Flows in Water Tanks Induced by the Release of Air from a Manifold*. The purpose of the thesis was to study "currents and circulation patterns induced by the release of air from a manifold placed below water." A number of vertical and horizontal (surface) velocity measurements were made using a Pitot tube and the relationship that

$$v = 12.19\sqrt{\Delta P(\text{psi})}$$

where: v = velocity (ft/s)

ΔP = pressure difference between static and stagnation pressures

(Perry *et al.*, 1963, quoted in Provost, 1973).

The high reproducibility of Provost's velocity measurements indicated that the measurements were reliable.

The model was run for the conditions given in the thesis. Unfortunately, Provost did not provide all the values required to run the model requiring that some estimations be made. Oxygen concentration, nitrogen concentration, and dissolved solids concentrations were not available. Oxygen concentration in the ambient water was assumed to be 0.29 mol/m³ which is the saturation value at 20^o C (Sincero and Sincero, 1996) and nitrogen concentration was assumed to be 0.71 mol/m³ which is the saturation value at 20^o C (Lide, 1995). The total dissolved solids concentration was estimated to be 0.20 mg/g, which seemed to be a reasonable value based on an examination of several sources. Since the best method for estimating the total dissolved solids concentration was unclear, the salinity was varied between 0.0 and 0.40 mg/g to determine the effect on plume velocity. Bubble size had to be estimated, as well. Estimates of bubble size were calculated using an equation derived by Bischof *et al.* (1994) for bubble formation from a submerged diffuser in 20^o C water:

$$D = 3.236 \times \sqrt[3]{D_o}$$

where: D = bubble diameter (mm) and

D_o = orifice diameter (mm).

After it was determined that the model overpredicted the velocities given by Provost (1973), the method for determining the initial velocity was examined. The possibility of using Bulson's (1969) relationship that velocity is proportional to the air flowrate raised to the 1/3 power according to the equations

$$v_m^3 = kgQ,$$

$$\sqrt[3]{k} = 1.46, \text{ and}$$

$$w = 0.75v_m,$$

where: v_m = horizontal surface current velocity,

g = acceleration due to gravity,

Q = quantity of air per second per foot of pipe, and

w = vertical plume velocity

to calculate initial velocity was examined. However, since these constants were reported by Bulson for only one set of conditions (measured in the ocean at approximately 30m depth), they were used with caution in predicting the results of this laboratory scale experiment. Both the initial velocities derived from the model and the initial velocities using Bulson's relationships were compared to Provost's data to determine which method more accurately predicted the data.

All other parameters, including water temperature, water depth, length and width of diffuser, and air flowrate were provided. The values used to run the model are provided in Table 8.

Wen (1974). Chung Wen performed a study to expand upon the work performed by Provost. While he focused on surface velocities produced by plumes, he also examined the effect of the plume on the oxygen concentration in a tank of water from which all of the oxygen had been removed. The oxygen was removed using anhydrous sodium sulfite and the catalyst cobalt chloride. Dissolved oxygen concentrations were measured using a Chemtrix Type 30 Dissolved Oxygen Meter which, according to the manufacturer, was accurate to ± 0.2 ppm. Wen demonstrated that his dissolved oxygen measurements were extremely reproducible.

Again, not all numbers required by the linear program were provided in the thesis. The dissolved nitrogen concentration was assumed to be 0.95 mol/m^3 which is the saturation value at the water temperature reported by Wen (4.44°C) (Lide, 1995). The dissolved solids concentration was assumed to be 0.20 mg/g as in Provost's (1973) study and was varied holding one gas

Table 8. Values from Provost (1973) Used to Test Linear Model Velocity Predictions.

Parameter	Test 1 (Variable Gas Flowrate)	Test 2 (Variable Water Depth)
Length of Diffuser (m)	0.31	0.31
Width of Diffuser (m)	0.02	0.02
Initial Bubble Radius (m) (calculated)	0.0019	0.0019
Water Temperature (C)	20	20
Dissolved Solids Concentration (g/1000g) (assumed)	0.20	0.20
Dissolved Oxygen Concentration (mol/m³) (assumed)	0.29	0.29
Dissolved Nitrogen Concentration (mol/m³) (assumed)	0.71	0.71
Gas Input Rate (Nm³/s)	0.00052 0.0010 0.0015	0.0013
Water Depth (m)	0.25	0.20 0.30 0.40 0.60

flowrate constant to determine whether it affected the oxygen concentration calculations. Initial plume velocity was calculated using the Froude number equation and initial bubble radius was calculated using Bischof *et al.*'s (1994) equation. The temperature, dissolved oxygen concentration (zero initially), and all required dimensions were included in the thesis. The linear model was run using these conditions which are shown in Table 9.

TVA (1994). A limited amount of data was available for the Blue Ridge Reservoir in Tennessee into which a TVA diffused oxygen system had been installed. On the day on which the data was collected, one 549m line diffuser supplied 0.0510 Nm³/s of oxygen to the reservoir. Temperature and dissolved oxygen data were collected at three depths: 23.5, 30.0, and 35.0 meters from the surface. These values for the area of the reservoir outside the influence of the plume were used as the ambient profiles. The dissolved nitrogen concentration was assumed to be at saturation and the dissolved solids concentration was assumed to be a constant 0.39 g/1000g, a typical value based on Wuest *et al.* (1992), for lack of any better information. The total depth of the reservoir was assumed to be 40m when the model was run. (For a summary of input values, see Table 10.) The temperature and dissolved oxygen concentrations predicted by the model were compared to the data collected to determine how well the model predicted full scale values.

Linear Model Sensitivity Analysis.

A sensitivity analysis identical to that performed on the circular model was performed on the linear model. The same variables, including initial bubble radius, oxygen input rate, initial plume area, initial Froude number, entrainment coefficient, nitrogen concentration, and temperature, dissolved solids, and dissolved oxygen profiles were altered. The variables were

altered by the same amounts as described in the circular model section except for initial plume area, which was altered over a range of 0.25 to 50 m². The conditions under which the linear model was run for the sensitivity analysis were the same as those used to determine the predictions the model would make in full scale conditions, described in a preceding section.

Table 9. Values from Wen (1974) Used to Test Linear Model Oxygen Transfer Predictions.

Parameter	Value
Length of Diffuser (m)	0.31
Width of Diffuser (m)	0.02
Initial Bubble Radius (m) (calculated)	0.0019
Water Temperature (C)	4.44
Dissolved Solids Concentration (g/1000g) (assumed)	0.20
Dissolved Oxygen Concentration (mol/m³)	0.0
Dissolved Nitrogen Concentration (mol/m³) (assumed)	0.95
Gas Input Rates (Nm³/s)	0.0019 0.0017 0.00078 0.00039 0.00021
Water Depth (m)	0.25
Water Volume (m³)	0.46

Table 10. Profiles Used to Test Linear Model Predictions of TVA Data.

Parameter	10 Meters Above Diffuser	16.5 Meters Above Diffuser	40 Meters Above Diffuser (Lake Surface)
Temperature (C)	18.40	19.05	19.75
Dissolved Solids (g/1000g)	0.39	0.39	0.39
Dissolved Oxygen (mol/m³)	0.123	0.125	0.131
Dissolved Nitrogen (mol/m³)	0.725	0.717	0.709

IV. RESULTS AND DISCUSSION

Circular Plume Model vs. Wuest *et al.* Model.

The circular plume model was implemented under the conditions provided in the Wuest *et al.* (1992) paper which were shown in Table 5. Since the Wuest *et al.* conditions were used in this test the circular plume model, a comparison of the circular model's results with the results provided in the Wuest *et al.* paper could determine whether the circular model correctly solved and implemented the paper's equations for a circular plume.

A comparison of the circular model's results with the results obtained by Wuest *et al.* showed significant differences for both July and November conditions. While the bubble radii and plume temperatures from both the July and November conditions were a fairly good match to the data presented in the Wuest *et al.* paper, the plume velocities, water volume fluxes, plume densities, and ambient densities were very different. The velocities predicted by the circular plume model were higher than those in Wuest *et al.*'s model. The July plume rose higher in the circular plume model which was consistent with the higher velocities. Unlike in the Wuest *et al.* model, the circular model velocities showed an initial increase before they decreased. The initial increase was consistent with the model proposed by Milgram (1983) and the experimental results of Provost (1973) but was not shown in the paper by Wuest *et al.* (1992).

Volume flux values were slightly higher in the circular plume model at any given height. The change in the volume flux with height was greater in the circular model than in the Wuest *et al.* paper. Differences existed in the density predictions as well. Although the circular model's ambient and plume density data followed the same general trends as Wuest *et al.*'s density data,

the values predicted by the circular model were different. The difference in the density data, particularly in the ambient density data, warranted further investigation.

The plume velocity at a given height was calculated by dividing the momentum by the water volume flux at that height. Because the momentum flux is strongly dependent upon density (See Table 2.) the density difference could have caused the velocity difference. The volume flux depends on the plume velocity, so the density difference could have resulted in the difference in the circular plume model's predicted volume fluxes as well. Finally, the ambient density was calculated using a simple equation that was a function of the ambient temperature and dissolved solids concentration; therefore, there should be no significant difference between the ambient density calculated by the circular model compared to the Wuest *et al.* model.

Wuest *et al.* provided a copy of the program they used by to implement their model in a different lake than was described in their paper. An examination of the program revealed the equation used for the ambient and plume water density equations was not the same as that provided in the paper. However, substituting the Wuest *et al.* program equation into the circular model program still did not result in identical density profiles. Apparently, a third version of the density equation was used to calculate the ambient and plume water densities in the paper. As that equation was unavailable, the ambient density profile was manipulated until it matched the profile provided by Wuest *et al.* By running the model with this new equation for the ambient and plume water densities, it could be determined whether the difference in calculated density was the cause of the differences in predicted plume velocity and water volume flux. The new density equation was

$$\rho = (0.059385T^3 - 8.56272T^2 + 65.4891T) \times 10^{-3} + 999.84298 + 0.28 + 0.802\left(\frac{S}{1000}\right)$$

where: ρ = ambient or plume water density,

T = ambient or plume water temperature, and

S = ambient or plume water dissolved solids concentration.

The circular program was then run with the adjusted ambient density profiles to determine whether the altering the density equation eliminated the differences between the circular plume model and the Wuest *et al.* model. The results for the July and November conditions are shown in Figures 2 through 8.

The July ambient density predicted by the two models is nearly identical (Figure 7) which is to be expected since the density equation was manipulated to fit the Wuest *et al.* results. The plume density profile is very similar with some difference in the bottom portion of the plume. Very small differences exist in the July plume velocity and water volume flux data (Figures 2 and 3). These differences are so small that they are likely attributable to slight differences between the temperature, dissolved solids, dissolved oxygen, and dissolved nitrogen profiles used in the circular model compared to the actual data points used by Wuest *et al.* The height of maximum plume rise in July with the altered density equations is within 0.5 m of that predicted by Wuest *et al.*

The bubble radius predicted by the circular model in July is consistently larger at any given depth than that predicted in the paper except at the top of the plume (Figure 4). This is likely due to a mistake in the paper which was found by the authors after the paper was published

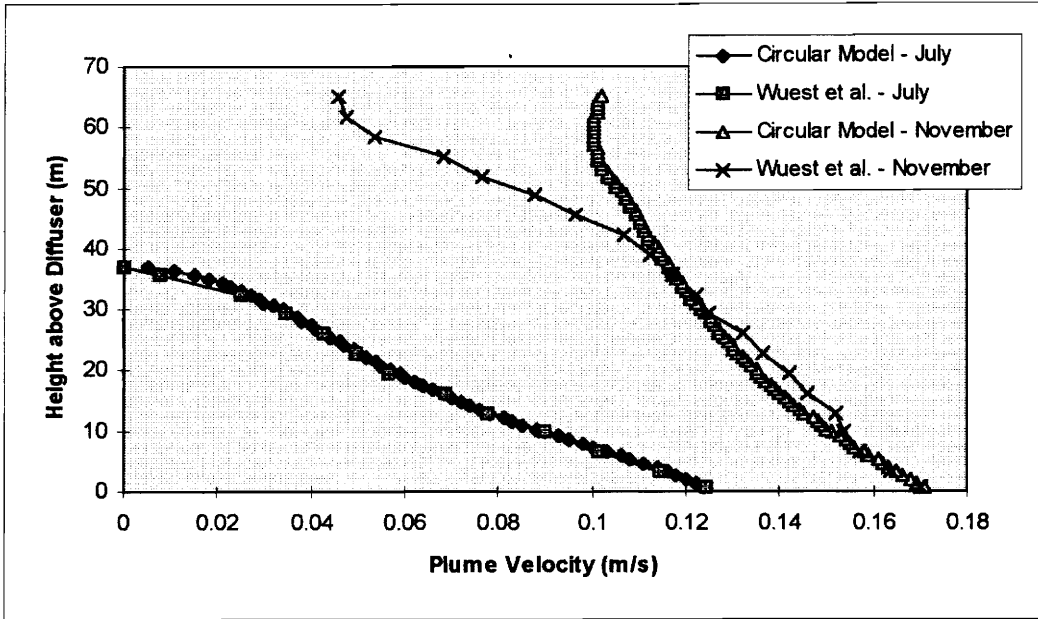


Figure 2. Comparison of Plume Velocities for Circular Model with Adjusted Ambient Density Profile with Wuest *et al.*'s Results for July and November.

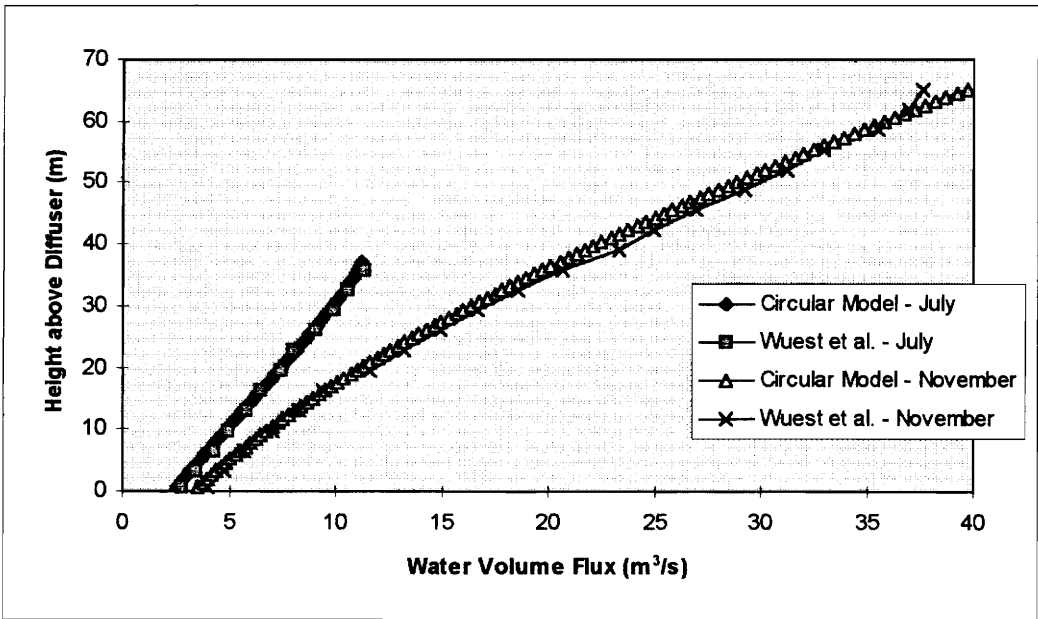


Figure 3. Comparison of Water Volume Fluxes for Circular Model with Adjusted Ambient Density Profile with Wuest *et al.*'s Results for July and November.

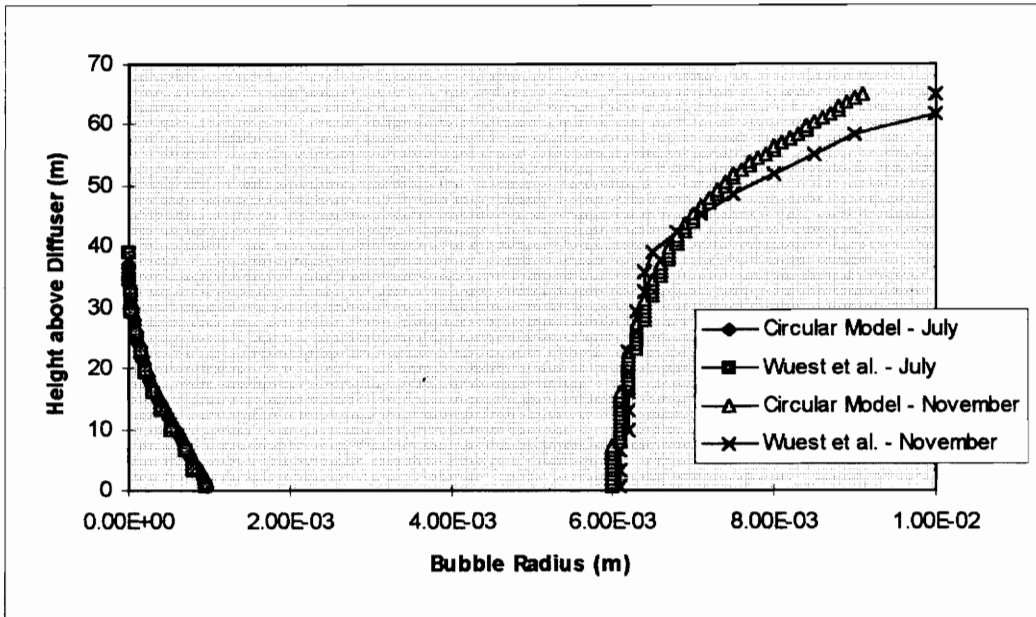


Figure 4. Comparison of Bubble Radii for Circular Model with Adjusted Ambient Density Profile with Wuest *et al.*'s Results for July and November.

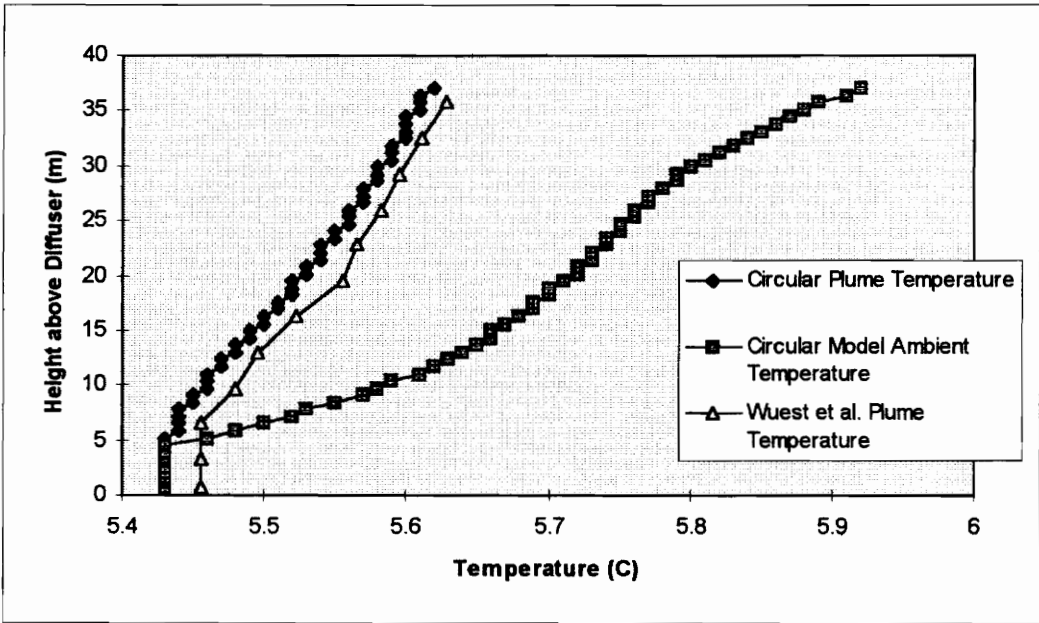


Figure 5. Comparison of Temperatures for Circular Model with Adjusted Ambient Density Profile with Wuest *et al.*'s Results for July.

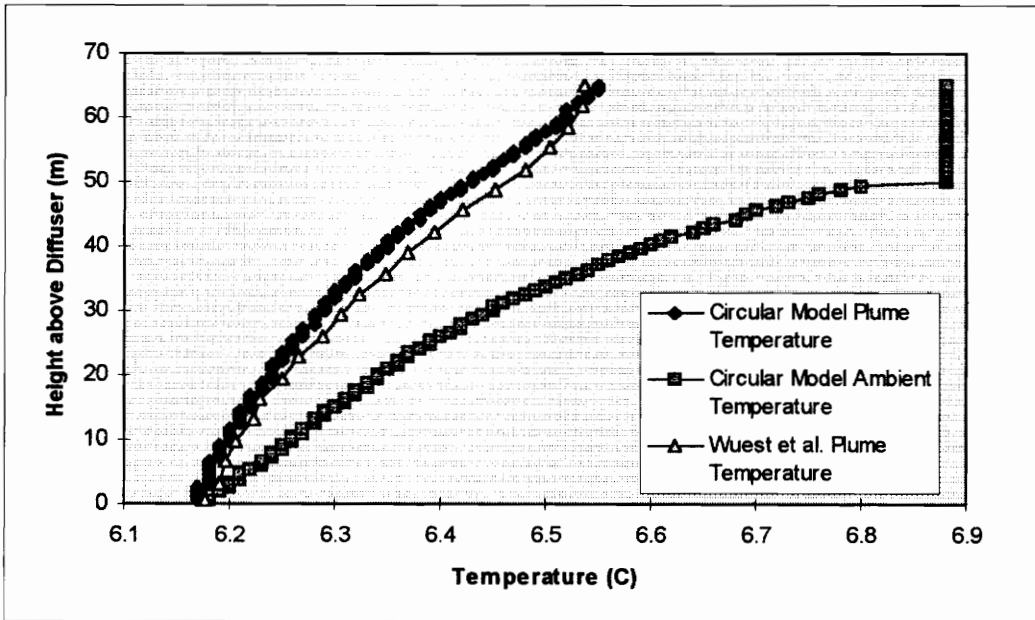


Figure 6. Comparison of Temperatures for Circular Model with Adjusted Ambient Density Profile with Wuest *et al.*'s Results for November.

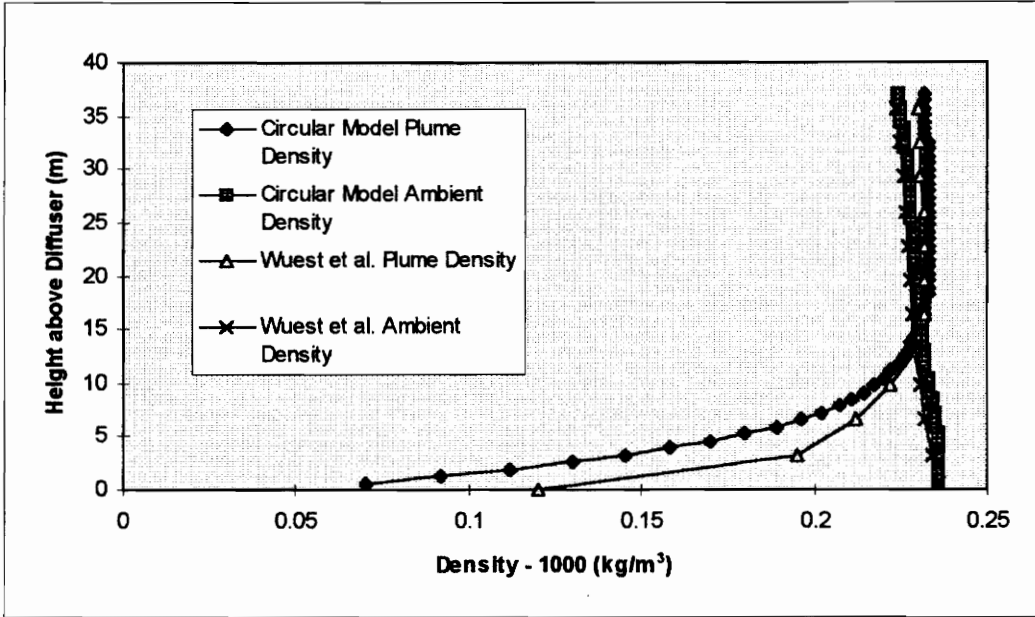


Figure 7. Comparison of Densities for Circular Model with Adjusted Ambient Density Profile with Wuest *et al.*'s Results for July.

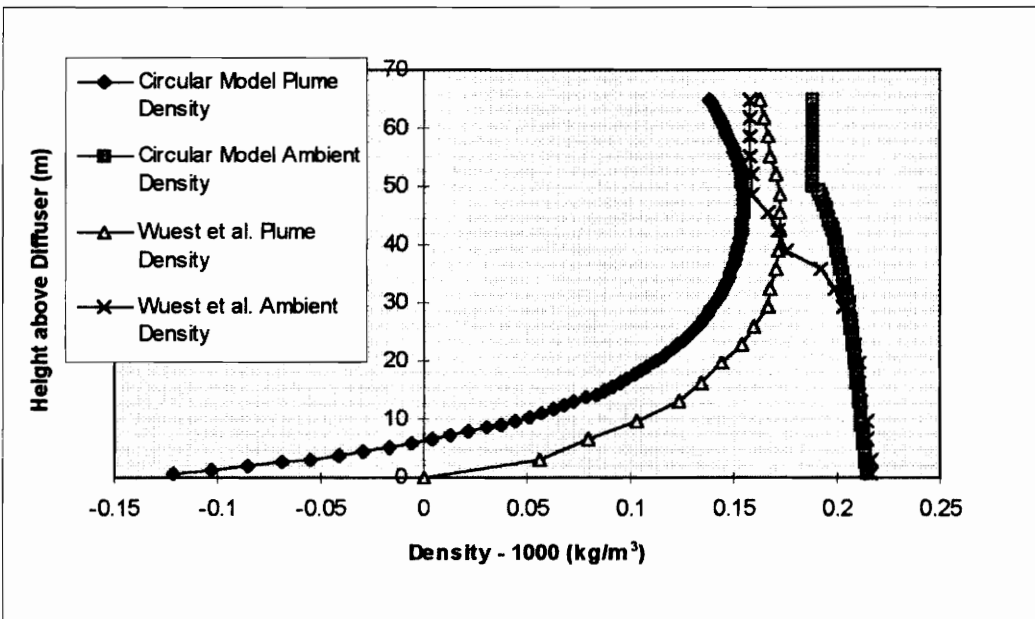


Figure 8. Comparison of Densities for Circular Model with Adjusted Ambient Density Profile with Wuest *et al.*'s Results for November.

(Wuest, 1996). The bubble radius equation in the paper contained a π term in the denominator that should not have been in the equation. Removing this term from their results would have produced a slightly larger bubble radius.

The July plume temperature predicted by the circular plume is approximately 0.025°C cooler than that predicted by Wuest *et al.* (Figure 5). The most likely explanation for this is that it is due to the fitting of curves to the ambient temperature profile. The ambient temperature is the basis for the initial plume temperature calculation. Once the initial plume temperature is calculated, subsequent calculations add incremental temperature to the initial value. Therefore, an inaccurate estimation of the ambient temperature and the resulting error in initial plume temperature could result in an inaccurate plume temperature throughout the depth of the lake.

The same altered ambient and plume water density equations were used for the November conditions. As is shown in Figure 8, the ambient density using the new equation was a good match to the Wuest *et al.* results in the bottom portions of the lake under November conditions but showed less similarity at the top. The predicted plume density was consistently smaller than the plume density reported in the paper. However, the predicted volume flux was again very similar to that predicted by Wuest *et al.* (Figure 3). The plume velocity data (Figure 2) followed the same pattern as the density data: it was similar to the Wuest *et al.* data in the bottom part of the plume but deviated from the paper's data in the upper portions of the plume. This is to be expected due to the dependence of velocity on density as described previously.

The November bubble radii predicted by the circular plume model were similar to those predicted by Wuest *et al.* (Figure 4). However, no clear trend could be seen. At the top and bottom of the plume, the radii predicted by the circular model were smaller than predicted in the paper, which is the opposite of what is expected based on the error in the paper. In the middle

portion of the plume, the circular model predicts a slightly larger radius, which is consistent with the error in the paper.

Similar to the July case, the November plume temperature predicted by the circular model is slightly cooler than that predicted by Wuest *et al.* (Figure 6). While the same possibilities for error exist as explained previously, the actual reason for this difference is not clear.

Although some small differences exist, the similarity in the predictions made by the circular model when the density equations were altered to match the Wuest *et al.* densities to the results in the paper suggest that the large discrepancies found initially were due to the difference in calculated densities. Forcing the ambient densities to be similar resulted in very similar plume densities, plume velocities, and water volume fluxes in July and in November. The fact that the November predicted velocities in the upper portions of the plume varied from those provided in the paper confirmed that density was the reason for the differences as the ambient density also deviated from that in the paper in the upper part of the plume. The circular model's predictions for bubble radius and plume temperature were fairly accurate with both density equations; these calculations are less sensitive to density.

Another possible explanation exists for the small differences in the circular model and the Wuest *et al.* model's predictions. A careful examination of the program they provided revealed that in several cases Wuest *et al.* used slightly different values for constants in the program than were used in the paper. The difference in the density equation has already been discussed. Other differences include a different value for the bubble slip velocity (0.22 vs. 0.23 m/s for $7.0 \times 10^{-4} <$ bubble radius $< 5.1 \times 10^{-3}$ m) and for λ (1.0 vs. 0.8). These and other potential discrepancies in the Wuest *et al.* program compared to their paper could account for the differences in the circular

model, which was based on the equations in the paper, compared to the results of the Wuest *et al.* program.

Revised Circular Plume Model vs. Wuest *et al.* Model.

Once it was determined that differences in density calculations were the cause of the initial discrepancies in the circular plume model compared to the Wuest *et al.* paper, the ambient and plume water density equations were revised. The density of fresh water from 0 to 30° C, in 1° increments was obtained from the *CRC Handbook of Chemistry and Physics* (Lide, 1995) and a curve was fitted to the data. The resulting equation was

$$\rho = 6 \times 10^{-7} T^4 + 8.53 \times 10^{-5} T^3 - 8.91 \times 10^{-3} T^2 + 6.72 \times 10^{-2} T + 999.843 \text{ kg/m}^3$$

The salinity term provided by Wuest *et al.* was added to the above equation. The additional term was $0.802 \times S$ if dissolved solids concentration is given in grams per 1000 grams or $0.705 \times 10^{-3} \times S$ if salinity is provided in electrical conductivity ($\mu\text{S/cm}$) at 20° C.

The method used for calculating the initial plume velocity was revised as well. Previously, the initial conditions for the circular plume model were forced to be identical to those given in the Wuest *et al.* paper by setting the initial velocity equal to that given in the paper. This was done after it was determined that the use of the Froude number equation given in the paper did not result in the same initial velocity as that provided in the paper. However, to make the circular model more generally applicable, the initial velocity had to be calculated. Therefore, the program was altered to ask the user for a guessed initial velocity. From this guess, the program entered a do-loop in which the initial concentrations of dissolved oxygen and nitrogen, volume of gas, plume density (using the Table 4 equations), and initial velocity (using the Froude number equation) were

calculated through 30 iterations. Thirty iterations were considered very conservative as it was determined that the initial velocity value became stable after approximately ten iterations. Hereafter, the circular plume model with the new density equation and the iterative method of finding the initial plume velocity will be called the revised circular plume model or simply the revised model.

The revised circular plume model was run under Wuest *et al.*'s July and November conditions and the results were compared to those reported in the Wuest *et al.* paper. The results are shown in Figures 9-14.

The ambient and plume densities for the two seasons (Figures 13 and 14) show approximately the same shapes as those provided in the paper; however, the values are different. Again, the July densities are more similar to the paper than are the November densities. The November densities vary most from the Wuest *et al.* model densities near the top of the plume. As shown in Figure 9, the velocities are very similar to those predicted by Wuest *et al.* for both July and November conditions. Once again, the November velocity data differs near the top of the plume where the model and paper's ambient densities are different. Another noticeable difference is that the July plume rises higher than Wuest *et al.*'s and the November plume does not rise to the top of the lake with the revised circular plume model. The small differences in the predicted velocities and in the height of maximum plume rise likely result from iterating to obtain the initial velocity rather than forcing the initial velocity to be the same as reported in the paper. The new ambient and plume water density equations play a part in these differences as well.

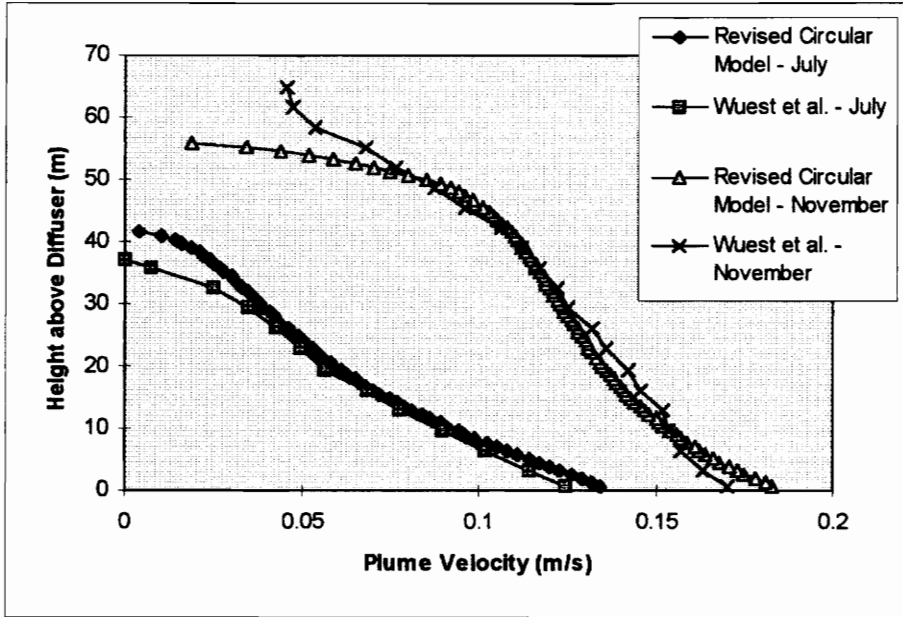


Figure 9. Comparison of Plume Velocities for Revised Circular Model with Wuest *et al.*'s Results for July and November.

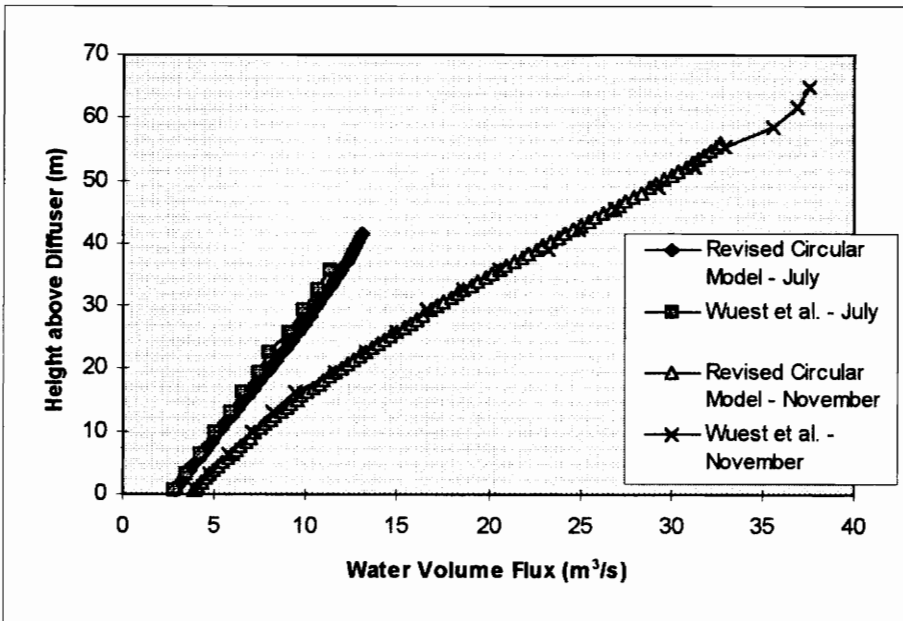


Figure 10. Comparison of Water Volume Fluxes for Revised Circular Model with Wuest *et al.*'s Results for July and November.

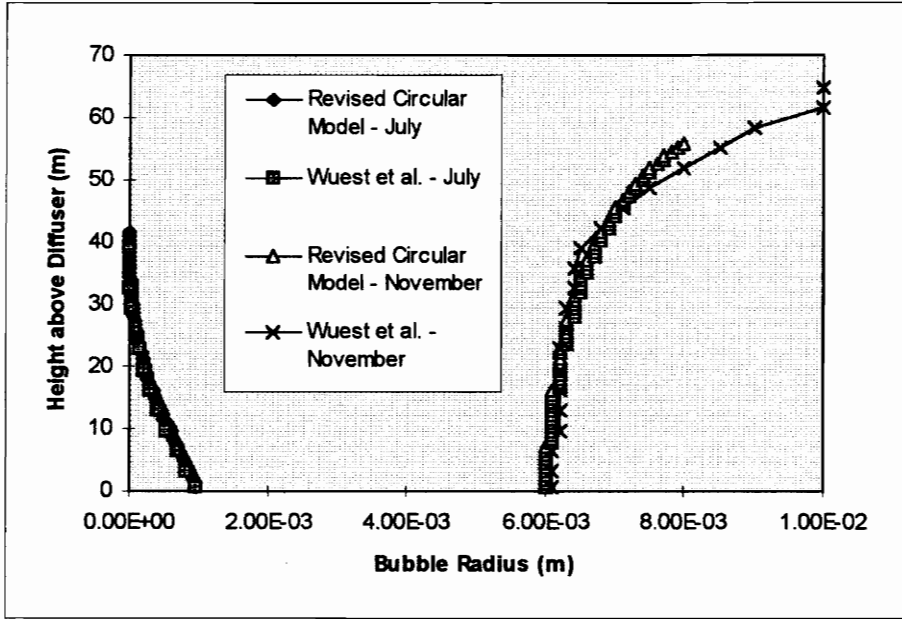


Figure 11. Comparison of Bubble Radii for Revised Circular Model with Wuest *et al.*'s Results for July and November.

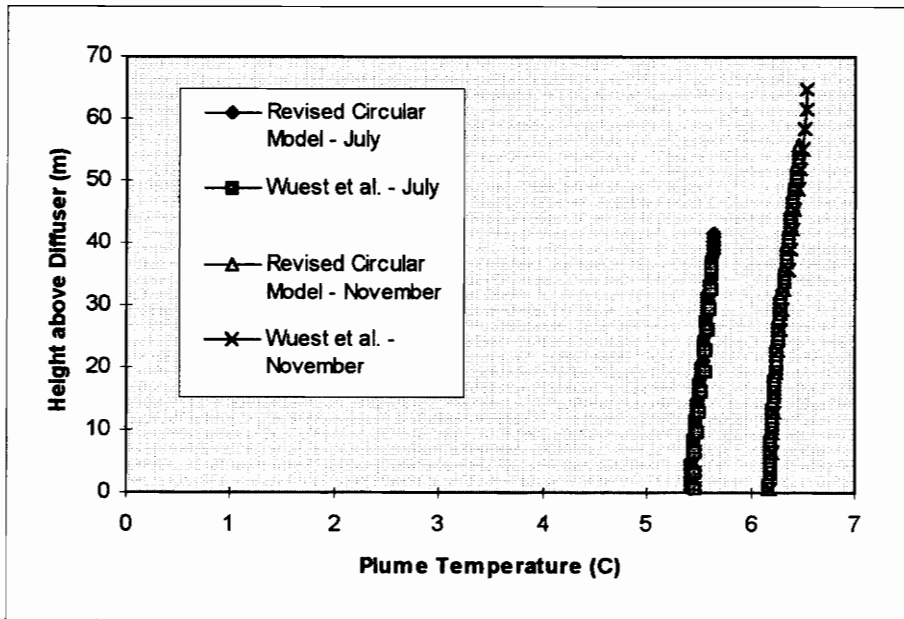


Figure 12. Comparison of Plume Temperatures for Revised Circular Model with Wuest *et al.*'s Results for July and November.

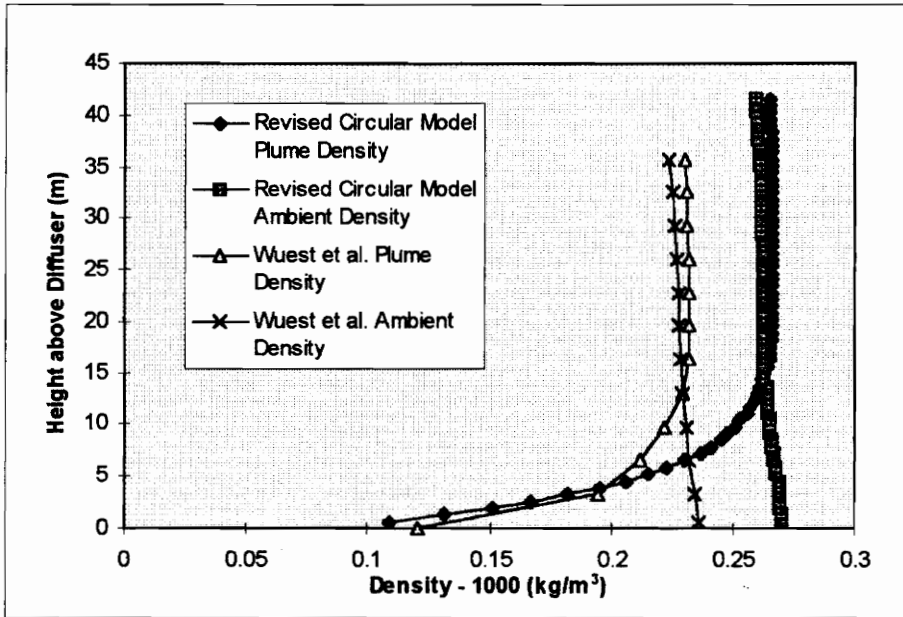


Figure 13. Comparison of Densities for Revised Circular Model with Wuest *et al.*'s Results for July.

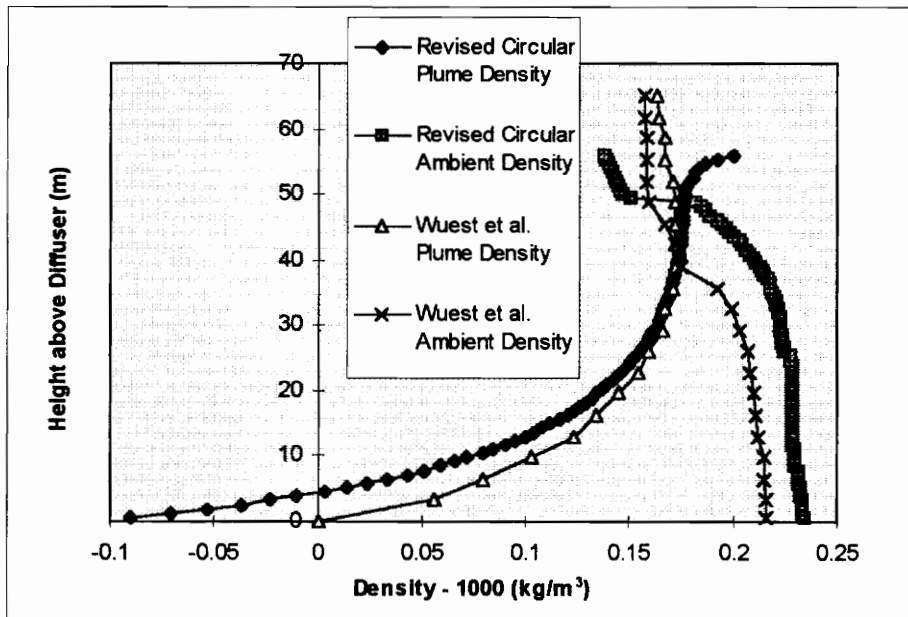


Figure 14. Comparison of Densities for Revised Circular Model with Wuest *et al.*'s Results for November.

The water volume fluxes predicted by the revised model were very similar to those predicted in the Wuest *et al.* paper (Figure 10). The bubble radius predictions are also similar but show the same trends as in the original circular model with the ambient and plume water densities forced to Wuest *et al.*'s densities (Figure 11). Similarly, the plume temperature predictions are similar to Wuest *et al.*'s but are slightly cooler than the plume temperatures predicted in the paper (Figure 12).

After examining the results of the revised circular plume model compared to the results obtained by Wuest *et al.*, it was concluded that the revised model accurately solved the equations presented by Wuest *et al.* for a circular plume. After running a sensitivity analysis, then, the next step was to convert the revised circular plume model into a linear model. The results are described in the following section.

Linear Plume Model vs. Revised Circular Plume Model.

After the linear model was completed based on the revised circular plume model, its results were compared to those obtained from the revised circular model to determine whether the linear model was performing as expected. To do this, the conditions under which the linear model was run had to be similar to those under which the revised circular plume model was run. Therefore, the "linear" source was assumed to be a 2.45m x 2.45m square, which provides approximately the same area as the circular source with a 2.5m radius. The linear model was run under July and November conditions with temperature, dissolved solids, dissolved oxygen, and dissolved nitrogen profiles; gas input rates; and initial bubble size identical to those provided in Wuest *et al.*'s paper (Table 5) to duplicate the conditions under which the revised circular plume model was run. In

addition, the linear model's assumption that entrainment at the ends of the plume could be neglected was tested by comparing the linear model's predictions with and without end entrainment to the results obtained from the revised circular model. The assumption was tested both under the condition described above, in which the model is run in a square configuration, and under full scale conditions. As an example of how the model was implemented with end entrainment, the equation for the change in water volume flux with height was changed from

$$\frac{d\mu}{dz} = 2\alpha Lw$$

to

$$\frac{d\mu}{dz} = 2\alpha(L + b)w .$$

Equations for temperature flux, salinity flux, and dissolved gas flux were changed in a similar manner.

The linear model was run for July and November conditions. The July results are shown in Figures 15, 17, 19, 21, and 23 and the November results in Figures 16, 18, 20, 22, and 24. The results from both seasons clearly showed that the assumption that end effects could be neglected was incorrect in this situation, as the linear model with end entrainment considered performed much more like the revised circular model than the linear model with end effects neglected. Therefore, for this case in which the "linear" plume is a square, entrainment at the ends of the plume must be included in the model. In this section of the paper, the linear model with end entrainment considered will be the basis for comparison of the linear model to the revised circular model. This assumption will again be tested when the model is run as a long linear source as it was meant to be implemented.

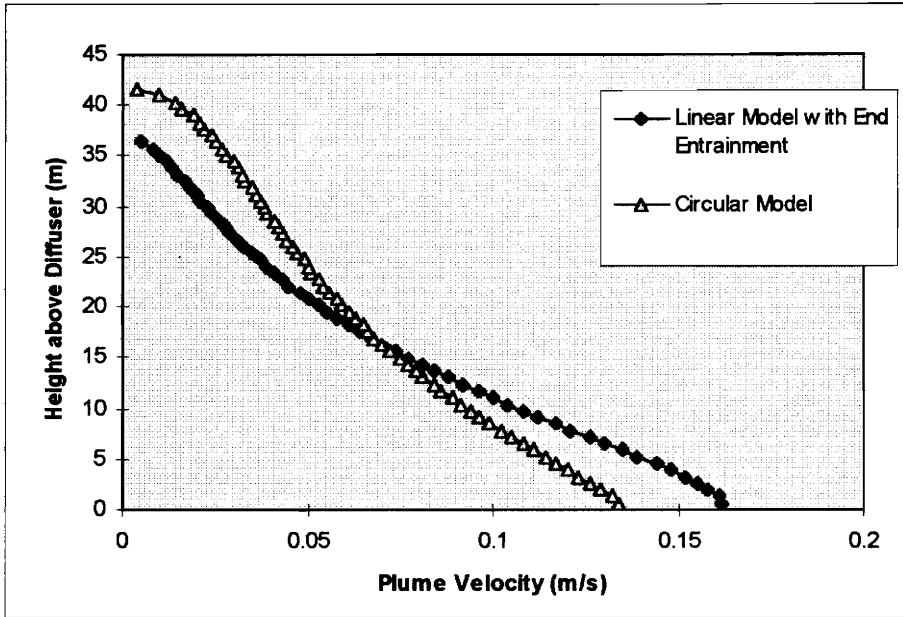


Figure 15. Comparison of Plume Velocities for Linear Model with End Entrainment with Revised Circular Model for July.

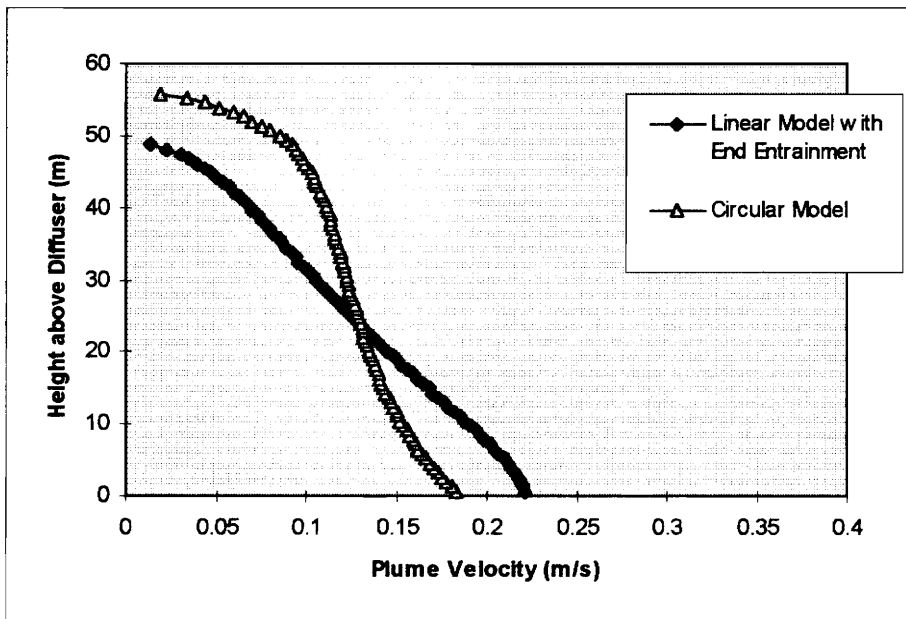


Figure 16. Comparison of Plume Velocities for Linear Model with End Entrainment with Revised Circular Model for November.

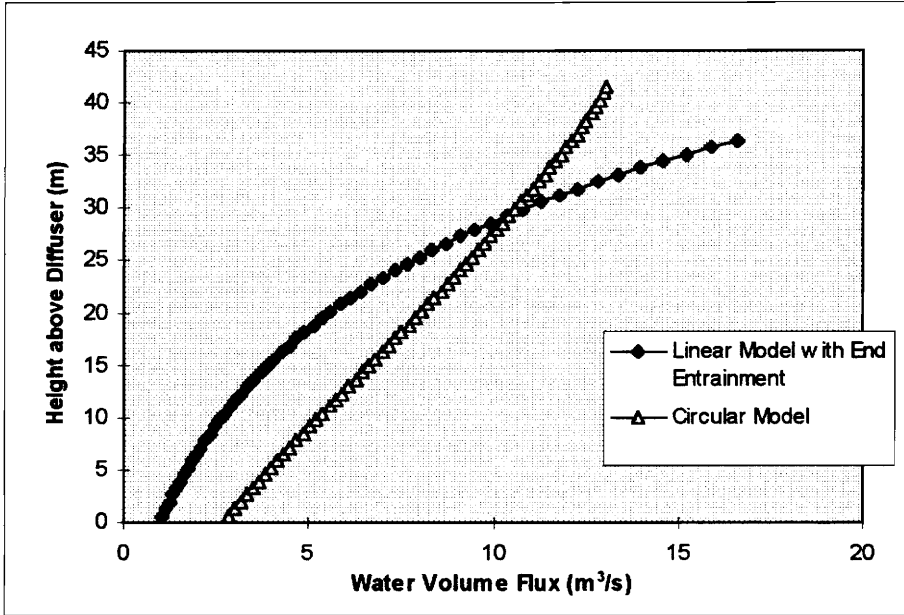


Figure 17. Comparison of Water Volume Fluxes for Linear Model with End Entrainment with Revised Circular Model for July.

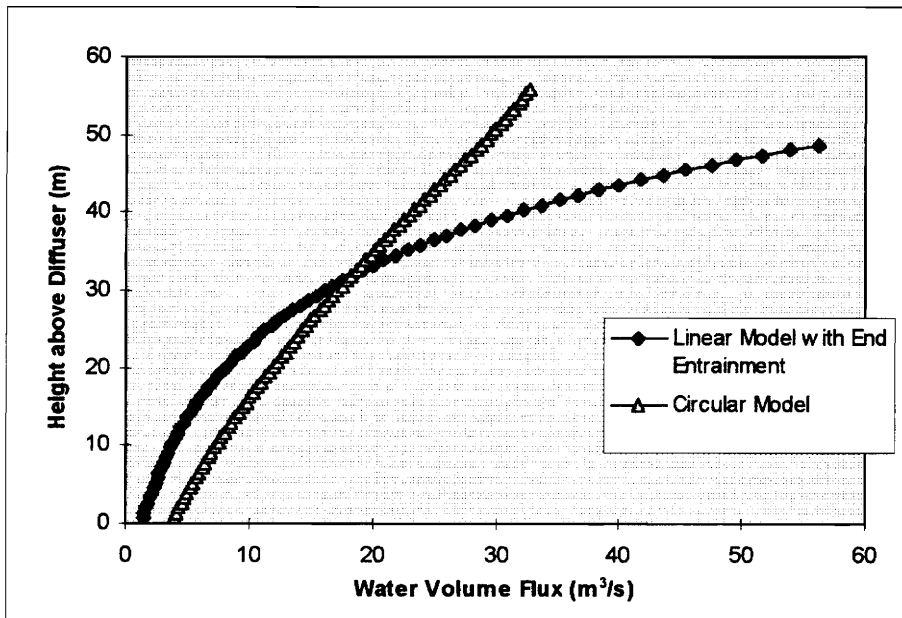


Figure 18. Comparison of Water Volume Fluxes for Linear Model with End Entrainment with Revised Circular Model for November.

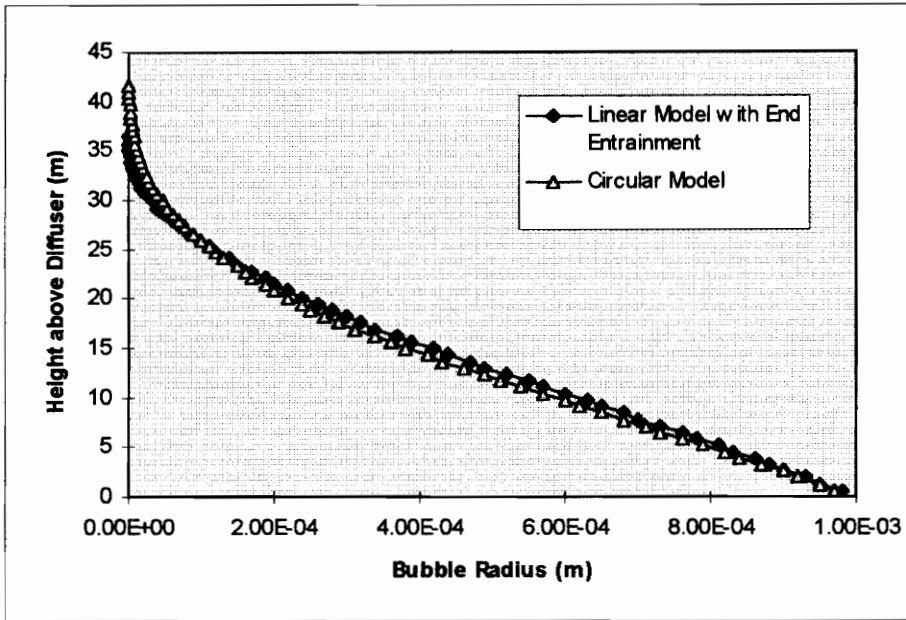


Figure 19. Comparison of Bubble Radii for Linear Model with End Entrainment with Revised Circular Model for July.

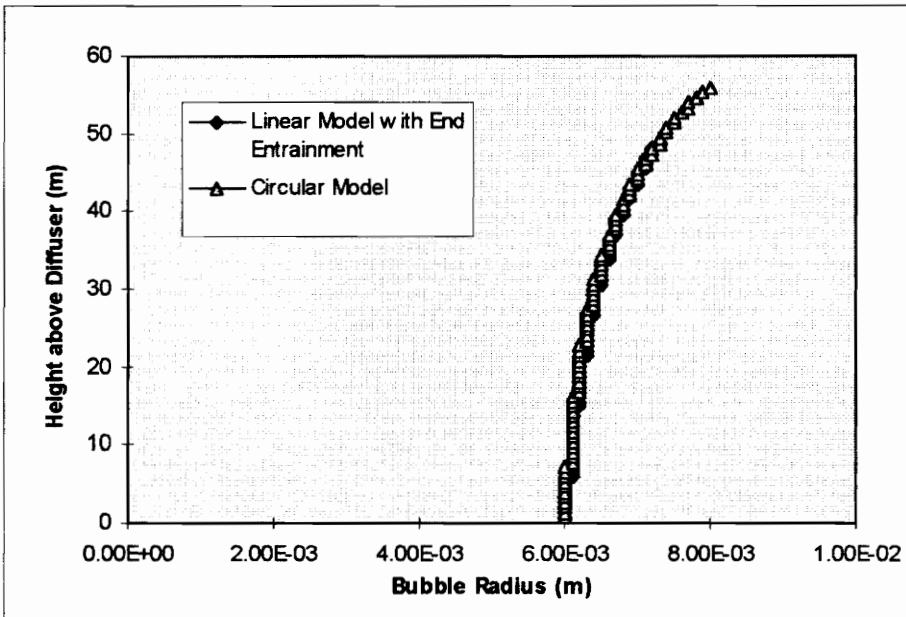


Figure 20. Comparison of Bubble Radii for Linear Model with End Entrainment with Revised Circular Model for November.

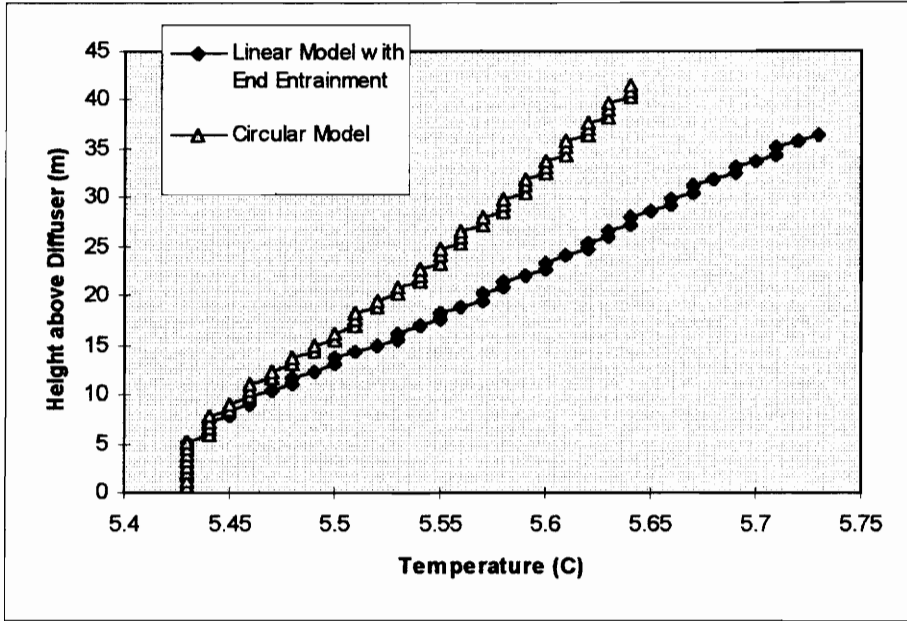


Figure 21. Comparison of Plume Temperatures for Linear Model with End Entrainment with Revised Circular Model for July.

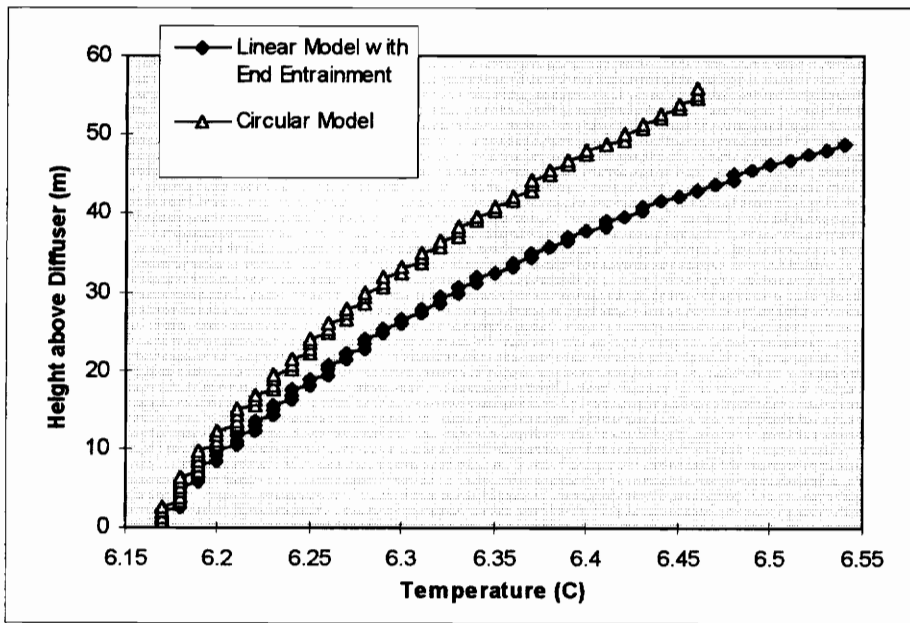


Figure 22. Comparison of Plume Temperatures for Linear Model with End Entrainment with Revised Circular Model for November.

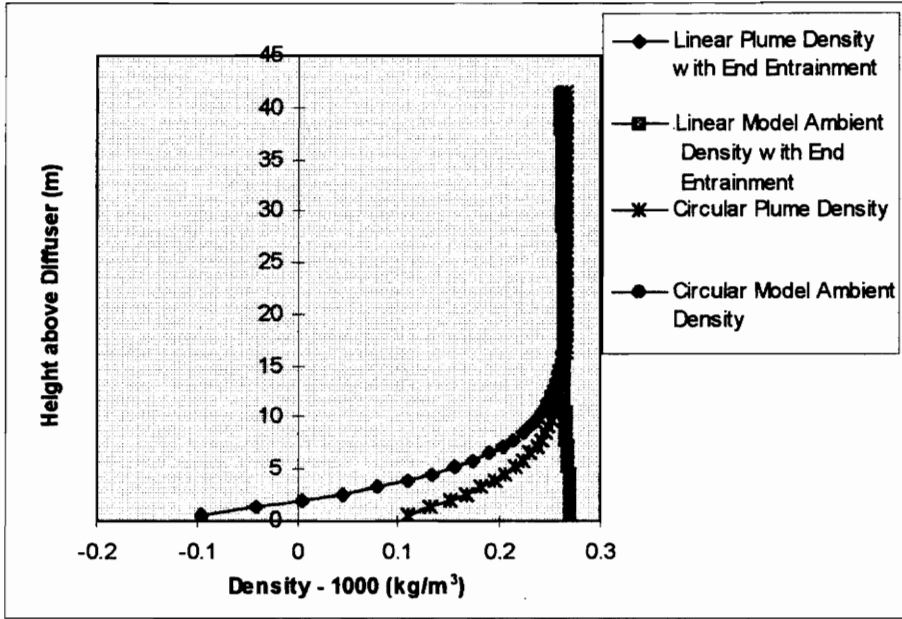


Figure 23. Comparison of Plume Densities for Linear Model with End Entrainment with Revised Circular Model for July.

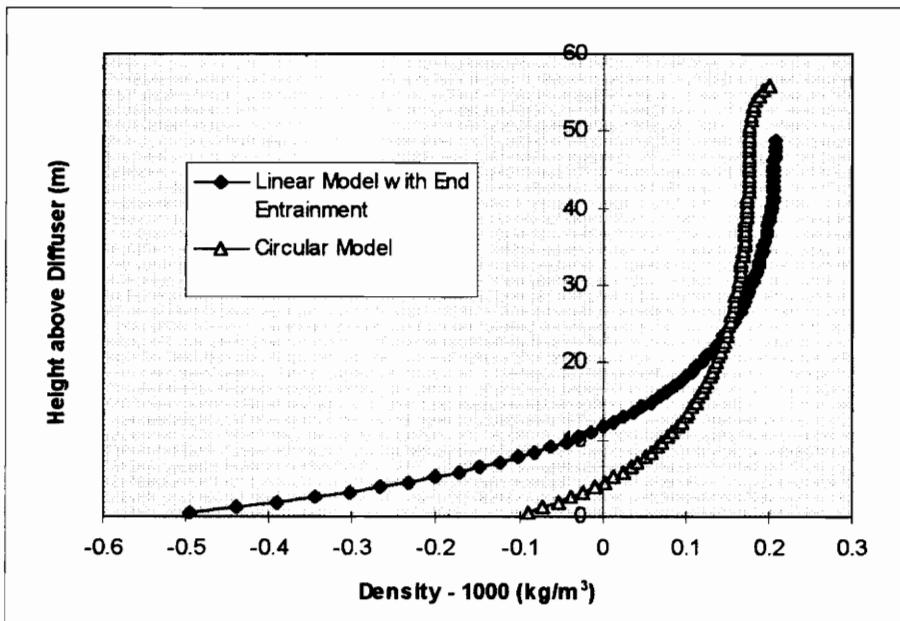


Figure 24. Comparison of Plume Densities for Linear Model with End Entrainment with Revised Circular Model for November.

A comparison of the linear model with end entrainment considered with the revised circular model reveals very similar performance of the two models. Since a comparison of the revised circular model with Wuest *et al.*'s data demonstrated that the revised model performed well, the similarity of the linear model to the revised model implied that it too was performing as expected.

For the July conditions, Figure 23 shows that the ambient densities are identical for the two models. This was expected since the same density equation, temperature profile, and dissolved solids profile were used in testing both models. Slight differences can be seen in plume density, but these differences are restricted to the bottom 10 meters of the plume.

The predicted plume velocities for July are similar in the linear and the revised circular models (Figure 15). The linear model velocity is approximately 0.025 m/s faster than the revised circular model at the bottom of the plume. However, the linear velocity slows more quickly than the circular velocity and therefore the linear model predicts a maximum plume rise of approximately 5 meters less than is predicted by the revised circular model.

While the bubble radii predicted by the two models for July are practically identical (Figure 19), the plume temperatures show significant differences. The linear plume temperature at any given height above 5 meters is colder than predicted by the revised circular plume, and the difference becomes more pronounced as the plume rises. (See Figure 21.) However, the difference can be explained. As the plume rises, it flows through warmer and warmer ambient water. As it entrains this warmer water, the plume itself becomes warmer. Due to the shape of the circular plume compared to the linear plume (which is in this case a square), the circular plume has less "plume surface area" with which to entrain water. Since entrainment is proportional to the distance around the plume and the perimeter of a square is larger than the circumference of a circle with the same area, the plume modeled as a square entrains more water and thus becomes warmer more

quickly. (The linear model neglecting end effects, which entrains water on only two sides of the square, was found to warm more slowly than either the revised circular model or the linear model including end entrainment.) The entrainment coefficient, α , is slightly smaller for the linear plume model (0.08) than for the circular plume model (0.11), but this small difference is not enough to counteract the effect of the increased plume surface area.

A significant difference can be seen in the July water volume flux data as well (Figure 17). Rather than slowing with height as in the revised circular model, the volume flux predicted by the linear model with end entrainment remains constant with height. The linear volume flux is larger than the revised circular volume flux in approximately the bottom two-thirds of the plume but becomes smaller near the top. This is a result of the assumptions that L , the plume length, is constant, and that the entrainment is proportional to L . Initially, the larger surface area of the linear plume compared to the circular plume allows the linear plume to entrain more water. Therefore, initially the linear plume has a higher flowrate than the circular plume. However, as the plume rises, the width alone increases. Eventually, the surface area of the square plume with the length of two sides held constant is surpassed by the surface area of the round plume with an increasing radius, and as a result a smaller volume of water flows in the linear plume than in the circular plume per unit time.

Similar trends are seen in the November data. Again, the ambient densities for the linear and revised circular plume models are identical and therefore not shown in Figure 24, which shows the predicted plume densities. The linear plume density follows the same general trend as the circular plume density but shows significant difference, especially towards the bottom of the plume.

The predicted November velocities (Figure 16) show the same pattern as the July plume velocities. The linear plume with end entrainment considered has a higher initial velocity than the revised circular plume. However, its speed diminishes more quickly than the circular plume as it rises and predicts that the plume will rise approximately 6 to 7 meters less than predicted by the revised circular model. The bubble radii predicted by the linear model (Figure 20) are virtually identical to those predicted by the revised circular model.

As in the July conditions, the linear model with end entrainment in November starts at the same plume temperature as the revised circular plume but warms more quickly as it rises. (See Figure 22.) This is due to entrainment as explained previously.

The November water volume flux (Figure 18) follows the same trend as the July water volume flux. At the bottom of the square shaped linear plume a greater water volume flux occurs because it entrains more water than the circular plume. However, since the plume length is assumed constant, the volume of water transported per unit time decreases relative to the revised circular plume model until the linear volume flux is less than the circular water volume flux.

Testing End Entrainment Assumption under Simulated Full Scale Conditions.

The linear model was next run under the conditions in the Wuest *et al.* paper for a diffuser similar to that designed by TVA (Mobley and Brock, 1996) to test the assumption that end entrainment could be neglected when the model was implemented for a linear source. The diffuser unit modeled was 100 meters long and 0.25 meters wide. Other initial conditions, such as gas input rate and initial bubble size, were as given in the Wuest *et al.* paper (Table 5).

The only notable differences in the model's predictions with and without end entrainment were in the plume velocity, water volume flux, and plume width predictions. The most striking

difference between the two versions of the linear model was seen in the plume width calculations. For both seasons, the two versions predicted very similar plume widths throughout most of the height of the plume. Near the top of the plume, the model that included end entrainment began to predict slightly larger plume widths than the model that did not include end entrainment. However, at the height of maximum plume rise for both July and November, the version in which end entrainment was considered predicted a much larger value for the plume width which should not occur in the zone of established flow based on the results of previous studies. This dramatic increase in predicted plume width at the top of the plume implies that the model including the effects of end entrainment may not be as reliable as the model neglecting the end effects for full scale applications when the source is linear rather than square as in the previous case.

Other than the plume width predictions, both versions of the linear model appeared to make reasonable predictions. The variables followed the trends of the circular plume model and therefore seemed to be performing well. For applications in which the model is run as it was designed, the best results were obtained when end effects were neglected. If the shape of the linear model source is modified to a square shape, end entrainment must be considered to obtain accurate predictions, and, in fact, it may not be advisable to run the linear model for configurations other than that for which it was developed. A square source could perhaps be better simulated by the revised circular model.

Linear Plume Model vs. Provost's (1973) Velocity Data.

The linear model was compared to vertical plume velocity data collected by Provost (1973). The model was run under two sets of conditions for which Provost collected data. In the first, the air flowrate was varied and the velocity was measured at one height above the diffuser. In

the second, the air flowrate was kept constant and the depth of the water in the tank was varied. In the second situation, velocity was measured at four heights above the diffuser. Since Provost's experiments were set up as line sources in a laboratory tank of water, the linear plume model was run with the assumption that end entrainment was negligible.

The water temperature was provided in the thesis; however, the dissolved oxygen, dissolved nitrogen, and dissolved solids concentrations in the water were not given. Therefore, the saturation values for oxygen and nitrogen in 20° C water were used as estimates. An appropriate value for the total dissolved solids concentration was not as apparent. An average reservoir total dissolved solids concentration was estimated to be approximately 0.20 mg/g (Snoeyink and Jenkins, 1980). Therefore, the salinity in the tap water used by Provost was varied from 0.0 to 0.40 mg/g in the model to determine the effect of dissolved solids concentration on velocity. Altering the salinity through this range in 0.10 mg/g increments had no effect on the plume velocity for an air flowrate of 0.00052 Nm³/s. Therefore, all subsequent calculations were performed with the salinity assumed to be 0.20 mg/g. A summary of the values used in executing the linear model for comparison with Provost's data was provided in Table 8.

Before the model could be used to make predictions, an appropriate number of steps had to be determined to minimize error due to the numerical solution procedure. A total of 20,000 steps was found to be adequate as adding additional steps did not change the outcome of the predicted values.

The results from the implementation of the model at different gas flowrates are shown in Table 11. The velocity measurements were made at 0.15 m above the diffuser. The linear plume model overpredicts the velocity data by over 40 percent for all three air flowrates. The error increases as flowrate increases.

Due to the possibility that the reason for the overprediction of the velocities was a result of the initial velocity calculation using the Froude number for a circular area, the Bulson method for predicting velocity was examined. Unfortunately, this approach led to higher predictions for initial plume velocity. It is likely that Bulson's findings were applicable only to the situation in which he made his measurements. For these reasons, this method of calculating initial plume velocity was abandoned.

The results of the second set of conditions are shown in Figures 25-28. The model overpredicted the velocities at all four depths but seemed to be more accurate as depth increased. The shape of the curves predicted did not match the shape of the curves of the data collected by Provost.

Since the diffuser in Provost's experiments was not very long, the model was implemented once again for the same conditions with end entrainment included in order to ascertain whether the inaccurate predictions of the linear model resulted from neglecting entrainment at the ends of the plume. The predictions made by the linear model when end entrainment was considered were slightly closer to the actual data than when end effects are neglected. The predictions of the linear model with end entrainment more closely resembled the data as the total water depth increased and as the plume rose. However, the more accurate predictions near the top of the plume were likely a result of the more rapid decrease in velocity with height when end entrainment is considered rather than an actual better fit to the data. Therefore, it should not be concluded that the linear model with end entrainment more accurately predicted the data.

Table 11. Predicted and Measured Plume Velocities at Different Air Flowrates.

Air Flowrate (Nm³/s)	Predicted Velocity (m/s)	Measured Velocity (m/s)	Percent Error (%)
0.00052	0.56	0.40	40.3
0.0010	0.72	0.49	46.6
0.0015	0.84	0.56	48.6

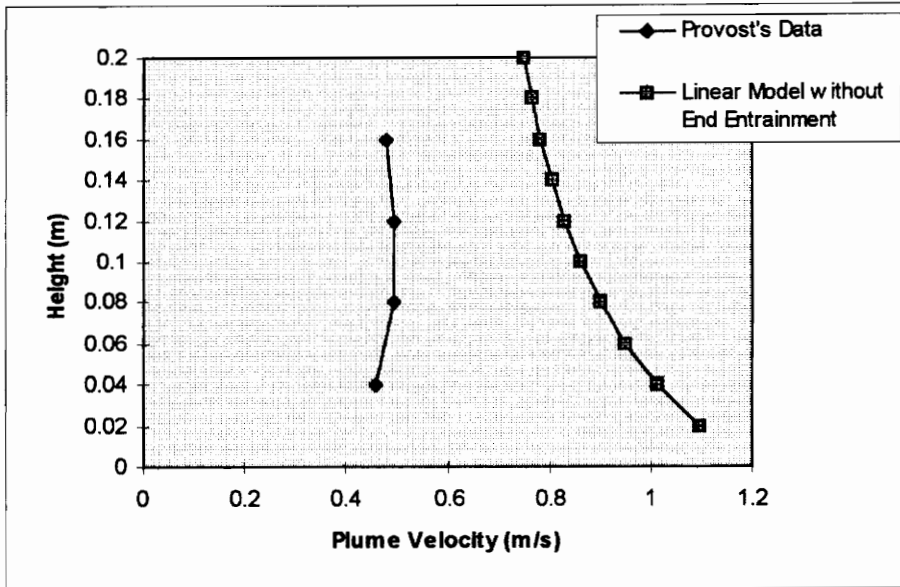


Figure 25. Comparison of Linear Models without End Entrainment to Provost's Plume Velocity Data for 0.20 Meter Depth.

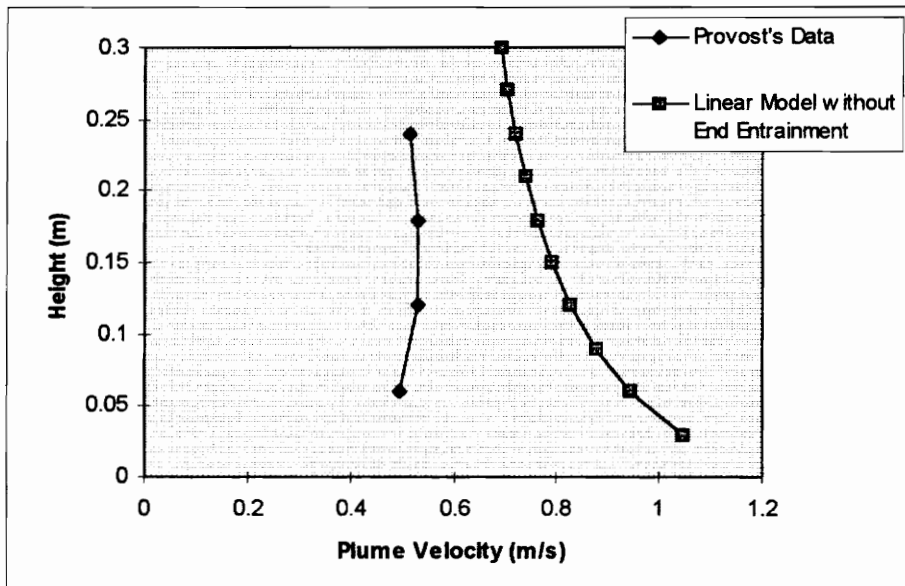


Figure 26. Comparison of Linear Models without End Entrainment to Provost's Plume Velocity Data for 0.30 Meter Depth.

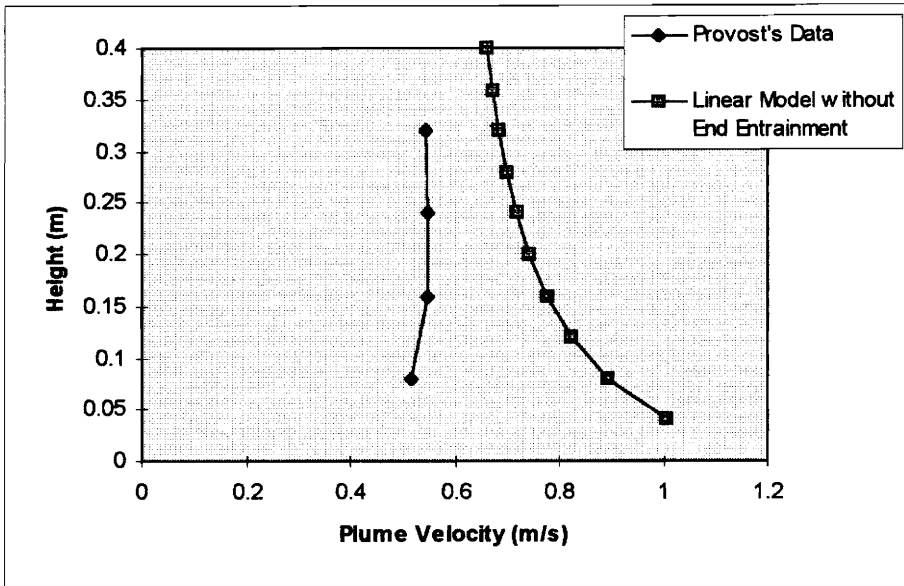


Figure 27. Comparison of Linear Models without End Entrainment to Provost's Plume Velocity Data for 0.40 Meter Depth.

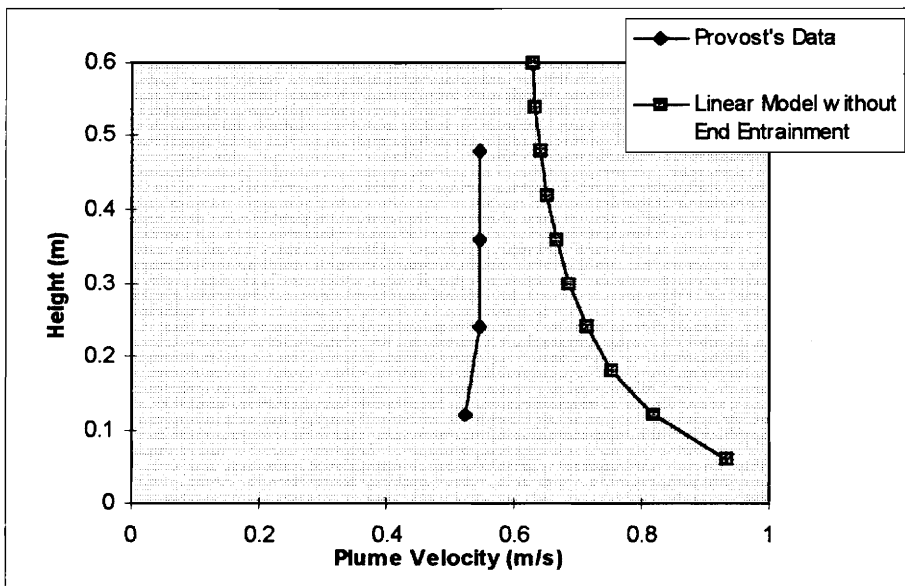


Figure 28. Comparison of Linear Models without End Entrainment to Provost's Plume Velocity Data for 0.60 Meter Depth.

As bubble size is notoriously difficult to predict, the possibility existed that the inaccuracies in the linear model velocity predictions were a result of incorrect initial bubble radius. Therefore, the effects of varying the initial bubble radius by ± 30 percent were examined. Variations of the initial bubble size over this range did not affect the predicted vertical velocities.

Because the Froude number used to calculate initial velocity was measured for a circular, rather than a linear plume, it was hypothesized that the Froude number could have been the basis for the difference between the predicted and measured values. Therefore, the Froude number was varied from 0.3 to 1.6 in 0.1 increments; the results for a Froude number of 0.5, which gave the best results, are shown in Table 12 for the experiments in which gas input rate was varied and in Figures 29-32 for the case in which water depth was modified.

A Froude number equal to 0.5 produced much more accurate predictions of Provost's data. The error for the situation in which gas flowrate was altered was only 6.7 percent for the lowest flowrate and was below 17 percent for all three flowrates examined. Again, predictions became less accurate as gas input rate increased. The results from the experiments in which water depth was varied show closer predictions of the data than were shown previously. In addition, the Froude number of 0.5 results in a shape for the velocity profile that is more similar to the actual data. As before, the predictions appeared to be increasingly accurate as water depth increased. However, whether a Froude number of 0.5 is a reasonable value for a linear plume is not known; further study should be done to determine the appropriate value for use in the linear model.

Several possible reasons exist for the discrepancies between the predicted velocities and the measured velocities. First, basing the initial velocity calculation on a circular Froude number could have caused the difference, as explained previously. Second, the Wuest *et al.* model on which the linear model was based was developed for the zone of established flow. It is possible

Table 12. Comparison of Linear Model Plume Velocity Predictions with Froude Number Equal to 0.5 to Provost's (1973) Measured Data.

Air Flowrate (Nm³/s)	Predicted Velocity with Froude = 0.5 (m/s)	Measured Velocity (m/s)	Percent Error (%)
0.00052	0.42	0.40	6.7
0.0010	0.55	0.49	13.6
0.0015	0.66	0.56	16.8

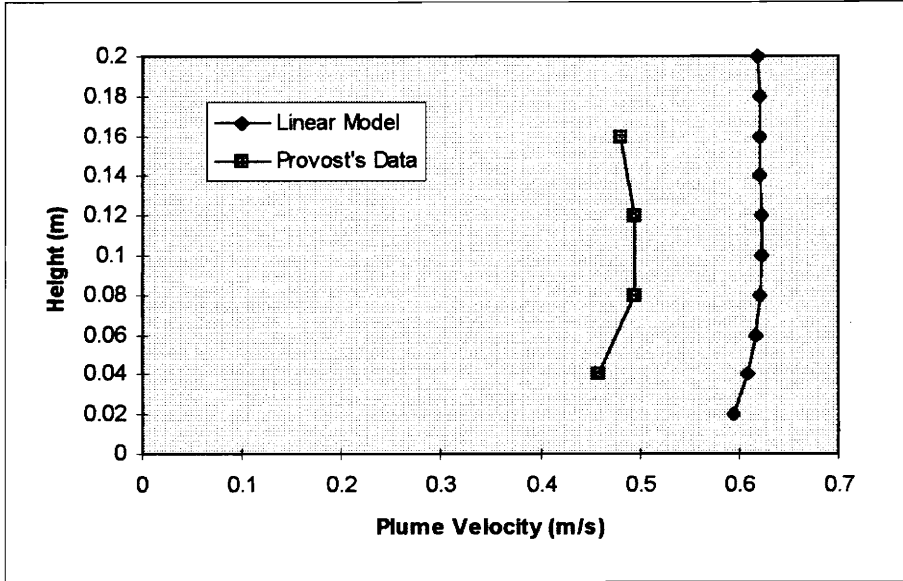


Figure 29. Comparison of Linear Model without End Entrainment with Froude Number of 0.5 to Provost's Plume Velocity Data for 0.20 Meter Depth.

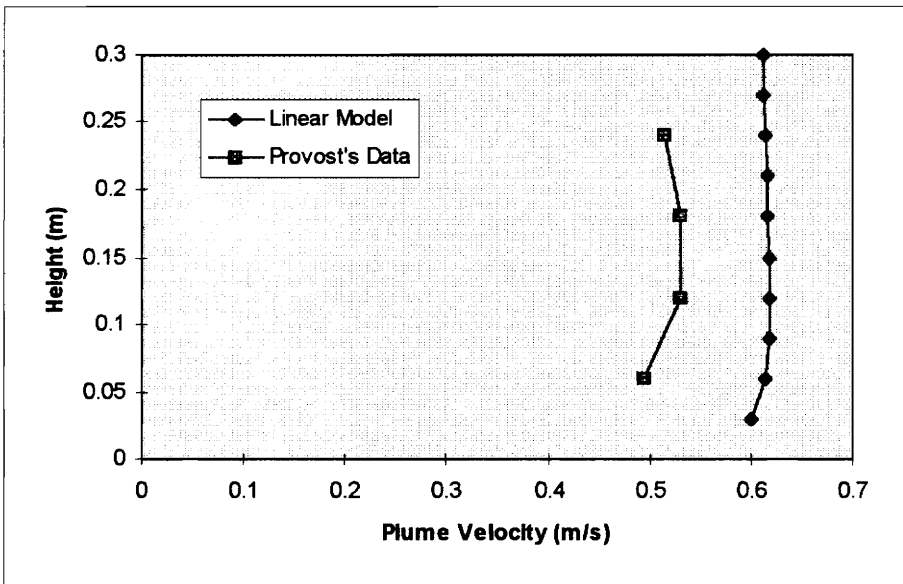


Figure 30. Comparison of Linear Model without End Entrainment with Froude Number of 0.5 to Provost's Plume Velocity Data for 0.30 Meter Depth.

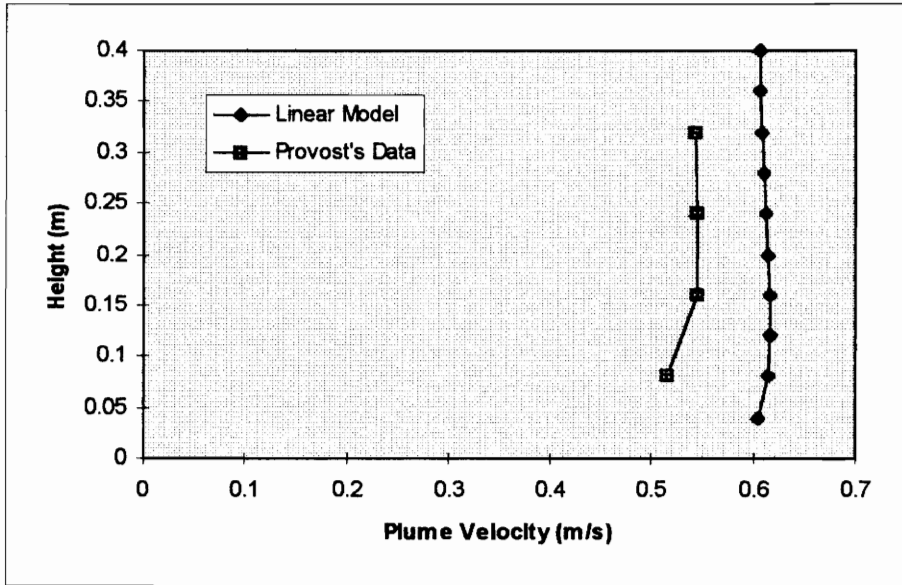


Figure 31. Comparison of Linear Model without End Entrainment with Froude Number of 0.5 to Provost's Plume Velocity Data for 0.40 Meter Depth.

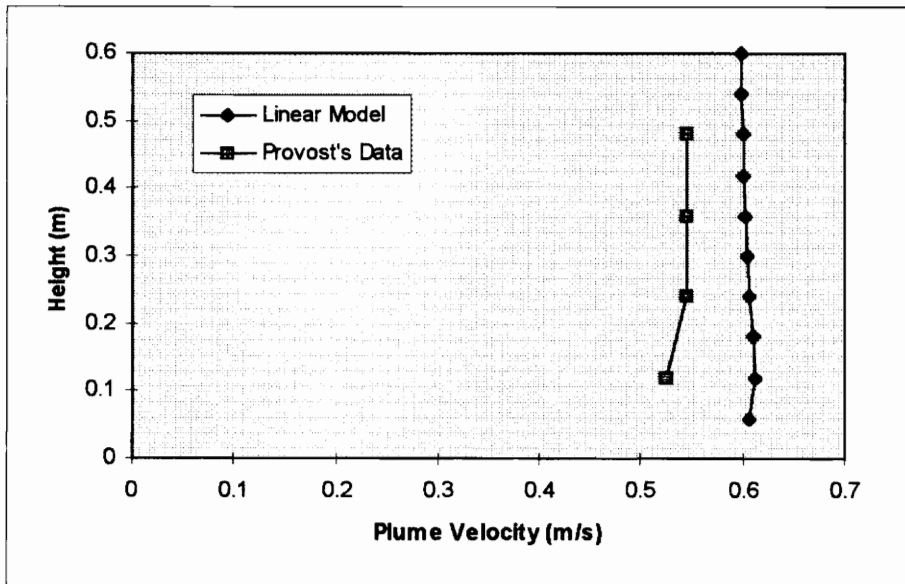


Figure 32. Comparison of Linear Model without End Entrainment with Froude Number of 0.5 to Provost's Plume Velocity Data for 0.60 Meter Depth.

that the shallow depths used in Provost's laboratory scale study were not deep enough for the plume to reach the zone of established flow. If this were the case, the plume would be in the zone of flow establishment which no bubble plume model has attempted to describe. It is also possible that the model, which was intended for use with full scale plumes, could not accurately predict the laboratory scale data due to the differences in full scale and laboratory scale plumes noted by Wilkinson (1979). Finally, the possibility exists that Provost's velocity measurements or calculations contained systematic errors that resulted in his unknowingly reporting velocities that were smaller than actually occurred.

Linear Plume Model vs. Wen's (1974) Oxygen Concentration Data.

The majority of the laboratory conditions used by Wen (1974) were the same as those used by Provost (1973). Exceptions were the water temperature of 4.44° C (compared to Provost's 20° C water) and the absence of dissolved oxygen in the water as dissolved oxygen was removed prior to Wen's experiments. The colder water temperature resulted in a higher saturation value for dissolved nitrogen: 0.953 mol/m³. The initial values used in implementing the model to predict Wen's data were shown in Table 9.

Before the linear model could be implemented, an appropriate number of steps for solving using Euler's method had to be selected. It was determined that 30,000 steps were adequate. The linear model used did not consider end entrainment as Wen's source was linear.

The model was used to predict initial oxygen input rates into the laboratory tank. The measured oxygen input rates were determined by finding the slopes of data graphed in Wen's thesis. The linear model overpredicted the oxygen input rates by 183 to 515 percent as shown in Table 13.

Four possibilities exist for the discrepancy between predicted and measured values. First, the gas transfer coefficient provided by Wuest *et al.* may have been too large. The second possibility is the miscalculation of initial plume velocity demonstrated in the comparison of the linear model to Provost's thesis. A high value for initial velocity would result in a high value for initial volume flux, and therefore in initial gaseous oxygen input rate. Since the dissolved oxygen input rate was determined based on the difference between gaseous oxygen concentration at the bottom of the plume compared to the gaseous concentration at the top of the plume this could result in an overprediction of dissolved oxygen supplied to the surrounding water. Third, the problems of using a full scale model for a laboratory scale experiment, as discussed previously, could have accounted for the differences. Fourth, an inaccurate estimation of initial bubble radius could have resulted in incorrect calculations of the amount of oxygen imparted to the water. The effect of altering the initial bubble radius by ± 30 percent is shown in Table 14. As the results in Table 14 show, it is unlikely that an error in the calculation of initial bubble radius was responsible for the entire discrepancy between predicted and measured oxygen input rates, but such an error could have exacerbated the difference caused by another factor.

The linear model with the Froude number equal to 0.5 was run to determine whether predictions of Wen's data were improved with the modified Froude number. Unfortunately, the oxygen imparted to the water was highly underpredicted when the new Froude number value was used. (For example, the initial oxygen input rates were 0.273 and 0.349 mg/L-min for air flowrates of 0.0019 and 0.0017 Nm³/s, respectively.) Therefore, altering the Froude number does change the predicted oxygen transferred, but the Froude number value that resulted in the best predictions of Provost's velocity data did not provide the best predictions of oxygen concentration

Table 13. Comparison of Linear Model Oxygen Input Rate Predictions to Wen's (1974) Measured Data.

Air Flowrate (Nm³/s)	Predicted Oxygen Input Rate (mg/L-min)	Measured Oxygen Input Rate (mg/L-min)
0.0019	5.74	1.71
0.0017	5.35	0.87
0.00078	2.80	0.68
0.00039	1.60	0.45
0.00021	0.96	0.34

Table 14. Effect of Varying Initial Bubble Size on Linear Model's Oxygen Transfer Predictions for Gas Flowrate Equal to 0.0017 Nm³/s.

	Initial Bubble Radius = 0.00132 m	Initial Bubble Radius = 0.00189 m	Initial Bubble Radius = 0.00246 m
Predicted Oxygen Imparted to Water (mg/L-min)	5.48	5.35	5.27

based on Wen's data. Wen did not provide vertical plume velocity data with which the Froude number could be calibrated for his experiments.

Linear Plume Model vs. TVA Data.

A limited amount of temperature and dissolved oxygen concentration data was available for Blue Ridge Reservoir in Tennessee for comparison with the linear model. While this data did not allow a comprehensive test of the linear model under full scale conditions, it did give an indication of how well the model predicted the temperature and dissolved oxygen concentration in the plume. Table 15 compares the predicted and measured values. The results showed that the model tended to underpredict the oxygen that dissolved into the plume water and to overpredict the effect of the rising plume on temperature. The measured values indicated that the plume temperature was nearly identical to that in the surrounding water. The temperatures predicted by the model were not as strongly affected by the surrounding water temperature except at the diffuser depth. The measured dissolved oxygen concentration decreased as the plume ascended from 30.0m below the surface to 23.5m below the surface. This is likely due to dilution from surrounding water. Therefore, it is possible that the entrainment coefficient used in the linear model is not appropriate in this situation.

Again, the possibility exists that the reason for the discrepancies was that the Froude number, which was derived for a circular rather than a linear source, was incorrect. However, varying the Froude number between 0.5 and 2.0 did not result in correct predictions, although decreasing the Froude number below 1.6 did produce slightly more accurate dissolved oxygen predictions. Another possible reason for the discrepancies is that the available temperature and

Table 15. Comparison of Linear Model Oxygen and Plume Temperature Predictions to TVA (1994) Measured Data.

	Predicted Values	Measured Data	Percent Error
Dissolved Oxygen (mol/m³) at 35.0m Depth	0.123	0.127	3.25
Dissolved Oxygen (mol/m³) at 30.0m Depth	0.124	0.170	37.1
Dissolved Oxygen (mol/m³) at 23.5m Depth	0.125	0.150	20.0
Plume Temperature (C) at 35.0m Depth	18.40	18.40	0.0
Plume Temperature (C) at 30.0m Depth	18.40	19.10	3.80
Plume Temperature (C) at 23.5m Depth	18.53	19.75	6.58

dissolved oxygen profiles were incomplete and that the dissolved solids and dissolved nitrogen profiles were estimated from the literature. The sensitivity of the model to temperature through the density equation has already been discussed; thus the limited ambient temperature data provided could have resulted in less accurate predictions of plume behavior. However, as the error in all but one measured compared to predicted value was 20 percent or less, the model did appear to provide reasonable predictions.

Sensitivity Analyses.

The sensitivity analyses performed on the revised circular model and the linear model produced similar results. Wuest *et al.* (1992) noted that the best conditions under which to examine the effects of various factors on the height of maximum plume rise were the July conditions as the plume rose to the lake surface under November conditions. Therefore, only the July conditions were considered here. Wuest *et al.* found that, based on the effect on maximum plume rise height, their model was most sensitive to initial bubble radius and gas input rate. Both the circular and the linear models show sensitivity to these parameters, especially at small bubble sizes and low gas input rates. (See Figures 33 and 34.) The models were not found to be overly sensitive to initial area (Figure 35), except perhaps at small initial areas, or Froude number (Figure 36), although a 5 meter difference in plume rise height was obtained by doubling the Froude number from 1.0 to 2.0. Varying the entrainment coefficient from 0.05 to 0.2 had a greater effect on the linear model than on the circular model, decreasing the circular model's maximum rise height by approximately 8 meters and the linear model's by over 10 meters (Figure 37).

The effects of changing the ambient profiles required by the models were investigated as well. The effects on the circular model and linear models are shown in Figures 38-45. The

temperature profile was altered by 1.0, 2.0, and 5.0 degrees in either direction. The slope of the profiles was changed as well so that the temperature increased more rapidly from the bottom to the top of the water body (denoted "T more with H" on the axis label) and less rapidly from the bottom to the top ("T less with H"). The dissolved solids, oxygen, and nitrogen profiles were altered by the amounts shown on the graphs. Each graph shows the original height of maximum plume rise without any changes in the profiles; these are designated T, S, O₂, and N₂ on the axis labels. As shown in the figures, only changes in the temperature profile had a noticeable effect on the height of maximum plume rise. Changes in the salinity profile produced almost no effect. This illustrates the necessity of obtaining an accurate temperature profile for a lake or reservoir in which the circular or linear model is to be implemented.

The model is sensitive to temperature due to the density equation. The sensitivity of the models to the density equation has already been demonstrated. As shown in Table 4, the density is highly dependent upon temperature. Salinity plays a role as well, but only a very small one.

In summary, then, the linear and circular models are most sensitive to the ambient temperature profile. The models are quite sensitive to initial bubble radius, especially for small bubbles (radius less than 0.01m), and to gas input rate, particularly for low input rates. Varying the entrainment coefficient or the Froude number affect the models' predictions as well. Initial plume area, ambient salinity, ambient dissolved oxygen, and ambient dissolved nitrogen profiles have very little effect on the predictions.

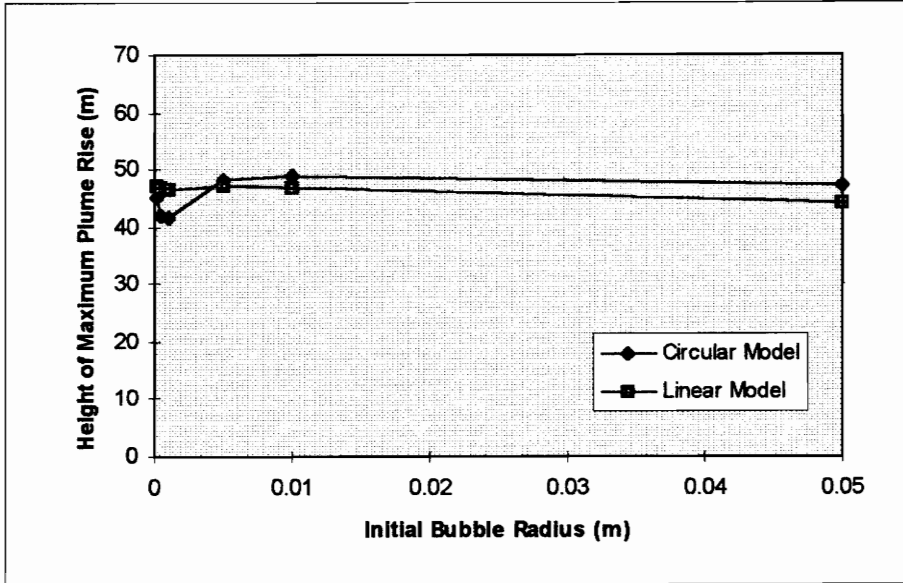


Figure 33. Sensitivity of Maximum Plume Rise Height to Initial Bubble Radius for Circular and Linear Models.

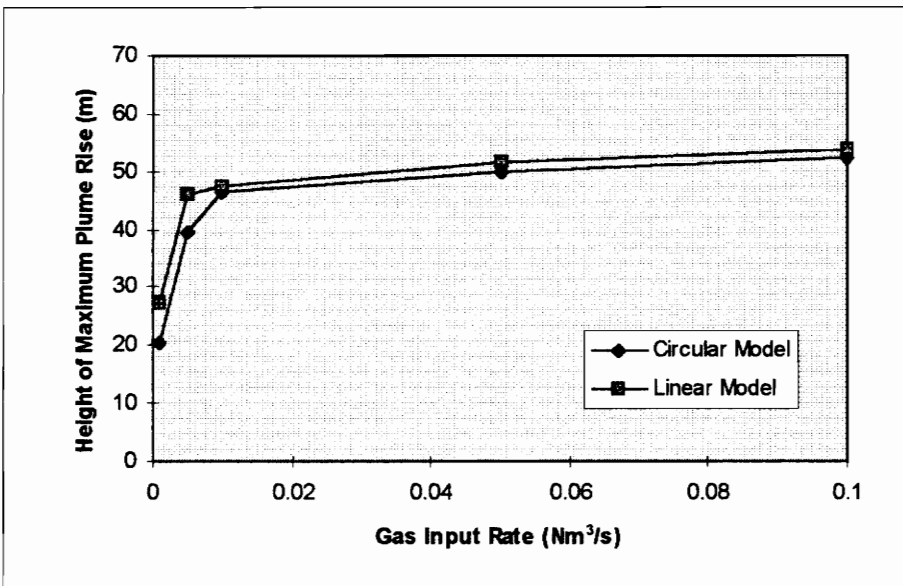


Figure 34. Sensitivity of Maximum Plume Rise Height to Gas Input Rate for Circular and Linear Models.

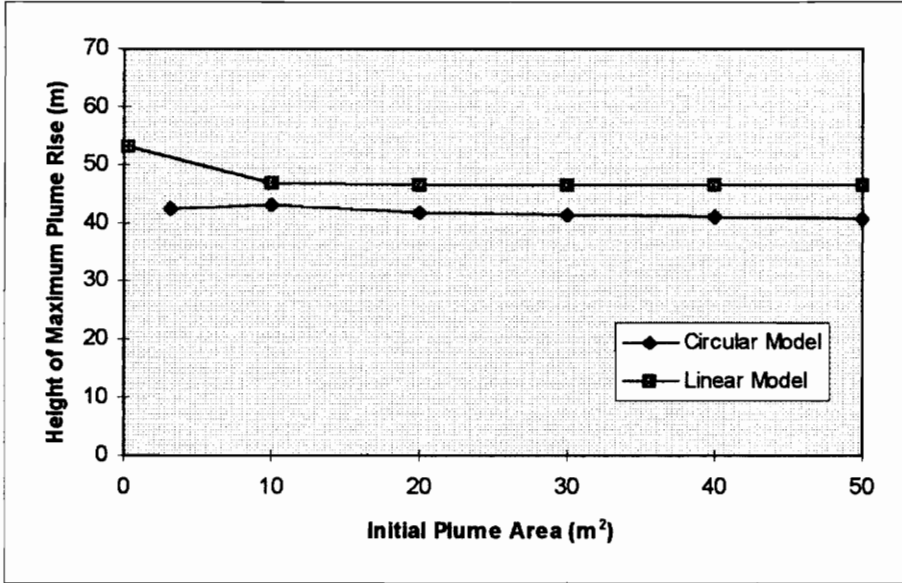


Figure 35. Sensitivity of Maximum Plume Rise Height to Initial Plume Area for Circular and Linear Models.

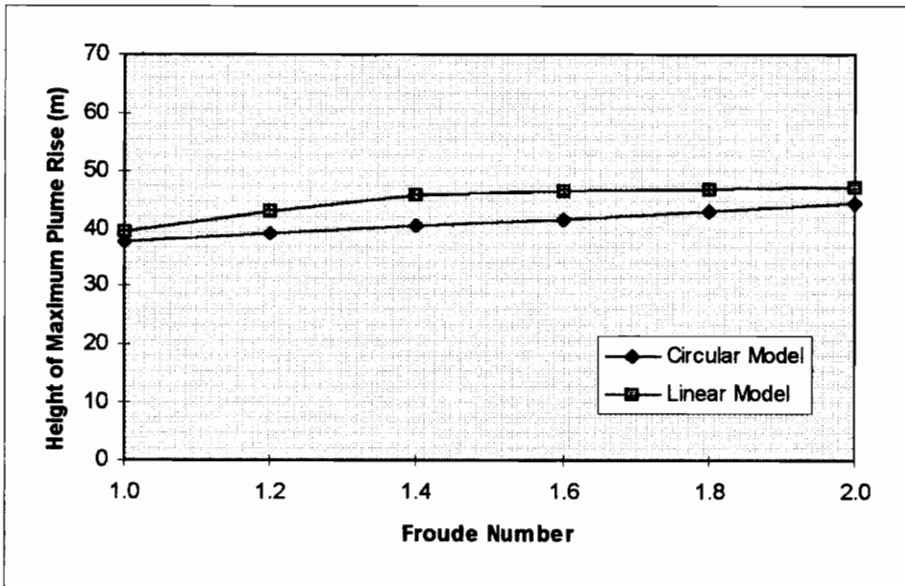


Figure 36. Sensitivity of Maximum Plume Rise Height to Froude Number for Circular and Linear Models.

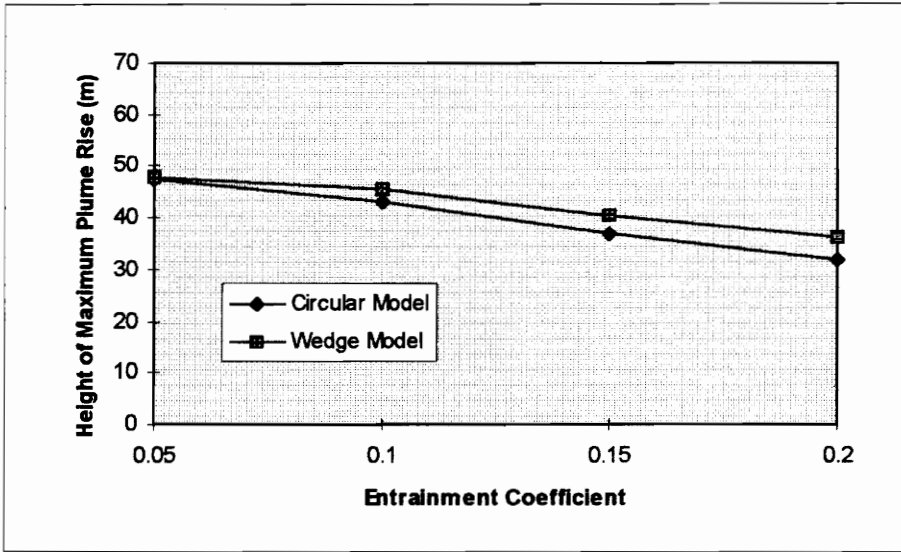


Figure 37. Sensitivity of Maximum Plume Rise Height to Entrainment Coefficient for Circular and Linear Models.

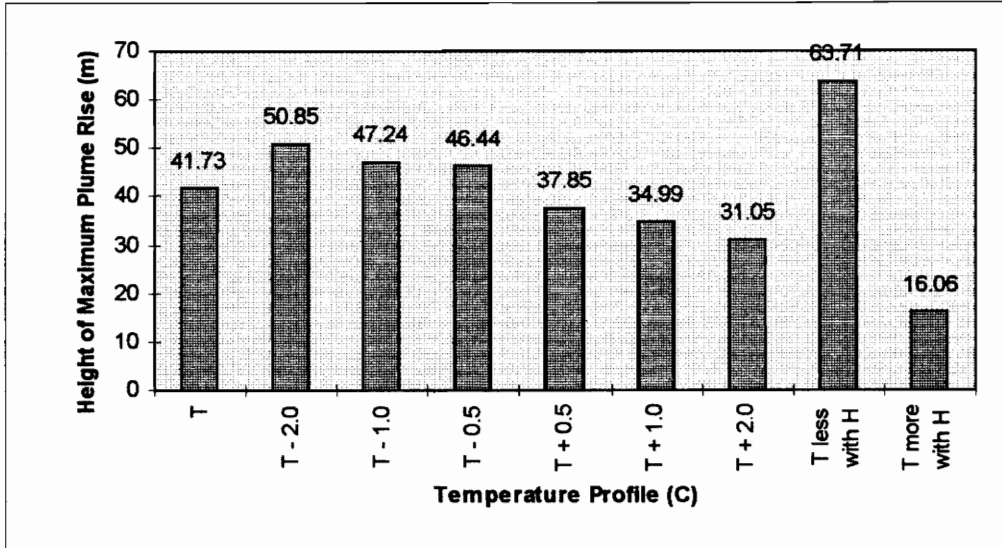


Figure 38. Sensitivity of Maximum Plume Rise Height to Ambient Temperature Profile for Circular Plume Model.

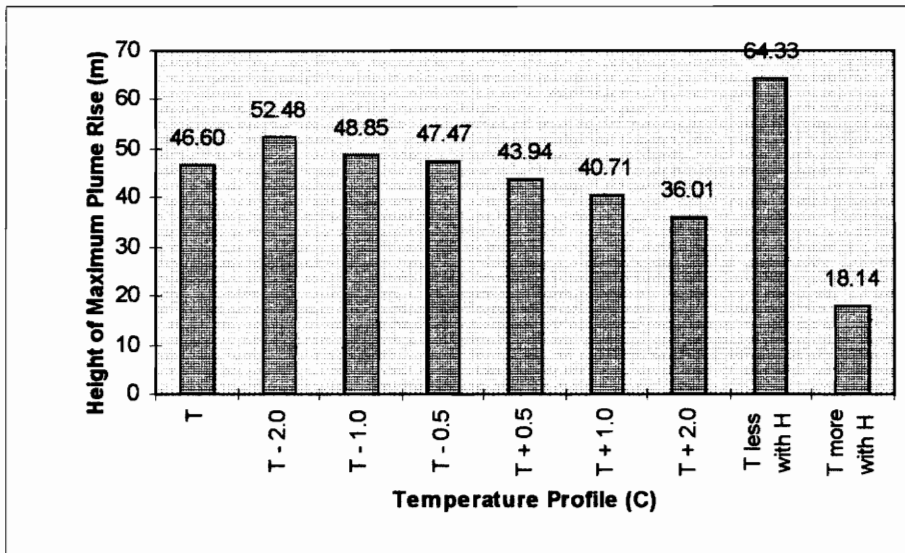


Figure 39. Sensitivity of Maximum Plume Rise Height to Ambient Temperature Profile for Linear Plume Model.

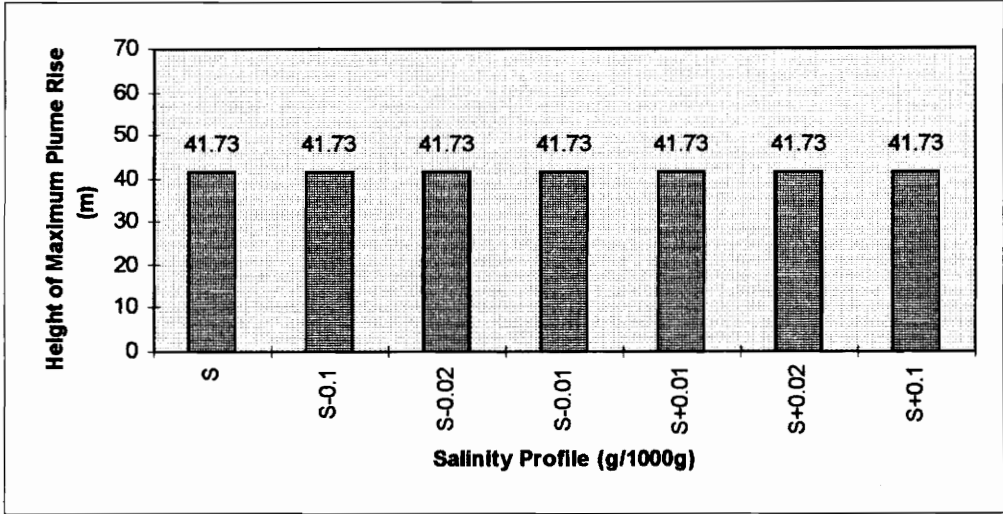


Figure 40. Sensitivity of Maximum Plume Rise Height to Ambient Dissolved Solids Profile for Circular Plume Model.

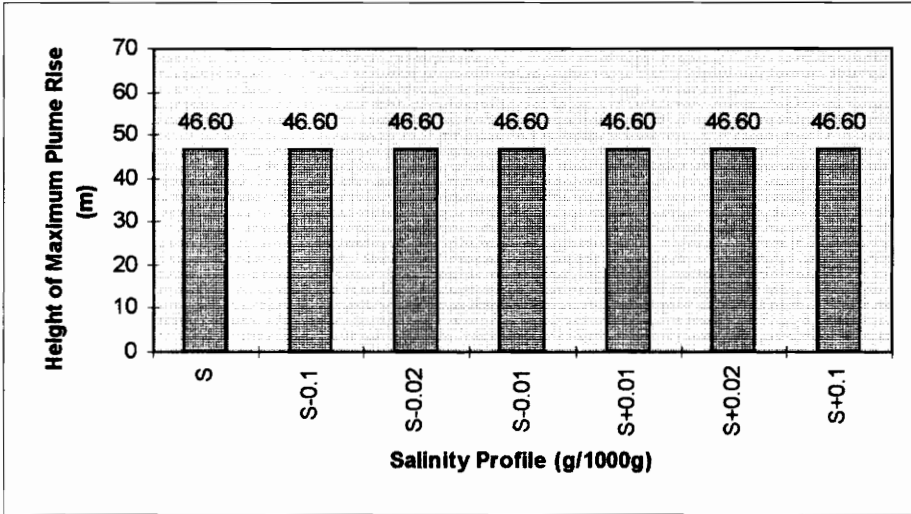


Figure 41. Sensitivity of Maximum Plume Rise Height to Ambient Dissolved Solids Profile for Linear Plume Model.

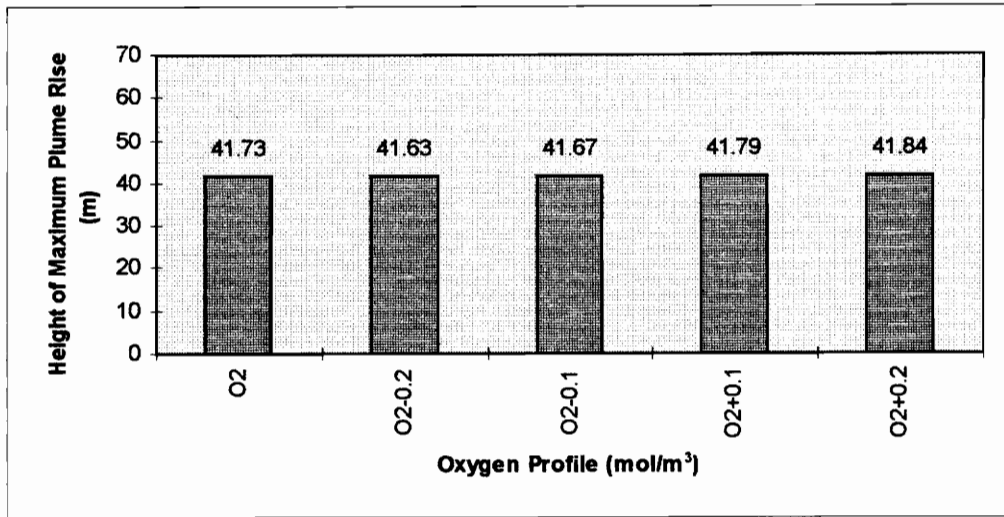


Figure 42. Sensitivity of Maximum Plume Rise Height to Ambient Dissolved Oxygen Profile for Circular Plume Model.

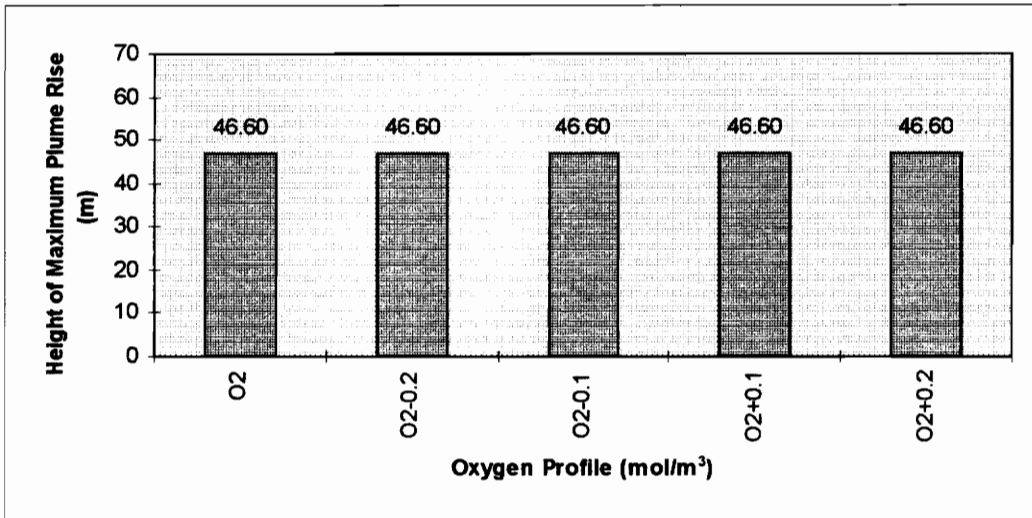


Figure 43. Sensitivity of Maximum Plume Rise Height to Ambient Dissolved Oxygen Profile for Linear Plume Model.

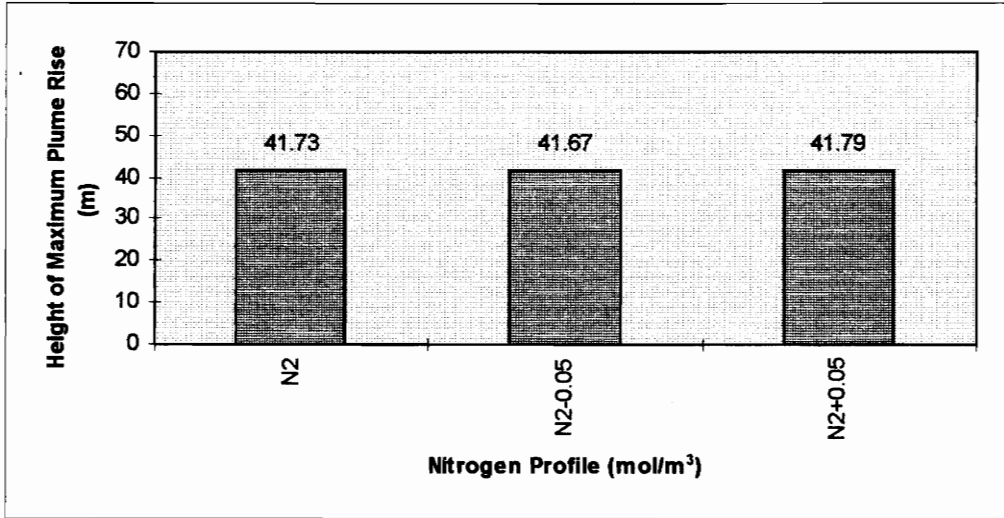


Figure 44. Sensitivity of Maximum Plume Rise Height to Ambient Dissolved Nitrogen Profile for Circular Plume Model.

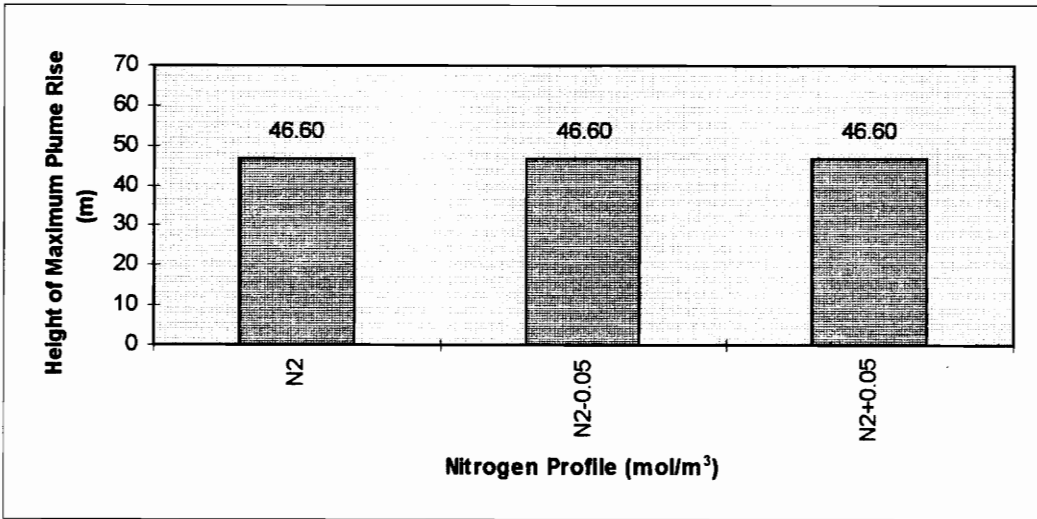


Figure 45. Sensitivity of Maximum Plume Rise Height to Ambient Dissolved Nitrogen Profile for Linear Plume Model.

V. SUMMARY AND CONCLUSIONS

The purposes of this research were first to implement the circular plume model developed by Wuest *et al.* (1992) and second to develop and verify a linear plume model based on the circular model. These objectives were achieved.

Based on the results presented in the Wuest *et al.* paper, the implementation of their model was successful. Results obtained from the circular model were comparable to the results presented in their paper, implying that the circular model performed as it was intended.

Comparisons of the linear model to the circular model indicated that the linear model also performed as intended. The assumption that entrainment at the ends of the plume could be neglected was verified except in the situation that the model was modified to be square, rather than linear, in configuration.

The use of the linear model to predict actual data measured in the laboratory and the field met with limited success. Comparisons of the model's predictions to plume velocity data collected by Provost (1973) resulted in errors of over 40 percent for a range of air flowrates and curves that did not reflect the shape of the data collected at various depths. However, changing Froude number from 1.6 to 0.5 resulted in less than 17 percent error for variable air flowrates and curves that captured the features of the data collected with variable depths. The linear model was found to greatly overpredict the amount of oxygen transferred to the water compared to Wen's (1974) data. Changing the Froude number affected the oxygen transfer predictions as well as the velocity predictions. Finally, a comparison of the linear model to a limited amount of temperature and dissolved oxygen concentration data collected in Blue Ridge Reservoir (TVA, 1994) was fairly

successful. With one exception, the model predicted the data to within 20 percent of the measured values.

Engineering Significance.

In a water body in which the ambient temperature, dissolved oxygen, dissolved nitrogen, and dissolved solids profiles are known and for a diffuser for which a good estimation of the initial bubble size can be made, this model can be used to predict the performance of the diffuser in the lake or reservoir. By running the model with a range of gas flowrates, the appropriate flowrate to achieve the desired height of maximum plume rise and oxygen transfer can be determined. The model may also help with diffuser selection by determining the best bubble size for aeration or destratification. Although bubble size is difficult to predict, it may be possible to select a diffuser known to produce the appropriate size bubbles for the required gas flowrate.

Recommendations.

It appears that the linear model can be used as a preliminary predictor of the performance of a bubble plume in a water body. However, a more thorough full scale test of the model is required before it should be used to design bubble plume systems. The major weakness of the linear model occurs in the prediction of initial plume velocity, as the Froude number used in the model was derived for a circular, rather than a linear, source. Once further study determines either the appropriate linear Froude number or a better method for estimating initial plume velocity, the linear model should accurately predict plume velocity, plume temperature, dissolved oxygen concentration, and height of maximum plume rise, thereby facilitating the design of linear diffused air hypolimnetic aeration and destratification systems in lakes and reservoirs.

LITERATURE CITED

- Abraham, G. (1960). "Jet Diffusion in Liquid of Greater Density." *Journal of the Hydraulics Division: Proceedings of the American Society of Civil Engineers*, 86, HY6, 1-13.
- Asaeda, T. and Imberger, J. (1993). "Structure of Bubble Plumes in Linearly Stratified Environments." *Journal of Fluid Mechanics*, 249, 35-57.
- Bernhardt, H. (1967). "Aeration of Wahnbach Reservoir without Changing the Temperature Profile." *Journal of the American Water Works Association*, 59, 8, 943-964.
- Bischof, F., Durst, F., Hofken, M., and Sommerfeld, M. (1994). "Theoretical Considerations about the Development of Efficient Aeration Systems for Activated Sludge." *Aeration Technology: ASME*, 187, 27-38.
- Boyce, W.E. and DiPrima, R.C. (1992). *Elementary Differential Equations and Boundary Value Problems: Fifth Edition*. John Wiley and Sons, Inc., New York, 680p.
- Bulson, P.S. (1968) "The Theory and Design of Bubble Breakwaters." *Proceedings of the 11th Coastal Engineering Conference*, London, England, 995-1015.
- Cederwall, K. and Ditmars, J.D. (1970). "Analysis of Air-Bubble Plumes." *W.M. Kech Laboratory Report No. KH-R-24*, California Institute of Technology, Pasadena, California.
- Chen, C.J. and Rodi, W. (1976). "A Review of Experimental Data of Vertical Turbulent Buoyant Jets." *Iowa Institute of Hydraulic Research Report No. 193*, University of Iowa, Iowa City, Iowa.
- Cole, G.A. (1983). *Textbook of Limnology: Third Edition*. Waveland Press, Inc., Prospect Heights, IL, 401p.
- Cooke, G.D., Welch, E.B., Peterson, S.A., and Newroth, P.R. (1993). *Restoration and Management of Lakes and Reservoirs: Second Edition*. Lewis Publishers, Boca Raton, FL, 548p.
- Cooke, G.D. and Carlson, R.E. (1989). *Reservoir Management for Water Quality and THM Precursor Control*. AWWA Research Foundation, Denver, CO, 387p.
- Durst, F., Schonung, B., Selanger, K., and Winter, M. (1986). "Bubble-Driven Liquid Flows." *Journal of Fluid Mechanics*, 170, 53-82.
- Fannelop, T.K., Hirschberg, S., and Kuffer, J. (1991). "Surface Current and Recirculating Cells Generated by Bubble Curtains and Jets." *Journal of Fluid Mechanics*, 229, 629-657.

- Fischer, H.B., List, E.J., Koh, R.C.Y., Imberger, J., and Brooks, N.H. (1979). *Mixing in Inland and Coastal Waters*. Academic Press, Inc., Boston, MA, 483p.
- Hussain, N.A. and Narang, B.S. (1977). "Analysis of Two-Dimensional Air-Bubble Plumes." *American Institute of Chemical Engineers Journal*, 23,4, 596-599.
- Jones, W.T. (1972). "Air Barriers as Oil-Spill Containment Devices." *Society of Petroleum Engineers Journal*, 12, 2, 126-142.
- Kobus, H.E. (1968) "Analysis of the Flow Induced by Air-Bubble Systems." *Proceedings of the 11th Coastal Engineering Conference, London, England*, 995-1015.
- Kortmann, R.W, Knoecklein, G.W, and Bonnell, C.H. (1994). "Aeration of Stratified Lakes: Theory and Practice." *Lake and Reservoir Management*, 8, 2, 99-120.
- Kotsovinos, N.E. and List, E.L. (1977). "Plane Turbulent Buoyant Jets. Part 1. Integral Properties." *Journal of Fluid Mechanics*, 81, 1, 25-44.
- Laureshen, C.J. and Rowe, R.D. (1987). Modeling of Plane Bubble Plumes. *Buoyant Plumes*, The 24th National Heat Transfer Conference and Exhibition, August 9-12, 1987, 15-22.
- Leitch, A.M. and Baines, W.D. (1989). "Liquid Volume Flux in a Weak Bubble Plume." *Journal of Fluid Mechanics*, 205, 77-98.
- Lide, D.L., ed. (1995). *CRC Handbook of Chemistry and Physics: 76th Edition*. CRC Press, Boca Raton, FL.
- Lorenzen, M.W. and Fast, A.W. (1977). "A guide to Aeration/Circulation Techniques for Lake Management." Environmental Resources Services, EPA- 600/3-77-004, USEPA, Washington, D.C.
- McDougall, T.J. (1978). "Bubble Plumes in Stratified Environments." *Journal of Fluid Mechanics*, 85, 4, 655-672.
- Milgram, J.H. (1983). "Mean Flow in Round Bubble Plumes." *Journal of Fluid Mechanics*, 113, 345-376.
- Mobley, M.H. and Brock, W.G. (1996). "Aeration of Reservoirs and Releases Using TVA Porous Hose Line Diffuser." submitted to ASCE North American Congress on Water and Environment, Anaheim, CA June 22-28, 1996.
- Morton, (1959). "Forced Plumes." *Journal of Fluid Mechanics*, 5, 1, 151-163.
- Orlob, G.T., ed. (1983). *Mathematical Modeling of Water Quality: Streams, Lakes, and Reservoirs*. John Wiley and Sons, Chichester, Great Britain, 518p.

- Priven, M., Atkinson, J.F., Bemporad, G.A., and Rubin, H. (1995). "Theoretical Study of a Laminar Jet in a Double Diffusion Environment." *Journal of Fluids Engineering*, 117, 3, 341-354.
- Provost, R.L. (1973). *Circulation and Flows in Water Tanks Induced by the Release of Air from a Manifold*. Master's Thesis, University of New Hampshire.
- Rayyan, F. and Speece, R.E. (1977). "Hydrodynamics of Bubble Plumes and Oxygen Absorption in Stratified Impoundments." *Progress in Water Technology*, 9, 129-142.
- Rouse, H., Yih, C.S., and Humphreys, H.W., (1952). "Gravitational Convection from a Boundary Source." *Tellus*, 4, 201-210.
- Schladow, S.G. (1992). "Bubble Plume Dynamics in a Stratified Medium and the Implications for Water Quality Amelioration in Lakes." *Water Resources Research*, 28, 2, 313-321.
- Schladow, S.G. (1993). "Lake Destratification by Bubble-Plume Systems: Design Methodology." *Journal of Hydraulic Engineering*, 119, 3, 350-368.
- Sincero, A.P. and Sincero, G.A. (1996). *Environmental Engineering: A Design Approach*. Prentice Hall, Upper Saddle River, NJ, 795p.
- Snoeyink, V.L. and Jenkins, D. (1980). *Water Chemistry*. John Wiley and Sons, New York, NY, 463p.
- Speece, R.E. and Murfee, G. (1973). "Hypolimnetic Aeration with Commercial Oxygen. Volume II: Bubble Plume Gas Transfer." Environmental Protection Technology Series No. EPA-660/2-73-025b, USEPA, Washington, D.C.
- Speece, R.E. and Rayyan, F. (1973). "Hypolimnetic Aeration with Commercial Oxygen. Volume I: Dynamics of Bubble Plume." Environmental Protection Technology Series No. EPA-660/2-73-025a, USEPA, Washington, D.C.
- Tennessee Valley Authority (TVA) (1994). Field Data.
- Tsang, G. (1984). "Modelling [sic] Criteria for Bubble Plumes - A Theoretical Approach." *Canadian Journal of Civil Engineering*, 11, 293-298.
- Tsang, G. (1990). "Theoretical Investigation of Oxygenating Bubble Plumes." *Air-Water Mass Transfer*, Selected Papers from the Second International Symposium on Gas Transfer at Water Surfaces, September 11-14, 1990, Minneapolis, MN, 715-727.
- Wen, C.J. (1974). *An Experimental Study of Flow and Oxygen Transfer in Circulation Induced by Air Bubble Plumes*. Master's Thesis, University of New Hampshire.

- Wilkinson, D.L. (1979). "Two-Dimensional Bubble Plumes." *Journal of the Hydraulics Division, Proceedings of the American Society of Civil Engineers*, 105, HY2, 139-154.
- Wuest, A., Brooks, N.H., and Imboden, D.M. (1992). "Bubble Plume Modeling for Lake Restoration." *Water Resources Research*, 28, 12, 3235-3250.
- Wuest, A. (1996). Personal Communication.

APPENDIX A
AMBIENT PROFILES

Temperature Profiles.

Table A-1. July Temperature Profiles.

	Height of Top of Region above Diffuser (m)	Profile (T in C)
Hypolimnion	5.12	$T = 5.43$
Metalimnion	46.36	$T = -1.0 \times 10^{-7} z^4 + 3.4 \times 10^{-5} z^3 - 1.99 \times 10^{-3} z^2 + 5.05 \times 10^{-2} z + 5.25$
Epilimnion	65.0 (lake surface)	$T = 8.13 \times 10^{-4} z^4 - 0.172z^3 + 13.59z^2 - 4.78 \times 10^2 z + 6.301 \times 10^3$

Table A-2. November Temperature Profiles.

	Height of Top of Region above Diffuser (m)	Profile (T in C)
Hypolimnion	34.63	$T = -2.0 \times 10^{-6} z^4 + 1.37 \times 10^{-4} z^3 - 2.47 \times 10^{-3} z^2 + 2.00 \times 10^{-2} z + 6.175$
Metalimnion	50.0	$T = 4.0 \times 10^{-6} z^3 - 1.39 \times 10^{-4} z^2 + 9.73 \times 10^{-3} z + 6.172$
Epilimnion	65.0 (lake surface)	$T = 4.0 \times 10^{-6} z^3 - 1.39 \times 10^{-4} z^2 + 9.73 \times 10^{-3} z + 6.172$

Dissolved Solids Profiles.

Table A-3. July Dissolved Solids Profiles.

	Height of Top of Region above Diffuser (m)	Profile (S in g/1000g)
Hypolimnion	20.0	$S = 1.08 \times 10^{-8} z^4 - 1.15 \times 10^{-6} z^3 + 4.01 \times 10^{-5} z^2 - 5.04 \times 10^{-4} z + 0.389$
Metalimnion	50.0	
Epilimnion	65.0 (lake surface)	

Table A-4. November Dissolved Solids Profiles.

	Height of Top of Region above Diffuser (m)	Profile (S in g/1000g)
Hypolimnion	25.57	$S = -4.2 \times 10^{-8} z^4 + 1.72 \times 10^{-6} z^3 - 1.37 \times 10^{-5} z^2 - 1.68 \times 10^{-4} z + 0.370$
Metalimnion	49.06	$S = 2.98 \times 10^{-7} z^4 - 4.60 \times 10^{-5} z^3 + 2.50 \times 10^{-3} z^2 - 5.84 \times 10^{-2} z + 0.867$
Epilimnion	65.0 (lake surface)	$S = -3.79 \times 10^{-6} z^3 + 6.44 \times 10^{-4} z^2 - 3.63 \times 10^{-2} z + 1.002$

Dissolved Oxygen Profiles.

Table A-5. July Dissolved Oxygen Profiles.

	Height of Top of Region above Diffuser (m)	Profile (O_2 in mol/m³)
Hypolimnion	30.0	$O_2 = 5.18 \times 10^{-7} z^4 - 3.14 \times 10^{-5} z^3 + 3.12 \times 10^{-4} z^2 + 6.64 \times 10^{-3} z + 0.175$
Metalimnion	55.0	$O_2 = 6.66 \times 10^{-7} z^4 - 1.17 \times 10^{-4} z^3 + 7.68 \times 10^{-3} z^2 - 0.224z + 2.718$
Epilimnion	65.0 (lake surface)	$O_2 = 0.525$

Table A-6. November Dissolved Oxygen Profiles.

	Height of Top of Region above Diffuser (m)	Profile (O_2 in mol/m³)
Hypolimnion	56.0	$O_2 = -8.8 \times 10^{-8} z^4 + 1.17 \times 10^{-5} z^3 - 4.71 \times 10^{-4} z^2 + 7.87 \times 10^{-3} z + 0.200$
Metalimnion	63.0	$O_2 = 1.06 \times 10^{-3} z^2 - 8.58 \times 10^{-2} z + 1.927$
Epilimnion	65.0 (lake surface)	$O_2 = 8.9 \times 10^{-7} - 2.00 \times 10^{-4} z^3 + 1.68 \times 10^{-2} z^2 - 0.625z + 8.901$

Dissolved Nitrogen Profiles.

July and November.

$N_2 = 0.714 \text{ mol/m}^3$ throughout depth of lake for both seasons.

APPENDIX B

CIRCULAR PLUME PROGRAM

PROGRAM CIRCPLUME

C define variables
C rad = radius of plume (=radius of diffusor unit initially)
C w = vertical velocity of the plume water
C mu = volume flux of plume water
C T = temperature
C S = total dissolved solids
C dens = density
C am = ambient
C pl = plume
C plw = plume water
C conco = concentration of dissolved oxygen
C concn = concentration of dissolved nitrogen
C mo = concentration of gaseous oxygen
C mn = concentration of gaseous nitrogen
C mom = momentum flux
C FT = temperature flux
C FS = TDS flux
C disso = dissolved oxygen flux
C dissn = dissolved nitrogen flux
C gaso = gaseous oxygen flux
C gasn = gaseous nitrogen flux
C z = vertical direction
C zsurf = height from water surface to diffusor (measured up
C from the diffusor)
C press = pressure (total)
C presso, pressn = partial pressures of oxygen and nitrogen
C vg = volume of gas
C bubrad = bubble radius
C numbub = number of bubbles
C numbub = real number for numbub
C bubslp = bubble slip velocity
C betao, betan = gas transfer coefficient for oxygen and nitrogen
C Ko, Kn = solubility constant for oxygen and nitrogen
C alpha = entrainment coefficient
C lambda = wedge width ratio
C airin = air input rate from the pump at the surface
C psurf = atmospheric pressure at the lake surface
C densave = average density of the lake water
C amopro, amnpro = ambient oxygen and nitrogen profiles
C g = acceleration due to gravity

C R = gas constant

REAL*8 w, mu, T, S, densam, denspl, densplw, conco,
+concn, mo, mn, mom, FT, FS, disso, dissn, gaso, gasn, z, zsurf,
+press, presso, pressn, vg, bubrad, bubslp, betao, betan,
+Ko, Kn, alpha, lambda, mu0, mom0, FT0, FS0, moles, mumbub,
+disso0, dissn0, bubrad0, airin, psurf, densave, g, R, Pi, dmudz,
+dmomdz, dFTdz, dFSdz, dDOdz, dDNdz, dGODz, dGNdz, amTpro, amSpro, amopro,
+amnpro, aTh, bTh, cTh, dTh, eTh, aTm, bTm, cTm, dTm, eTm, aTe, bTe, cTe, dTe,
+eTe, aSh, bSh, cSh, dSh, eSh, aSm, bSm, cSm, dSm, eSm, aSe, bSe, cSe, dSe, eSe,
+aOh, bOh, cOh, dOh, eOh, aOm, bOm, cOm, dOm, eOm, aOe, bOe, cOe, dOe, eOe,
+aNh, bNh, cNh, dNh, eNh, aNm, bNm, cNm, dNm, eNm, aNe, bNe, cNe, dNe, eNe, rad,
+frac, nfrac

INTEGER I, numbub, Count, frac, season

C Constants

g = 9.81
alpha = 0.11
lambda = 0.8
R = 8.314
Pi = 3.1415927

C Input all known numbers

Write(*,*) "Enter the radius of the diffusor unit in meters."
Read(*,*) rad
Write(*,*) "Enter the air or oxygen input rate in m³/s,
+normalized to 1 m³ gas at 1 bar and 0 degrees C."
Read(*,*) airin
Write(*,*) "If the gas to be used is pure oxygen, enter 1.
+If the gas is air, enter 2."
Read(*,*) frac
Write(*,*) "Enter the initial radius of the bubbles produced
+in meters."
Read(*,*) bubrad0
Write(*,*) "Enter the pressure at the lake surface in bars.
+(1 atm = 1.013 bars.)"
Read(*,*) psurf
Write(*,*) "Enter the average density of the lake water."
Read(*,*) densave

C Input the temperature profile

Write(*,*) "Enter the temperature of the ambient water at the
+diffusor depth."
Read(*,*) amTpro

```
Write(*,*) "Enter the coefficients for the equation for the
+ temperature profile in the hypolimnion in the form  $ez^4 +$ 
+ $az^3 + bz^2 + cz + d$ . Separate the coefficients by commas."
Read(*,*) eTh, aTh, bTh, cTh, dTh
Write(*,*) "Enter the upper depth of the hypolimnion based on
+the temperature profile in meters, measured up from the diffusor
+depth."
Read(*,*) zTh
```

```
Write(*,*) "Enter the coefficients for the equation for the
+ temperature profile in the metalimnion in the form  $ez^4 +$ 
+ $az^3 + bz^2 + cz + d$ . Separate the coefficients by commas."
Read(*,*) eTm, aTm, bTm, cTm, dTm
Write(*,*) "Enter the upper depth of the metalimnion based on
+the temperature profile in meters, measured up from the diffusor
+depth."
Read(*,*) zTm
```

```
Write(*,*) "Enter the coefficients for the equation for the
+ temperature profile in the epilimnion in the form  $ez^4 +$ 
+ $az^3 + bz^2 + cz + d$ . Separate the coefficients by commas."
Read(*,*) eTe, aTe, bTe, cTe, dTe
Write(*,*) "Enter the upper depth of the epilimnion based on
+the temperature profile in meters, measured up from the diffusor
+depth. This should correspond with the lake surface."
Read(*,*) zTe
```

```
zsurf = zTe
```

C Input the salinity profile

```
Write(*,*) "Enter the total dissolved solids content of
+the ambient water at the diffusor depth in mass solids
+(micrograms) per mass water (grams)."
Read(*,*) amSpro
Write(*,*) "Enter the coefficients for the equation for the
+salinity profile in the hypolimnion in the form  $ez^4 +$ 
+ $az^3 + bz^2 + cz + d$ . Separate the coefficients by commas."
Read(*,*) eSh, aSh, bSh, cSh, dSh
Write(*,*) "Enter the upper depth of the hypolimnion based on
+the salinity profile in meters, measured up from the diffusor
+depth."
Read(*,*) zSh
```

```
Write(*,*) "Enter the coefficients for the equation for the
+salinity profile in the metalimnion in the form  $ez^4 +$ 
+ $az^3 + bz^2 + cz + d$ . Separate the coefficients by commas."
```

Read(*,*) eSm, aSm, bSm, cSm, dSm
Write(*,*) "Enter the upper depth of the metalimnion based on
+the salinity profile in meters, measured up from the diffuser
+depth."
Read(*,*) zSm

Write(*,*) "Enter the coefficients for the equation for the
+salinity profile in the epilimnion in the form ez^4
+ $az^3 + bz^2 + cz + d$. Separate the coefficients by commas."
Read(*,*) eSe, aSe, bSe, cSe, dSe
Write(*,*) "Enter the upper depth of the epilimnion based on
+the salinity profile in meters, measured up from the diffuser
+depth. This should correspond with the lake surface."
Read(*,*) zSe

C Input the dissolved oxygen profile

Write(*,*) "Enter the dissolved oxygen concentration in
+the ambient water at the diffuser depth in mol per m^3 ."
Read(*,*) amopro
Write(*,*) "Enter the coefficients for the equation for the
+oxygen profile in the hypolimnion in the form ez^4
+ $az^3 + bz^2 + cz + d$. Separate the coefficients by commas."
Read(*,*) eOh, aOh, bOh, cOh, dOh
Write(*,*) "Enter the upper depth of the hypolimnion based on
+the oxygen profile in meters, measured up from the diffuser
+depth."
Read(*,*) zOh

Write(*,*) "Enter the coefficients for the equation for the
+oxygen profile in the metalimnion in the form ez^4
+ $az^3 + bz^2 + cz + d$. Separate the coefficients by commas."
Read(*,*) eOm, aOm, bOm, cOm, dOm
Write(*,*) "Enter the upper depth of the metalimnion based on
+the oxygen profile in meters, measured up from the diffuser
+depth."
Read(*,*) zOm

Write(*,*) "Enter the coefficients for the equation for the
+oxygen profile in the epilimnion in the form ez^4
+ $az^3 + bz^2 + cz + d$. Separate the coefficients by commas."
Read(*,*) eOe, aOe, bOe, cOe, dOe
Write(*,*) "Enter the upper depth of the epilimnion based on
+the oxygen profile in meters, measured up from the diffuser
+depth. This should correspond with the lake surface."
Read(*,*) zOe

```

C   Input the dissolved nitrogen profile
    Write(*,*) "Enter the dissolved nitrogen concentration in
+the ambient water at the diffuser depth in mol per m^3."
    Read(*,*) amnpro
    Write(*,*) "Enter the coefficients for the equation for the
+nitrogen profile in the hypolimnion in the form ez^4
+az^3 + bz^2 + cz + d. Separate the coefficients by commas."
    Read(*,*) eNh, aNh, bNh, cNh, dNh
    Write(*,*) "Enter the upper depth of the hypolimnion based on
+the nitrogen profile in meters, measured up from the diffuser
+depth."
    Read(*,*) zNh

    Write(*,*) "Enter the coefficients for the equation for the
+nitrogen profile in the metalimnion in the form ez^4
+az^3 + bz^2 + cz + d. Separate the coefficients by commas."
    Read(*,*) eNm, aNm, bNm, cNm, dNm
    Write(*,*) "Enter the upper depth of the metalimnion based on
+the nitrogen profile in meters, measured up from the diffuser
+depth."
    Read(*,*) zNm

    Write(*,*) "Enter the coefficients for the equation for the
+nitrogen profile in the epilimnion in the form ez^4
+az^3 + bz^2 + cz + d. Separate the coefficients by commas."
    Read(*,*) eNe, aNe, bNe, cNe, dNe
    Write(*,*) "Enter the upper depth of the epilimnion based on
+the nitrogen profile in meters, measured up from the diffuser
+depth. This should correspond with the lake surface."
    Read(*,*) zNe

```

C Calculate initial pressures, densities, ν , and num bub

```

z = 0
T = amTpro
S = amSpro
conco = amopro
concn = amnpro
Tsurf = 0.0
press = psurf+(1.0*10.0**(-5.0))*densave*g*(zsurf-z)

```

Froude = 1.6

```

C   Bubleslp:
    bubrad = bubrad0
    If (bubrad.LE.7.0*(10.0**(-4.0))) Then

```

```

    bubslp = 4474.0*(bubrad**1.357)
    Else if(7.0*(10.0**(-4.0)).LT.bubrad.AND.bubrad.LE.
+    5.1*(10.0**(-3.0)))Then
        bubslp = 0.23
    Else
        bubslp = 4.202*(bubrad**0.547)
Endif

If (frac.EQ.1) Then
    ofrac=1.0
Else If (frac.EQ.2) Then
    ofrac=0.21
Endif

If (frac.EQ.1) Then
    nfrac=0.0
Else If (frac.EQ.2) Then
    nfrac=0.78
Endif

moles=airin/((R*10.0**(-5.0))*(273.15))
gaso=moles*ofrac
gasn=moles*nfrac

Write(*,*)"Enter guess for initial plume velocity."
Read(*,*)wguess

presso = (gaso/(gaso+gasn))*press
pressn = (gasn/(gaso+gasn))*press

densam = -6.0*10.0**(-7.0)*T**4.0+0.0000853*T**3-0.0089173*T**2.0
++0.0672279*T+999.8430939+0.802*S

C  densam = (999.84298+(65.4891*T-8.56272*T**2.0+0.059385*T**3.0)*
C  +(1.0*10.0**(-3.0)))+0.802*S/1000.0+0.28

densplw = densam

w = wguess

DO 30 K=1,30,1
mo = gaso/(Pi*(rad**2.0)*(lambda**2.0)*(w+bubslp))
mn = gasn/(Pi*(rad**2.0)*(lambda**2.0)*(w+bubslp))

vg = ((mo+mn)/press)*(R*10.0**(-5.0))*(273.15+T)
denspl = (1.0-vg)*densplw

```

```
w = Froude*(SQRT(2.0*lambda*rad*g*((densam-denspl)/denspl)))
```

```
30 Continue
```

C Initial conditions

```
mu0 = Pi*(rad**2)*w  
mom0 = mu0*w  
FT0 = mu0*amTpro  
FS0 = (mu0*amSpro*densplw)/1000.0  
disso0 = mu0*amopro  
dissn0 = mu0*amnpro
```

```
denspl = (1-vg)*densplw  
numbub = (3.0*(vg)*(lambda**2.0)*(rad**2.0)*(w+bubslp))  
+/(4.0*(bubrad0**3.0))
```

```
numbub=numbub
```

```
If (bubrad.LE.0.000667) Then
```

```
    betao = 0.6*bubrad
```

```
    Else
```

```
        betao = 4.0*10.0**(-4)
```

```
Endif
```

```
betan = betao
```

```
Ko = 2.125-0.05021*T+(5.77*10.0**(-4.0))*T**2.0
```

```
Ko = 1.042-0.0245*T+(3.171*10.0**(-4.0))*T**2.0
```

```
Write(*,*) "Enter the number of intervals into which to divide  
+the depth of the lake in order to solve using Euler's Method."
```

```
Read(*,*) I
```

```
deltaz = zsurf/I
```

```
mu = mu0
```

```
mom = mom0
```

```
FT = FT0
```

```
FS = FS0
```

```
disso = disso0
```

```
dissn = dissn0
```

```
Count = 0
```

```
OPEN(6,file = 'pm')
```

```
Open(8,file='output.dat',status='new')
```

```

Write(8,62)"z","w","mu","mom","brad","T","amT","den","amden"
62 Format(1X,A1,8X,A1,6X,A2,4X,A3,4X,A4,5X,A1,5X,A3,3X,A3,4X,A5)

```

C DO LOOP STARTS HERE!!!

```
DO 100 J=1,I,1
```

```
z = z+deltaz
```

```
If (mom.LT.0.0) Then
```

```
Write(*,*)"Because momentum is negative at z=",z,"the change
+ in volume flux can no longer be calculated.Press enter to
+ continue."
```

```
Read(*,*)
```

```
Go To 1000
```

```
Else
```

```
Continue
```

```
Endif
```

```
dmudz=2.0*alpha*((Pi*mom)**0.5)
```

```
dmomdz=(((densam-denspl)/denspl)*g*(lambda**2.0)*((mu**2.0)/mom))
++((1.0-(lambda**2.0))*((densam-densplw)/denspl)*g*((mu**2.0)/mom))
```

```
dFTdz=2.0*alpha*((Pi*mom)**0.5)*amTpro
```

```
dFSdz=2.0*alpha*densam*(amSpro/1000.0)*((Pi*mom)**0.5)
```

```
dDOdz=2.0*alpha*((Pi*mom)**0.5)*amopro+((4.0*Pi*(bubrad**2.0)*
+rnumbub)/((mom/mu)+bubslp))*betao*((Ko*presso)-(disso/mu))
```

```
dDNdz=2.0*alpha*((Pi*mom)**0.5)*amnpro+((4.0*Pi*(bubrad**2.0)*
+rnumbub)/((mom/mu)+bubslp))*betan*((Kn*pressn)-(dissn/mu))
```

```
dGOdz=((-4.0*Pi*(bubrad**2.0)*rnumbub)/((mom/mu)+bubslp))*betao*
+((Ko*presso)-(disso/mu))
```

```
dGNdz=((-4.0*Pi*(bubrad**2.0)*rnumbub)/((mom/mu)+bubslp))*betan*
+((Kn*pressn)-(dissn/mu))
```

```
mu = mu+(dmudz*deltaz)
```

```
mom = mom+(dmomdz*deltaz)
```

```
FT = FT+(dFTdz*deltaz)
```

```
T=FT/mu
```

FS = FS+(dFSdz*deltaz)
S=(FS/(mu*densplw))*1000

disso = disso+(dDOdz*deltaz)

dissn = dissn+(dDNdz*deltaz)

gaso = gaso+(dGOdz*deltaz)

gasn = gasn+(dGNdz*deltaz)

If (z.LE.zTh)Then

amTpro = eTh*z**4.0+aTh*z**3.0+bTh*z**2.0+cTh*z+dTh

Else if (z.LE.zTm)Then

amTpro = eTm*z**4.0+aTm*z**3.0+bTm*z**2.0+cTm*z+dTm

Else

amTpro = eTe*z**4.0+aTe*z**3.0+bTe*z**2.0+cTe*z+dTe

Endif

If (z.LE.zSh)Then

amSpro = eSh*z**4.0+aSh*z**3.0+bSh*z**2.0+cSh*z+dSh

Else if (z.LE.zSm)Then

amSpro = eSm*z**4.0+aSm*z**3.0+bSm*z**2.0+cSm*z+dSm

Else

amSpro = eSe*z**4.0+aSe*z**3.0+bSe*z**2.0+cSe*z+dSe

Endif

If (z.LE.zOh)Then

amopro = eOh*z**4.0+aOh*z**3.0+bOh*z**2.0+cOh*z+dOh

Else if (z.LE.zOm)Then

amopro = eOm*z**4.0+aOm*z**3.0+bOm*z**2.0+cOm*z+dOm

Else

amopro = eOe*z**4.0+aOe*z**3.0+bOe*z**2.0+cOe*z+dOe

Endif

If (z.LE.zNh)Then

amnpro = eNh*z**4.0+aNh*z**3.0+bNh*z**2.0+cNh*z+dNh

Else if (z.LE.zNm)Then

amnpro = eNm*z**4.0+aNm*z**3.0+bNm*z**2.0+cNm*z+dNm

Else

amnpro = eNe*z**4.0+aNe*z**3.0+bNe*z**2.0+cNe*z+dNe

Endif

press = psurf+(1.0*10.0**(-5.0))*densave*g*(zsurf-z)

```

presso = (gaso/(gaso+gasn))*press
pressn = (gasn/(gaso+gasn))*press

```

```

If (mom.LT.0.0) Then
  Write(*,*)"Because momentum is negative at z=",z,"the change
+   in volume flux can no longer be calculated.Press enter to
+   end program."
  Read(*,*)
  Go To 1000
  Else
    Continue
  Endif

```

```
rad = SQRT((mu**2)/(mom*Pi))
```

```

densam = -6.0*10.0**(-7.0)*amTpro**4.0+0.0000853*amTpro**3.0
+0.0089173*amTpro**2.0+
+0.0672279*amTpro+999.8430939+0.802*amSpro

```

```

C   densam = (999.84298+(65.4891*amTpro-8.56272*amTpro**2.0+
C   +0.059385*amTpro**3.0)*(1.0*10.0**(-3.0)))+0.802*amSpro/1000.0+
C   +0.28

```

```

densplw = -6.0*10.0**(-7.0)*T**4.0+0.0000853*T**3.0-0.0089173*
+T**2.0+0.0672279*T+999.8430939+0.802*S

```

```

C   densplw = (999.84298+(65.4891*T-8.56272*T**2.0+
C   +0.059385*T**3.0)*(1.0*10.0**(-3.0)))+0.802*S/1000.0+0.28

```

```
w = mom/mu
```

```

If (w.LE.0.0)Then
  Write(*,*)"The plume velocity has reached zero at z=",z,".
+   Press enter to continue."
  Read(*,*)
  Else
    Continue
  Endif

```

```

C   This bubrad eqn is using previous bubsplp and vg!!
C   bubrad=(totvg/((4.0/3.0)*Pi*numbub))**(1.0/3.0)
  bubrad = ((vg*lambda**2*(rad**2)*(bubsplp+w))/
+((4.0/3.0)*rnumbub))**(1.0/3.0)

```

```

C   bubrad = ((vg*(mu*(1.0+mu*(bubsplp/mom))))/

```

```

C  +((4.0/3.0)*mumbub)**(1.0/3.0)
  If (bubrad.LE.0.0)Then
    Write(*,*)"The bubbles have completely dissolved. Press enter
+   to continue."
    Read(*,*)
  Endif

  If (bubrad.LE.(7.0*10.0**(-4.0))) Then
    bubslp = 4474.0*(bubrad**1.357)
    Else if ((7.0*10.0**(-4.0)).LT.bubrad.AND.bubrad.LE.
+   (5.1*10.0**(-3.0)))Then
      bubslp = 0.23
      Else
        bubslp = 4.202*(bubrad**0.547)
  Endif

C  mo = gaso/((mu)*(1.0+(mu*(bubslp/mom))))
C  mn = gasn/((mu)*(1.0+(mu*(bubslp/mom))))
mo = gaso/(Pi*(rad**2.0)*(lambda**2.0)*(w+bubslp))
mn = gasn/(Pi*(rad**2.0)*(lambda**2.0)*(w+bubslp))

vg = ((mo+mn)/press)*(R*10.0**(-5.0))*(T+273.15)

denspl = (1-vg)*densplw

If (bubrad.LE.6.67*(10.0**(-4.0)))Then
  betao = 0.6*bubrad
  Else
    betao = 4.0*(10.0**(-4.0))
  Endif

If (bubrad.LE.6.67*(10.0**(-4.0)))Then
  betan = 0.6*bubrad
  Else
    betan = 4.0*(10.0**(-4.0))
  Endif

Ko = 2.125-0.05021*T+5.77*(10.0**(-4.0))*T**2.0
Kn = 1.042-0.0245*T+3.171*(10.0**(-4.0))*T**2.0

Count = Count+1
IF (Count.EQ.5000)THEN
  Write(8,92)z,w,mu,mom,bubrad,T,amTpro,denspl-1000,densam-1000
92  Format(1X,F6.2,1X,F6.3,1X,F5.2,1X,F6.3,1X,E8.2,1X,F5.2,1X,
+   F5.2,1X,F6.3,1X,F6.3)
  Count = 0

```

ENDIF

100 Continue

1000 END

APPENDIX C

LINEAR PLUME PROGRAM

PROGRAM LINEPLUME

C define variables
C b = width of plume(width of diffuser unit initially)
C L = length of diffuser unit
C w = vertical velocity of the plume water
C mu = volume flux of plume water
C T = temperature
C S = total dissolved solids
C dens = density
C am = ambient
C pl = plume
C plw = plume water
C conco = concentration of dissolved oxygen
C concn = concentration of dissolved nitrogen
C mo = concentration of gaseous oxygen
C mn = concentration of gaseous nitrogen
C mom = momentum flux
C FT = temperature flux
C FS = TDS flux
C disso = dissolved oxygen flux
C dissn = dissolved nitrogen flux
C gaso = gaseous oxygen flux
C gasn = gaseous nitrogen flux
C z = vertical direction
C zsurf = height from water surface to diffuser (measured up
C from the diffuser)
C press = pressure (total)
C presso, pressn = partial pressures of oxygen and nitrogen
C vg = volume of gas
C bubrad = bubble radius
C numbub = number of bubbles
C numbub = real number for numbub
C bubslp = bubble slip velocity
C betao, betan = gas transfer coefficient for oxygen and nitrogen
C Ko, Kn = solubility constant for oxygen and nitrogen
C alpha = entrainment coefficient
C lambda = wedge width ratio
C airin = air input rate from the pump at the surface
C psurf = atmospheric pressure at the lake surface
C densave = average density of the lake water
C amopro, amnpro = ambient oxygen and nitrogen profiles

- C g = acceleration due to gravity
- C R = gas constant

```

REAL*8 w, mu, T, S, densam, denspl, densplw, conco,
+concn, mo, mn, mom, FT, FS, disso, dissn, gaso, gasn, z, zsurf,
+press, presso, pressn, vg, bubrad, bubslp, betao, betan,
+Ko, Kn, alpha, lambda, mu0, mom0, FT0, FS0, moles, mumbub,
+disso0, dissn0, bubrad0, airin, psurf, densave, g, R, Pi, dmudz,
+dmomdz, dFTdz, dFSdz, dDOdz, dDNdz, dGOdz, dGNdz, amTpro, amSpro, amopro,
+ammpro, aTh, bTh, cTh, dTh, eTh, aTm, bTm, cTm, dTm, eTm, aTe, bTe, cTe, dTe,
+eTe, aSh, bSh, cSh, dSh, eSh, aSm, bSm, cSm, dSm, eSm, aSe, bSe, cSe, dSe, eSe,
+aOh, bOh, cOh, dOh, eOh, aOm, bOm, cOm, dOm, eOm, aOe, bOe, cOe, dOe, eOe,
+aNh, bNh, cNh, dNh, eNh, aNm, bNm, cNm, dNm, eNm, aNe, bNe, cNe, dNe, eNe,
+ofrac, nfrac, L, b, b0, wguess

```

```

INTEGER I, num bub, Count, frac

```

C Constants

```

g = 9.81
alpha = 0.08
lambda = 0.85

```

C lambda and alpha from Fannelop et al.

```

R = 8.314
Pi = 3.1415927

```

C Input all known numbers

```

Write(*,*) "Enter the length of the diffusor unit in meters."
Read(*,*) L
Write(*,*) "Enter the width of the diffusor unit in meters."
Read(*,*) b0
Write(*,*) "Enter the air or oxygen input rate in m^3/s,
+normalized to 1 m^3 gas at 1 bar and 0 degrees C."
Read(*,*) airin
Write(*,*) "If the gas to be used is pure oxygen, enter 1.
+If the gas is air, enter 2."
Read(*,*) frac
Write(*,*) "Enter the initial radius of the bubbles produced
+in meters."
Read(*,*) bubrad0
Write(*,*) "Enter the pressure at the lake surface in bars.
+(1 atm = 1.013 bars.)"
Read(*,*) psurf
Write(*,*) "Enter the average density of the lake water."
Read(*,*) densave

```

C Input the temperature profile

```
Write(*,*) "Enter the temperature of the ambient water at the
+diffusor depth."
Read(*,*) amTpro
Write(*,*) "Enter the coefficients for the equation for the
+ temperature profile in the hypolimnion in the form  $ez^4 +
+az^3 + bz^2 + cz + d$ . Separate the coefficients by commas."
Read(*,*) eTh, aTh, bTh, cTh, dTh
Write(*,*) "Enter the upper depth of the hypolimnion based on
+the temperature profile in meters, measured up from the diffusor
+depth."
Read(*,*) zTh
Write(*,*) "Enter the coefficients for the equation for the
+ temperature profile in the metalimnion in the form  $ez^4 +
+az^3 + bz^2 + cz + d$ . Separate the coefficients by commas."
Read(*,*) eTm, aTm, bTm, cTm, dTm
Write(*,*) "Enter the upper depth of the metalimnion based on
+the temperature profile in meters, measured up from the diffusor
+depth."
Read(*,*) zTm
Write(*,*) "Enter the coefficients for the equation for the
+ temperature profile in the epilimnion in the form  $ez^4 +
+az^3 + bz^2 + cz + d$ . Separate the coefficients by commas."
Read(*,*) eTe, aTe, bTe, cTe, dTe
Write(*,*) "Enter the upper depth of the epilimnion based on
+the temperature profile in meters, measured up from the diffusor
+depth. This should correspond with the lake surface."
Read(*,*) zTe
```

zsurf = zTe

C Input the salinity profile

```
Write(*,*) "Enter the total dissolved solids content of
+the ambient water at the diffusor depth in mass solids
+(micrograms) per mass water (grams)."
Read(*,*) amSpro
Write(*,*) "Enter the coefficients for the equation for the
+salinity profile in the hypolimnion in the form  $ez^4
+az^3 + bz^2 + cz + d$ . Separate the coefficients by commas."
Read(*,*) eSh, aSh, bSh, cSh, dSh
Write(*,*) "Enter the upper depth of the hypolimnion based on
+the salinity profile in meters, measured up from the diffusor
+depth."
Read(*,*) zSh
```

```
Write(*,*) "Enter the coefficients for the equation for the
```

+salinity profile in the metalimnion in the form ez^4
 $+az^3 + bz^2 + cz + d$. Separate the coefficients by commas."
 Read(*,*) eSm, aSm, bSm, cSm, dSm
 Write(*,*) "Enter the upper depth of the metalimnion based on
 +the salinity profile in meters, measured up from the diffusor
 +depth."
 Read(*,*) zSm
 Write(*,*) "Enter the coefficients for the equation for the
 +salinity profile in the epilimnion in the form ez^4
 $+az^3 + bz^2 + cz + d$. Separate the coefficients by commas."
 Read(*,*) eSe, aSe, bSe, cSe, dSe
 Write(*,*) "Enter the upper depth of the epilimnion based on
 +the salinity profile in meters, measured up from the diffusor
 +depth. This should correspond with the lake surface."
 Read(*,*) zSe

C Input the dissolved oxygen profile
 Write(*,*) "Enter the dissolved oxygen concentration in
 +the ambient water at the diffusor depth in mol per m^3 ."
 Read(*,*) amopro
 Write(*,*) "Enter the coefficients for the equation for the
 +oxygen profile in the hypolimnion in the form ez^4
 $+az^3 + bz^2 + cz + d$. Separate the coefficients by commas."
 Read(*,*) eOh, aOh, bOh, cOh, dOh
 Write(*,*) "Enter the upper depth of the hypolimnion based on
 +the oxygen profile in meters, measured up from the diffusor
 +depth."
 Read(*,*) zOh

Write(*,*) "Enter the coefficients for the equation for the
 +oxygen profile in the metalimnion in the form ez^4
 $+az^3 + bz^2 + cz + d$. Separate the coefficients by commas."
 Read(*,*) eOm, aOm, bOm, cOm, dOm
 Write(*,*) "Enter the upper depth of the metalimnion based on
 +the oxygen profile in meters, measured up from the diffusor
 +depth."
 Read(*,*) zOm

Write(*,*) "Enter the coefficients for the equation for the
 +oxygen profile in the epilimnion in the form ez^4
 $+az^3 + bz^2 + cz + d$. Separate the coefficients by commas."
 Read(*,*) eOe, aOe, bOe, cOe, dOe
 Write(*,*) "Enter the upper depth of the epilimnion based on
 +the oxygen profile in meters, measured up from the diffusor
 +depth. This should correspond with the lake surface."
 Read(*,*) zOe

```

C   Input the dissolved nitrogen profile
    Write(*,*) "Enter the dissolved nitrogen concentration in
+the ambient water at the diffuser depth in mol per m^3."
    Read(*,*) amnpro
    Write(*,*) "Enter the coefficients for the equation for the
+nitrogen profile in the hypolimnion in the form ez^4
+az^3 + bz^2 + cz + d. Separate the coefficients by commas."
    Read(*,*) eNh, aNh, bNh, cNh, dNh
    Write(*,*) "Enter the upper depth of the hypolimnion based on
+the nitrogen profile in meters, measured up from the diffuser
+depth."
    Read(*,*) zNh

    Write(*,*) "Enter the coefficients for the equation for the
+nitrogen profile in the metalimnion in the form ez^4
+az^3 + bz^2 + cz + d. Separate the coefficients by commas."
    Read(*,*) eNm, aNm, bNm, cNm, dNm
    Write(*,*) "Enter the upper depth of the metalimnion based on
+the nitrogen profile in meters, measured up from the diffuser
+depth."
    Read(*,*) zNm
    Write(*,*) "Enter the coefficients for the equation for the
+nitrogen profile in the epilimnion in the form ez^4
+az^3 + bz^2 + cz + d. Separate the coefficients by commas."
    Read(*,*) eNe, aNe, bNe, cNe, dNe
    Write(*,*) "Enter the upper depth of the epilimnion based on
+the nitrogen profile in meters, measured up from the diffuser
+depth. This should correspond with the lake surface."
    Read(*,*) zNe

```

Calculate initial pressures, densities, vg, and numhub

```

z = 0
T = amTpro
S = amSpro
conco = amopro
concn = amnpro
Tsurf = 0.0
press = psurf+(1.0*10.0**(-5.0))*densave*g*(zsurf-z)

```

Froude = 1.6

```

C   Bublesp:
    bubrad = bubrad0
    If (bubrad.LE.7.0*(10.0**(-4.0))) Then

```

```

    bubslp = 4474.0*(bubrad**1.357)
    Else if(7.0*(10.0**(-4.0)).LT.bubrad.AND.bubrad.LE.
+    5.1*(10.0**(-3.0)))Then
        bubslp = 0.23
    Else
        bubslp = 4.202*(bubrad**0.547)
Endif

If (frac.EQ.1) Then
    ofrac=1.0
Else If (frac.EQ.2) Then
    ofrac=0.21
Endif

If (frac.EQ.1) Then
    nfrac=0.0
Else If (frac.EQ.2) Then
    nfrac=0.78
Endif

moles=(airin)/((R*10.0**(-5.0))*(273.15))
gaso=moles*ofrac
gasn=moles*nfrac

Write(*,*)"Enter guess for initial plume velocity."
Read(*,*)wguess

presso = (gaso/(gaso+gasn))*press
pressn = (gasn/(gaso+gasn))*press

densam = -6.0*10.0**(-7.0)*T**4.0+0.0000853*T**3-0.0089173*T**2.0
++0.0672279*T+999.8430939+0.000705*S

C  densam = (999.84298+(65.4891*T-8.56272*T**2.0+0.059385*T**3.0)*
C  +(1.0*10.0**(-3.0)))+0.802*S/1000.0+0.28

densplw = densam

w = wguess
b = b0

DO 30 K=1,30,1
mo = gaso/(L*b*(lambda)*(w+bubslp))
mn = gasn/(L*b*(lambda)*(w+bubslp))

vg = ((mo+mn)/press)*(R*10.0**(-5.0))*(273.15+T)

```

```

denspl = (1.0-vg)*densplw
w = Froude*(SQRT(L*g*((densam-denspl)/denspl)))
30 Continue

```

C Initial conditions

```

mu0 = L*b0*w
mom0 = mu0*w
FT0 = mu0*amTpro
FS0 = (mu0*amSpro*densplw)/1000.0
disso0 = mu0*amopro
dissn0 = mu0*amnpro

```

```

numbub = (3.0*(vg)*lambda*b0*L*(w+bubslp))
+/(4.0*Pi*(bubrad0**3.0))

```

```

rnumbub=numbub

```

```

If (bubrad.LE.0.000667) Then

```

```

    betao = 0.6*bubrad

```

```

    Else

```

```

        betao = 4.0*10.0**(-4)

```

```

Endif

```

```

betan = betao

```

```

Ko = 2.125-0.05021*T+(5.77*10.0**(-4.0))*T**2.0

```

```

Kn = 1.042-0.0245*T+(3.171*10.0**(-4.0))*T**2.0

```

```

Write(*,*) "Enter the number of intervals into which to divide
+the depth of the lake in order to solve using Euler's Method."

```

```

Read(*,*) I

```

```

deltaz = zsurf/I

```

```

Open(8,file='output.dat',status='new')

```

```

mu = mu0

```

```

mom = mom0

```

```

FT = FT0

```

```

FS = FS0

```

```

disso = disso0

```

```

dissn = dissn0

```

```

Count = 0

```

```

OPEN(6,file = 'prm')

```

```

Write(8,62)"z","w","mu","b","brad","T","Oflx","DO","mo","denpl",
+"denam"
62 Format(A1,8X,A1,6X,A2,4X,A1,6X,A4,7X,A1,5X,A4,5X,A2,6X,A2,
+6X,A5,6X,A5)

```

C DO LOOP STARTS HERE!!!

```
DO 100 J=1,I,1
```

```
z = z+deltaz
```

```
If (mom.LT.0.0) Then
```

```
Write(*,*)"Because momentum is negative at z=",z,"the change
+ in volume flux can no longer be calculated.Press enter to
+ continue."
```

```
Read(*,*)
```

```
Go To 1000
```

```
Else
```

```
Continue
```

```
Endif
```

```
dmudz=2.0*alpha*(L)*(mom/mu)
```

```
dmomdz=((((densam-denspl)/denspl)*g*(lambda)*(b*L))
+((1.0-lambda)*((densam-densplw)/denspl)*g*(b*L))
```

```
dFTdz=2.0*alpha*(L)*(mom/mu)*amTpro
```

```
dFSdz=2.0*alpha*densam*(amSpro/1000)*(mom/mu)*(L)
```

```
dDOdz=2.0*(L)*alpha*(mom/mu)*amopro+((4.0*Pi*(bubrad**2.0)*
+rnumbub)/((mom/mu)+bubslp))*betao*((Ko*presso)-(disso/mu))
```

```
dDNdz=2.0*(L)*alpha*(mom/mu)*amnpro+((4.0*Pi*(bubrad**2.0)*
+rnumbub)/((mom/mu)+bubslp))*betan*((Kn*pressn)-(dissn/mu))
```

```
dGOdz=((-4.0*Pi*(bubrad**2.0)*rnumbub)/((mom/mu)+bubslp))*betao*
+((Ko*presso)-(disso/mu))
```

```
dGNdz=((-4.0*Pi*(bubrad**2.0)*rnumbub)/((mom/mu)+bubslp))*betan*
+((Kn*pressn)-(dissn/mu))
```

```
mu = mu+(dmudz*deltaz)
```

```
mom = mom+(dmomdz*deltaz)
```

FT = FT+(dFTdz*deltaz)
T=FT/mu

FS = FS+(dFSdz*deltaz)
S=(FS/(mu*densplw))*1000

disso = disso+(dDOdz*deltaz)
conco = disso/mu

dissn = dissn+(dDNdz*deltaz)
concn = dissn/mu

gaso = gaso+(dGOdz*deltaz)

gasn = gasn+(dGNdz*deltaz)

If (z.LE.zTh)Then
 amTpro = eTh*z**4.0+aTh*z**3.0+bTh*z**2.0+cTh*z+dTh
 Else if (z.LE.zTm)Then
 amTpro = eTm*z**4.0+aTm*z**3.0+bTm*z**2.0+cTm*z+dTm
 Else
 amTpro = eTe*z**4.0+aTe*z**3.0+bTe*z**2.0+cTe*z+dTe
Endif

If (z.LE.zSh)Then
 amSpro = eSh*z**4.0+aSh*z**3.0+bSh*z**2.0+cSh*z+dSh
 Else if (z.LE.zSm)Then
 amSpro = eSm*z**4.0+aSm*z**3.0+bSm*z**2.0+cSm*z+dSm
 Else
 amSpro = eSe*z**4.0+aSe*z**3.0+bSe*z**2.0+cSe*z+dSe
Endif

If (z.LE.zOh)Then
 amopro = eOh*z**4.0+aOh*z**3.0+bOh*z**2.0+cOh*z+dOh
 Else if (z.LE.zOm)Then
 amopro = eOm*z**4.0+aOm*z**3.0+bOm*z**2.0+cOm*z+dOm
 Else
 amopro = eOe*z**4.0+aOe*z**3.0+bOe*z**2.0+cOe*z+dOe
Endif

If (z.LE.zNh)Then
 amnpro = eNh*z**4.0+aNh*z**3.0+bNh*z**2.0+cNh*z+dNh
 Else if (z.LE.zNm)Then
 amnpro = eNm*z**4.0+aNm*z**3.0+bNm*z**2.0+cNm*z+dNm
 Else
 amnpro = eNe*z**4.0+aNe*z**3.0+bNe*z**2.0+cNe*z+dNe

Endif

press = psurf+(1.0*10.0**(-5.0))*densave*g*(zsurf-z)

presso = (gaso/(gaso+gasn))*press

pressn = (gasn/(gaso+gasn))*press

```
C If (mom.LT.0.0)Then
C   Write (*,*) "Because the momentum is less than zero, the
C + plume radius cannot be calculated at z=",z
C   Write(*,*)"Press enter to end program."
C   Read(*,*)
C   Go To 1000
C   Else
C     Continue
C Endif
```

densam = -6.0*10.0**(-7.0)*amTpro**4.0+0.0000853*amTpro**3.0
+0.0089173*amTpro**2.0+
+0.0672279*amTpro+999.8430939+0.000705*amSpro

```
C densam = (999.84298+(65.4891*amTpro-8.56272*amTpro**2.0+
C +0.059385*amTpro**3.0)*(1.0*10.0**(-3.0)))+0.802*amSpro/1000.0+
C +0.28
```

densplw = -6.0*10.0**(-7.0)*T**4.0+0.0000853*T**3.0-0.0089173*
+T**2.0+0.0672279*T+999.8430939+0.000705*S

```
C densplw = (999.84298+(65.4891*T-8.56272*T**2.0+
C +0.059385*T**3.0)*(1.0*10.0**(-3.0)))+0.802*S/1000.0+0.28
```

w = mom/mu

If (w.LE.0.0)Then

Write(*,*)"The plume velocity has reached zero at z=",z,".

+ Press enter to continue."

Read(*,*)

Go To 1000

Else

Continue

Endif

C This bubrad eqn is using previous bubsplp and vg!!

b = (mu**2)/(mom*L)

bubrad = ((vg*lambdab*L*(w+bubsplp))/

+((4.0/3.0)*Pi*rumbub))**(1.0/3.0)

```

C  bubrad = ((vg*(mu*(1.0+mu*(bubslp/mom))))/
C  +((4.0/3.0)*Pi*numbub)**(1.0/3.0)
  If (bubrad.LE.0.0)Then
    Write(*,*)"The bubbles have completely dissolved. Press enter
+   to continue."
    Read(*,*)
  Endif

  If (bubrad.LE.(7.0*10.0**(-4.0))) Then
    bubslp = 4474.0*(bubrad**1.357)
    Else if ((7.0*10.0**(-4.0)).LT.bubrad.AND.bubrad.LE.
+   (5.1*10.0**(-3.0)))Then
      bubslp = 0.23
      Else
        bubslp = 4.202*(bubrad**0.547)
  Endif

mo = gaso/(L*b*(lambda)*(w+bubslp))
mn = gasn/(L*b*(lambda)*(w+bubslp))

vg = ((mo+mn)/press)*(R*10.0**(-5.0))*(273.15+T)

moles = gaso+gasn

denspl = (1.0-vg)*densplw

  If (bubrad.LE.6.67*(10.0**(-4.0)))Then
    betao = 0.6*bubrad
    Else
      betao = 4.0*(10.0**(-4.0))
  Endif

  If (bubrad.LE.6.67*(10.0**(-4.0)))Then
    betan = 0.6*bubrad
    Else
      betan = 4.0*(10.0**(-4.0))
  Endif

Ko = 2.125-0.05021*T+5.77*(10.0**(-4.0))*T**2.0
Kn = 1.042-0.0245*T+3.171*(10.0**(-4.0))*T**2.0

Count = Count+1
IF (Count.EQ.1000)THEN
  Write(8,92)z,w,mu,b,bubrad,T,disso,conco,mo,denspl-1000
+ ,densam-1000
92  Format(1X,F6.2,1X,F6.3,1X,F8.4,1X,F7.3,1X,E8.2,1X,F5.2,1X,

```

```
+ F7.4,1X,F7.4,1X,F7.4,1X,F7.3,1X,F7.3)  
  Count = 0  
ENDIF
```

```
100 Continue
```

```
1000 END
```

VITA

Wendy Jean Cox Royston was born on November 25, 1969 in Richmond, Virginia. She attended the University of North Carolina at Chapel Hill from 1987 to 1991, graduating with a Bachelor of Arts Degree in Psychology and Economics with distinction and with highest honors. After spending two years traveling and working in the Western United States, Wendy decided to pursue her Master of Science Degree in Environmental Engineering at Virginia Tech in Blacksburg, Virginia.

Wendy Jean Cox Royston